CENTRE FOR ORE DEPOSIT AND EXPLORATION STUDIES

STRUCTURE AND MINERALISATION OF WESTERN TASMANIA

AMIRA PROJECT P.291A
Third Report
March 1995

UNIVERSITY OF TASMANIA

CONTENTS

SUMMARY

Ron Berry

The work defining a western margin for the Dundas Trough has reached an advance stage. Three types of work have been applied to this study. Detailed conventional provenance studies have indicated that the Crimson Creek Formation was being actively eroded as a source terrain throughout the Dundas Group deposition. The sedimentology supports a very close source. The need to erode Crimson Creek Formation throughout the depositional history of the Dundas Group means that it was not covered by Dundas Group at any time. No acid volcanic material is mixed with this source.

The provenance was also studied using heavy minerals. Several distinct source signatures were recognised. These are:

- The western source component has a distinctive high chromite/zircon ratio, high tourmaline, high apatite and low total Fe oxides. Most micaceous sandstones from Cycle 3 carry this signature.
- The eastern source signature (Tyennan region) was defined from the Sticht Range Formation. This signature (rounded zircon) has not been recognised in any of the other sandstones in this study.
- The CVC/ Yolande signature is high euhedral zircon and TiO_2
- The Tyndall Group signature is very high FeTi oxides

The difference between source signatures of Cycle 1 and Cycle 3 sandstones suggests the western source is transformed from a low relief deeply weathered area in the Middle Cambrian to an actively eroding area with fresh rocks exposed in the Late Cambrian. despite this transformation the western source has been recognised very widely as predicted by the more localised study on the western margin of the belt.

The sedimentological studies in the Stitt Quartzite have suggested the mature turbidite facies sandstones are transported along the graben axis while the pebbly sandstones are locally derived material eroding from horst blocks along the basin margin. Despite this difference both suites carry the western source signature. The Husskisson Group is consistent with a ramp facies. All three type of information are consistent with the structural interpretation which show a discrete graben margin along the western side of the Dundas Trough.

The S isotope work has been largely committed to a baseline study at Rosebery and has demonstrated evidence for complex sea-water circulation patterns. This work is now being extended out to growth faults throughout the Mt Read belt to define a growth fault signature.

Initial work on the new structural section near the Firewood Siding Fault has demonstrated the complex nature of Cambrian deformation based on the field relationships at the base of the Owen Conglomerate and its correlates. Further work is refining the pattern of Cambrian deformation in this area and its relationship to the Henty Fault wedge.

The project is now providing strong additional evidence for the existence of Cambrian faults in the Mt Read Volcanics. The sedimentological tests are supporting the general geometry defining which blocks are subaerial during the Cambrian. The outstanding result so far is that the western block is a major source during the Mt Read depositional cycles. The Tyennan block does not figure substantially until late in the sedimentary history. The S isotope work has shown that a Cambrian seawater can produce a detectable signature in an area of cold infiltration. This work is now being used to set up a growth fault signature to aid detailed identification of Cambrian growth faults.

Heavy minerals, provenance and lithostratigraphy

R.F. Berry and R. Fulton

Centre for Ore Deposit and Exploration Studies, Geology Department, University of Tasmania

ABSTRACT

The Mt Read Volcanics have been subdivided into three depositional cycles each with a distinct basin geometry and history. Samples of sandstones have been collect from each of these cycles. Cycle 2 sandstones are recognisable from the very large component of Fe oxides, including ilmenite and magnetite. Cycle 3 sandstones have much less Fe oxide and the major external contribution to the heavy minerals is chromite and rounded zircon. Chromite is apparently associated with a western source. Major points from this study are:

- The Animal Creek Greywacke has a distinctive high chromite/zircon ratio, high tourmaline, high apatite and low total Fe oxides. Most micaceous sandstones from Cycle 3 carry this signature.
- The eastern source signature (Tyennan region) was defined from the Sticht Range Formation. This signature has not been recognised in any of the other sandstones in this study.
- The Yolande River Group has a felsic magmatic source component very different from the andesitic source component of the Tyndall Group.
- The difference between source signatures of Cycle 1 and Cycle 3 sandstones suggests the western source is transformed from a low relief deeply weathered area in the Middle Cambrian to an actively eroding area with fresh rocks exposed in the Late Cambrian.

The heavy mineral suites have some potential to aid correlation of the stratigraphy. Noteworthy here is that initial data suggests the Eastern Quartz Phyric sequence is discernible from the Tyndall Group on heavy mineral content. The Cycle 2 sandstones form a very distinct group based on the uniform andesitic character of the source.

INTRODUCTION

A major aim of the combined ARC–AMIRA project is to define the basin geometry for the Mount Read Volcanics. A structural model was put forward in P291 which is being used as a template for this analysis. The project described here looks at the heavy mineral suite as a guide to what sources are available to the basin at each stage in its genesis.

The threefold classification of the Mount Read volcanics has been used to constrain the analysis of the heavy mineral provenance study.

CYCLE 1 — Denison Group biostratigraphic correlates
All the units which are Idamean or younger.

CYCLE 2 — Tyndall cycle of deposition
upper Boomerangian/Mindallyian

CYCLE 3 — Yolande Cycle of deposition
Undillian/lower Boomerangian (pre- to syn- granite intrusions).

Heavy minerals are a good test of the provenance of sandstones. They potentially survive minor alter-

ation and deformation. The phases are characteristic of their source. The distribution should place constraints on the basin architecture. In addition, if certain sources only become available during the history of the belt a separation of the stratigraphy should be possible. For example the existing problem with the definition of the Tyndall Group. At present some granitic clasts are required to recognise this group as distinct from the Eastern Quartz-phyric sequence. Sandstones from all cycles and scattered across the belt have been included in the initial study.

Thirty-seven samples have been collected and crushed gently as recommended by Henningsen (1967). The fine sand fraction (63–125 m) from these rocks was extracted by sieving, washed and then separated by heavy liquids. The heavy mineral grains were mounted on polished thin sections. Detailed point counting has been carried out on these samples and many have been checked by microprobe analysis. This is proving to be very labour intensive. Whole rock analyses are being carried out on these samples to compare the relative value of the two techniques.

PROVENANCE AND STRATIGRAPHIC CORRELATION

The heavy mineral contents are summarised in Tables 1 and 2. The results of this analysis are shown below. In these tables the lower dataset is normalised based on the total weight of sample processed and the weight of heavy minerals that were collected. The weight of heavy minerals varies from 0.001 to 1.53 gm despite the small range in amount of sandstone used (20–30 gm). Even on total heavy minerals alone the Cycle 1 and 2 sandstones are distinct from the Cycle 3 sandstones and volcaniclastics.

STATISTICAL ANALYSIS

The variability of the heavy minerals is very large. In order to put some order on this data the total dataset was processed in a multivariate statistical package (MVSP). The most distinctive analysis of provenance is obtained if sulphides, chlorite and goethite are excluded as these may reflect diagenetic and alteration processes. The dataset was normalised using the Aitchison centred log ratio method. The cross-correlation table for this analysis is shown in Table 3. The major correlations are:

1. magnetite–hematite–ilmenite
2. TiO_2–euhedral zircon
3. chromite–rounded zircon–tourmaline
4. apatite–tourmaline

Principal component analysis showed that the data set is very scattered with the maximum eigenvector only explaining 30% of the variance and the first four eigenvectors explaining 75% of the variance (Table 4). The first vector has the group magnetite–ilmenite–hematite as its positive direction (andesite/basalt magmatic source?) and chromite–zircon–tourmaline as the negative direction (Table 5). The second vector has euhedral zircon–TiO_2 in the positive direction and tourmaline – chromite in the negative direction. This is roughly a felsic magmatic component in the positive direction and a detrital component in the negative direction.

The graph of vector 1 versus vector 2 (Fig.1) spreads the data out very well. The most obvious features are that almost all Cycle 1 and 2 samples fall in the positive field for vector 1. In contrast most Cycle 3 samples have negative scores for vector 1. The vector 2 reflects the proportion of magmatic component. Thus the Tyndall Group in the south has a high score for vector 2 compared to the equivalent Mt Cripps Subgroup which contains less zircon and TiO_2. The Cycle 1 sandstones from Higgins Creek have high oxides but low felsic magmatic component so they fall in a similar field to the Mt Cripps Subgroup and the Southwell Subgroup.

The Cycle 3 sandstones have a large range of compositions. The Animal Creek Greywacke and probable correlates (Farrell Slates) have a very low magmatic component and are at the low end of vector 2. The Yolande River Group has a very large range reflecting the diverse range of rocks involved. Micaceous Yolande River Group rocks plot near the Animal Creek Greywackes while the volcaniclastic rocks have vector 2 values similar to the Tyndall Group but at lower oxide contents (lower vector 1 scores). This probably reflects the dominance of a dacitic source for these rocks with a more andesitic source required for the Tyndall Group. Most Dundas Group rocks (Stitt Quartzite, Boco Road samples, Cradle Mountain Link Road, Husskisson Group) lie within the range defined for the Yolande River Group. Exceptions are 94/3 (Browns Road member), 94/8 (Dundas Group on Boco Road), 94/39 (Yolande River Group from Strahan Road — this sample has very low total abundance of heavy minerals in contrast to most samples with high Vector 1 scores).

Table 1. Heavy mineral populations in sandstones from western Tasmania: Cycle 3 sandstones

	Stichl Range Format	Animal Creek Greywacke			Farrell Slate		Yolande River Group sst			Yolande River Group volcaniclastics				
							Strahan Road							
Field no	94/42	94/11	94/12	94/14	94/1	94/2	94/38	94/39	94/27	94/26	94/28	94/29	94/32	94/33
AMG	883699	811853	844897	853903	877833	874831	684297	662328	756475	753496	765467	789430	780338	795310
pyrite	52				39	61		1			2	6	100	
magnetite	4							3	1					
hematite	2		4		1	4		3		23	5			
ilmenite	2		7					9						
tourmaline	9	32	18	93	3	6		2	36			1	2	
zircon(euh)	2	5	3	11	6		4		4	1	47	210	2	171
zircon(round)	28	8	19	20	7	12	2	2	20	1	4	8		5
apatite	11	3	38	2	10	10	1	11	16		1	2	48	2
chromite	0	48	146	147	46	15	15	5	108					
TIO2	61	54	55	40	22	17	65	79	35	8	68	1		39
goethite	7	2		27	2	3	1	30	3	169	116	8	2	4
chlorite	3	6	1	3	13	1	1	3	2			3	0	3
other	34	3		2	7	8	4	9			8		74	
Total grains	215	161	291	345	156	137	93	157	225	202	251	239	228	224
weight(sample)	27.9	27.8	29.2	25.9	30.4	29.1	23.6	25.0	20.9	25.0	19.2	21.3	18.2	31.3
heavies	0.045	0.060	0.030	0.030	0.090	0.070	0.360	0.010	0.070	0.080	0.010	0.020	0.090	0.001
Heavy minerals in ppm by volume														
pyrite	390	0	0	0	740	1071	0	3	0	0	4	24	2174	0
magnetite	30	0	0	0	0	0	0	8	15	0	0	0	0	0
hematite	15	0	14	0	19	70	0	8	0	364	10	0	0	0
ilmenite	15	0	25	0	0	0	0	23	0	0	0	0	0	0
tourmaline	67	429	64	312	57	105	0	5	536	0	0	4	43	0
zircon(euh)	15	67	11	37	114	0	657	0	60	16	98	825	43	24
zircon(round)	210	107	67	67	133	211	328	5	298	16	8	31	0	1
apatite	82	40	134	7	190	176	164	28	238	0	2	8	1043	0
chromite	0	643	516	494	873	263	2463	13	1608	0	0	0	0	0
TIO2	457	724	194	134	417	298	10675	201	521	127	141	4	0	6
goethite	52	27	0	91	38	53	164	76	45	2677	241	31	43	1
chlorite	22	80	4	10	247	18	164	8	30	0	0	12	0	0
other	255	40	0	7	133	140	657	23	0	0	17	0	1609	0
zr/(zr+zrr)	0.07	0.38	0.14	0.35	0.46	0.00	0.67	0.00	0.17	0.50	0.92	0.96	1.00	0.97
zrr/(cr+zrr)	0.31	0.13	0.26	0.33	0.24	0.41	0.03	0.02	0.36	0.11	0.06	0.89		0.11
M +H +I	60	0	39	0	19	70	0	38	15	364	10	0	0	0

Table 1 cont.

	Central Volcanic Co		Dundas Group				EQPS	Rosebery Group			Husskisson Group	Southwell Subgroup
			Boco Rd			CradleLR	Murchison Volcanics	Stitt Qte	StittCorr	Westcott c	Merton Rd	Cradle LR
Field no	94/34	94/35	94/3	94/8	94/9	94/15	94/21	SQ-1	94/4	94/22	94/23	94/19
AMG	804302	823315	784850	793853	792853	910985	873755	772753	768846	758785	677794	947986
pyrite		8	36	148			42	7	30	2	35	4
magnetite	1		1	19			38	4		1		2
hematite		25	5	3	1	1		26	1	3		17
ilmenite	1	6	1	6	2	3		4		2		19
tourmaline	13			2	1	25		48	23		1	4
zircon(euh)	60	27	1		25	18	13	3	12		2	1
zircon(round)	20			4	2	16		47	12			
apatite	1	8	2		7	18	19	8	21		7	10
chromite	11			4		105		12		3	3	20
TiO2	106	23	44		94	50	40	9	61	115	10	10
goethite	19	79	13		151	2	3		11	15	122	
chlorite		2	1	6		1	81		17	119		1
other	16	81			5	2			4	30	9	
Total grains	248	259	104	192	288	241	236	168	192	290	189	88
weight(sample)	42.1	26.1	28.6	22.5	23.5	25.0	24.5	23.5	25.4	21.6	19.6	27.3
heavies	0.020	0.010	0.100	0.030	0.020	0.050	0.912	0.060	0.010	0.230	0.040	0.260
Heavy minerals in ppm by volume												
pyrite	0	12	1211	1029	0	0	6630	106	62	73	378	433
magnetite	2	0	34	132	0	0	5999	61	0	37	0	216
hematite	0	37	168	21	3	8	0	394	2	110	0	1839
ilmenite	2	9	34	42	6	25	0	61	0	73	0	2056
tourmaline	25	0	0	14	3	207	0	728	47	0	11	433
zircon(euh)	115	40	34	0	74	149	2052	46	25	0	22	108
zircon(round)	38	0	0	28	6	133	0	713	25	0	0	0
apatite	2	12	67	0	21	149	2999	121	43	0	76	1082
chromite	21	0	0	28	0	871	0	182	0	110	32	2164
TiO2	203	34	1480	0	277	415	6314	137	125	4217	108	1082
goethite	36	117	437	0	445	17	474	0	23	550	1318	0
chlorite	0	3	34	42	0	8	12787	0	35	4363	0	108
other	31	120	0	0	15	17	0	0	8	1100	97	0
zr/(zr+zrr)	0.75	1.00	1.00	0.00	0.93	0.53	1.00	0.06	0.50		1.00	1.00
zrr/(cr+zrr)	0.16	0.00	0.00	1.00	0.02	0.24	0.00	0.84	0.16	0.00	0.00	0.00
M +H +I	4	46	235	195	9	33	5999	516	2	220	0	4111

Table 2. Heavy mineral populations in sandstones from western Tasmania: Cycle 1 and 2 sandstones, Crimson Creek Formation

	Tyndall Group				Mt Cripps Formation		Higgins Creek Succession			Jukes Conglomerate	Crimson Creek
	Lynchford		Jukes Road		Cradle LR						
Field no	94/31	94/30	94/36	94/37	94/18	94/17	94/7	94/5	94/6	94/20	94/24
AMG	789378	790374	838306	846303	957987	967987	761861	753844	759844	863761	634813
pyrite					1				31		2
magnetite	101		8		49	15		18	1		6
hematite	3	3	2	108	72	13	3	93		3	3
ilmenite		2			5	23		30	37	207	69
tourmaline	1	1				0		4	1		3
zircon(euh)	1	15	9	7			1		6	6	7
zircon(round)	1		1			2	2			1	2
apatite	2				9	76		2	2	3	
chromite					0		2	1	8		8
TiO2	60	265	59	12	4		9	27	18	5	57
goethite	7	15	152	87		63	202	67	44	1	22
chlorite	9					0	1				33
other				15					57		7
Total grains	185	301	231	229	140	192	220	242	205	226	219
weight(sample	26.5	27.1	24.9	23.9	27.9	22.2	13.8	33.0	17.6	20.9	25.0
Heavies	0.390	0.020	0.110	0.120	0.470	0.710	0.050	1.530	0.006	0.520	0.230
Heavy minerals in ppm by volume											
pyrite	0	0	0	0	120	0	0	0	52	0	84
magnetite	8023	0	153	0	5900	2495	0	3454	2	0	252
hematite	238	7	38	2367	8670	2163	49	17844	0	331	126
ilmenite	0	5	0	0	602	3826	0	5756	62	22832	2899
tourmaline	79	2	0	0	0	0	0	768	2	0	126
zircon(euh)	79	37	172	153	0	0	16	0	10	662	294
zircon(round)	79	0	19	0	0	333	33	0	0	110	84
apatite	159	0	0	0	1084	12642	0	384	3	331	0
chromite	0	0	0	0	0	0	33	192	13	0	336
TiO2	4766	650	1131	263	482	0	148	5181	30	552	2395
goethite	556	37	2913	1907	0	10480	3322	12856	73	110	924
chlorite	715	0	0	0	0	0	16	0	0	0	1386
other	0	0	0	329	0	0	0	0	95	0	294
zr/(zr+zrr)	0.50	1.00	0.90	1.00		0.00	0.33		1.00	0.86	0.78
zrr/(cr+zrr)	0.02	0.00	0.02	0.00	0.00	1.00	0.18	0.00	0.00	0.17	0.03
M +H +I	8261	12	192	2367	15172	8484	49	27055	63	23163	3277

Table 3. Covariance matrix for heavy minerals after Aitchison centred log ratio transformation.

				CENTERED COVARIANCE MATRIX					
	magnetite	hematite	ilmenite	ourmaline	zircon(e)	zircon(r)	apatite	chromite	TiO2
magnetite	4.18	1.25	1.34	-1.13	-1.54	-1.20	-0.29	-1.84	-0.76
hematite		4.60	1.22	-1.85	-1.24	-0.91	-0.82	-2.00	-0.24
ilmenite			3.96	-1.00	-1.37	-1.73	-0.28	-0.94	-1.20
tourmaline				2.48	-0.62	0.85	0.52	1.56	-0.82
zircon(e)h					4.51	0.45	-0.33	-1.11	1.24
zircon(r)						2.84	-0.70	0.67	-0.27
apatite							3.43	-0.55	-0.99
chromite								4.45	-0.23
TiO2									3.28

Table 4. Variance scores from first 8 eigen vectors in Principal Component analysis.

AXIS	EIGENVALUE	PERCENT OF TOTAL	CUMULATIVE PERCENT
1	10.8	32.1	32.1
2	7.0	20.6	52.7
3	4.6	13.5	66.2
4	3.4	10.0	76.1
5	2.9	8.7	84.8
6	2.8	8.2	93.0
7	1.3	4.0	97.0
8	1.0	3.0	100.0

Table 5. Component loadings of first 3 eigenvectors.

EIGENVECTORS (COMPONENT LOADINGS)					
	AXIS 1	AXIS 2	AXIS 3	AXIS 4	AXIS 5
magnetite	0.45	-0.10	0.07	-0.15	0.76
hematite	0.48	0.13	-0.34	-0.36	-0.54
ilmenite	0.41	-0.21	0.02	0.54	-0.15
tourmaline	-0.30	-0.32	0.10	-0.13	0.05
zircon(euh)	-0.24	0.64	0.26	0.16	0.00
zircon(rou)	-0.29	0.02	-0.18	-0.58	0.07
apatite	-0.03	-0.17	0.74	-0.07	-0.28
chromite	-0.40	-0.44	-0.40	0.30	-0.05
TiO2	-0.11	0.44	-0.27	0.30	0.13

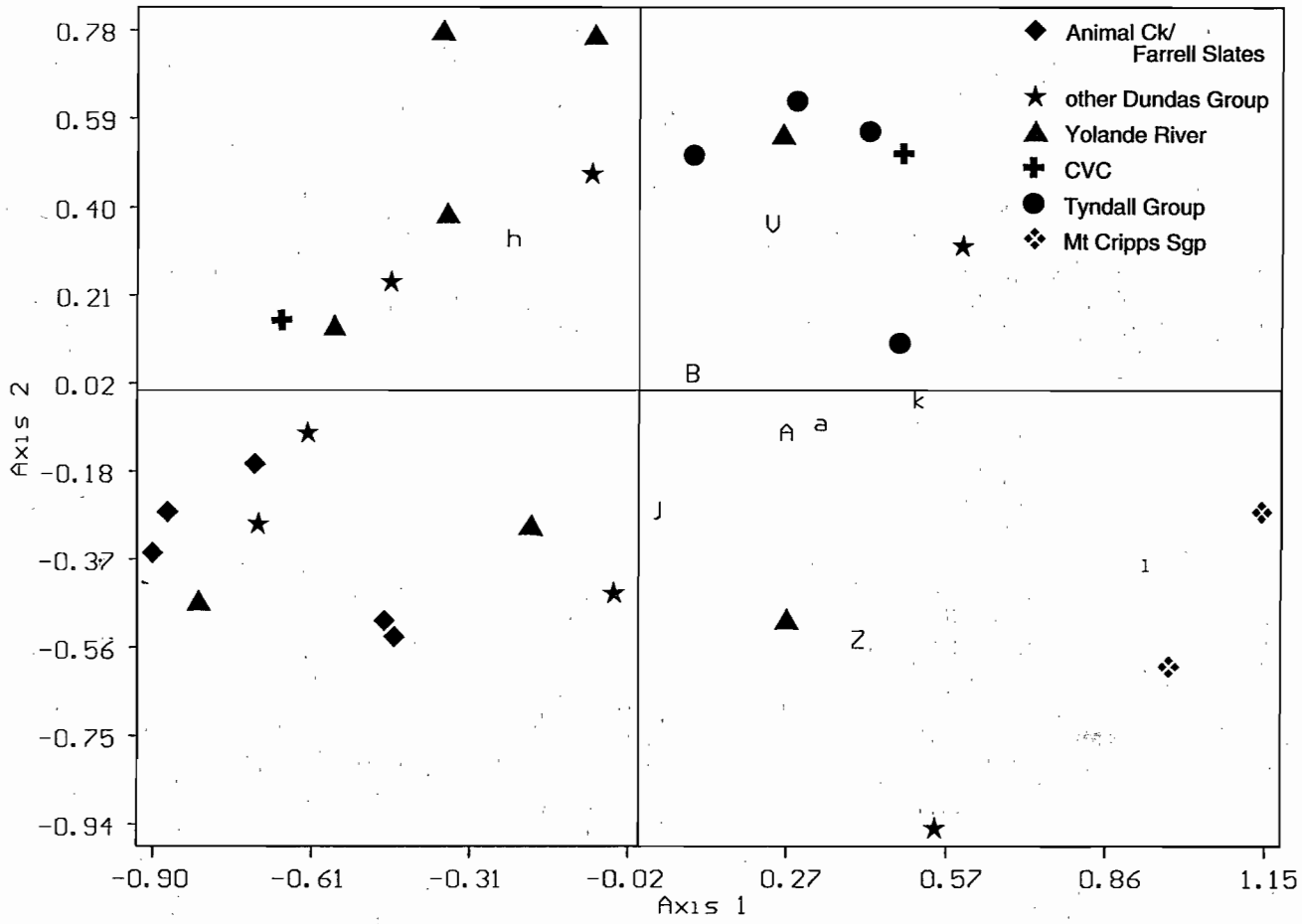

Figure 1. Plot of positions of samples in first two vectors of the Principal components space.

	Field no	Symbol
Crimson Creek Formation	94/24	A
Sticht Range Formation	94/42	B
Murchison Volcanics	94/21	V
Southwell Subgroup	94/19	Z
Westcott Argillite	94/22	a
Higgins Creek	94/7	h
Higgins Creek	94/6	j
Higgins Creek	94/5	i
Jukes Conglomerate	94/20	k

The spread due to vector 3 adds little to this story (Fig. 2). The major difference here is that the Murchison Volcanics sample(Eastern Quartz-phyric sequence) is separated from the Tyndall Group samples. Note that the Westcott Argillite is still very close to the Crimson Creek Formation sample as it is on Fig. 1. The large range in Yolande River Group is still similar to that of all the Dundas Group.

An alternative method for looking at the samples is to use a cluster analysis. Again this is based on the nine most diagnostic minerals and after normalising using the Aitchison centred log ratio method. The results of this clustering is shown in Fig. 3. The hierarchy of clustering recognises a clear Dundas association which includes the Animal Creek Greywacke (15, 12 ,11, 14), Farrell Slate (1, 2), Huskisson Group (23), Stitt Quartzite (SQ-1), Yolande River Group (27, 38 these are micaceous sandstone) and CVC (34). This group has a western basement source signature. Another more complex cluster is the Tyndall Group (30, 31, 36, 37) and volcanogenic Yolande River Group (26, 28, 29, 33), Murchison Volcanics (21) with volcanogenic Dundas Group (9), Stitt correlate (4) and the Sticht Range Formation. This group is largely composed of those rocks with little or no chromite, i.e. no western component. The third major cluster is dominated by the basaltic source material. This includes the Crimson Creek sample (24) , Higgins Creek sequence (5, 6), Westcott Argillite (22), Mt Cripps Subgroup (17, 18), Southwell Subgroup (19), CVC and Browns Road sequence (3, 35), and part of the Yolande River Group (39 on Strahan Road).

The major feature of this analysis is that the variation in provenance as defined by heavy minerals is not simply related to stratigraphy. There is a strong spatial association across the area which is reflecting the basin geometry. For example the Tyndall Group clusters with the volcanic components of the Yolande River Group. The Tyndall Correlate in the north, Mt Cripps Subgroup, has a different signature more closely aligned with the Cycle 1 sandstones of Higgins Creek.

Another examples of spatial as opposed to temporal control, are the trace garnet component found in both Yolande River Group samples from the Strahan Road. In contrast, garnet was not recognised in any other Mt Read sample studied including the Sticht Range Formation. Garnet is a minor component in the Crimson Creek Formation (94/24). The garnet source at this time was somewhere to the southwest.

SOURCE SIGNATURES

A better way to think about the various elements in this analysis is to consider the nature of the sources available. The Sticht Range Formation (94/42) is a good example. As a near shore facies on the eastern side of the basin, this unit has little chance to source material from the west. The sample has a very low component of felsic volcanic material as indicate by the low abundance of euhedral zircon. The major component of the heavies is TiO_2 and rounded zircon then apatite and tourmaline.

In contrast the work of Selley (this volume) indicates many of the conglomerates in the Dundas field are dominated by a western source (Crimson Creek Formation, Success Creek Group and MUC). The perfect example of this is the sample of Westcott Argillite taken from the Pieman Road very close to the boundary fault. This sample (94/22) lies very close to the Crimson Creek sample (94/24) in most plots. It has very high TiO_2 and low chromite with minor FeTi oxides. The high chlorite here probably reflects the basaltic source material. Surprisingly the chromite to TiO_2 ratio is low (0.03) suggesting there is little ultramafic component. Further north, the Higgins Creek samples have chromite to TiO_2 ratios up to 0.45. They also have higher FeTi oxides but with Fe >>Ti unlike the Westcott Argillite where Fe~Ti.

The best examples of a direct CVC source are the volcanogenic Yolande River Group (94/29, 94/33). These are dominated by euhedral zircon with low apatite and tourmaline. There is no chromite and TiO_2 abundance is less than a third of the zircon. The FeTi oxide contents are extremely low reflecting a very felsic composition. The sample 94/32 has high apatite but this is apparently an alteration product associate with high pyrite (see apatite section below).

The Tyndall Source can be from defined by samples from Lynchford and the Jukes Road. In contrast to the CVC, FeTi oxides >> euhedral zircon. Fe > Ti and apatite is apparently higher than the 0.01 * zircon found in the CVC source.

The Animal Creek Greywackes have some features of the western sources. They have high chromite suggesting a western source component. The high rounded zircon content, about 0.15 × chromite, is similar to the Crimson Creek Formation and does not require an additional eastern component. The magmatic source is recognised by the euhedral zircons and ?magmatic apatites. However a problem here is that apatite > euhedral zircon unlike

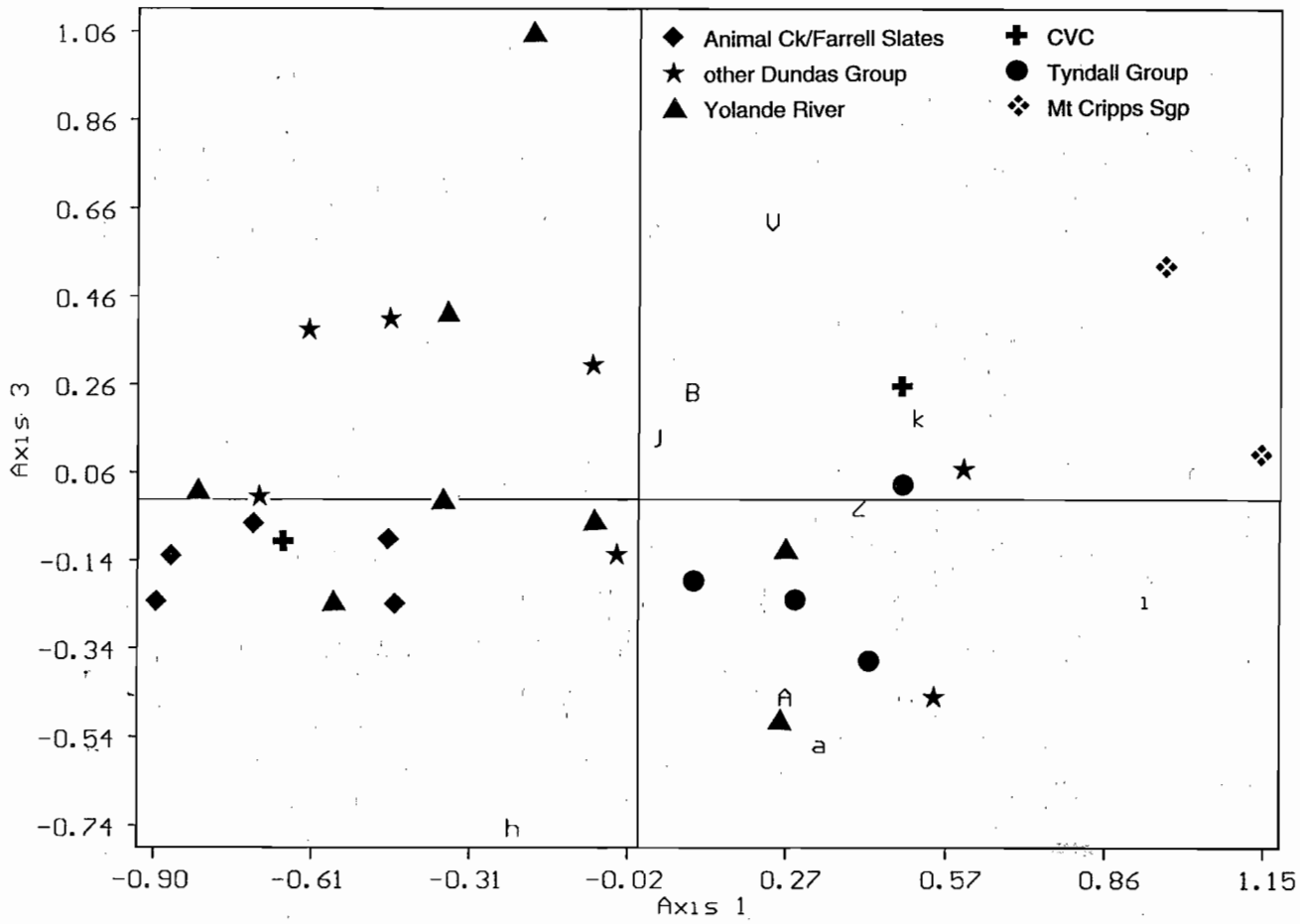

Figure 2. All samples in space defined by vector 1 and 3 of PC analysis.

	Field no	Symbol
Crimson Creek Formation	94/24	A
Sticht Range Formation	94/42	B
Murchison Volcanics	94/21	V
Southwell Subgroup	94/19	Z
Westcott Argillite	94/22	a
Higgins Creek	94/7	h
Higgins Creek	94/6	j
Higgins Creek	94/5	i
Jukes Conglomerate	94/20	k

Figure 3. Cluster analysis after log ratio transformation

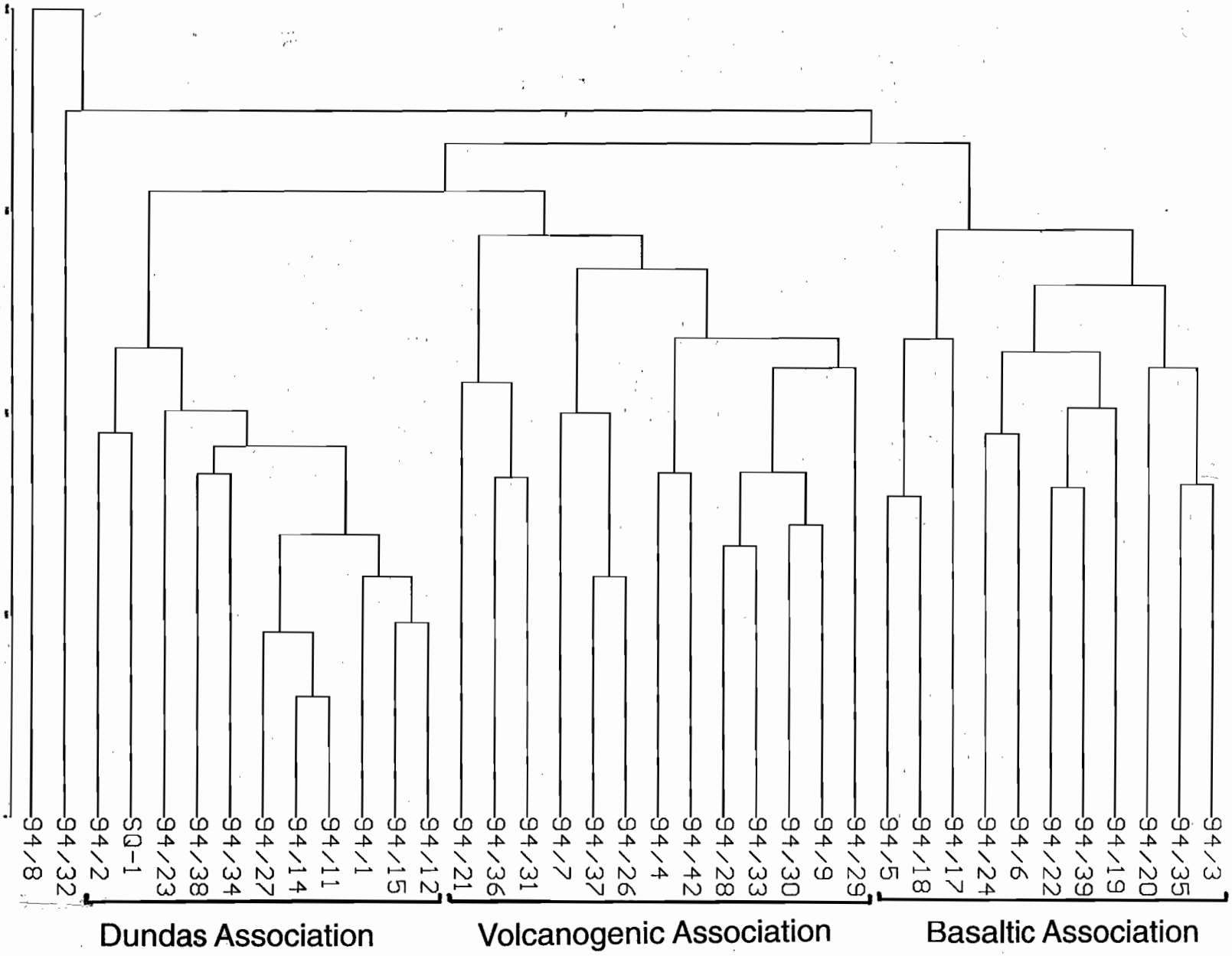

any of the magmatic sources listed above. Tourmaline is also very high compared to Cycle 1 and 2 sandstones. The apatite in these rocks is largely euhedral and extremely F-rich suggesting a magmatic source. The association with tourmaline is suggestive of a plutonic source rock (granite). However the tourmaline is not typical of granite (see Tourmaline section below). This source component is also seen in the Farrell Slates, Stitt Quartzite and the micaceous sandstone from the Dundas Group (94/15) and the Yolande River Group (94/27). The association with micaceous rocks has been used in the past to suggest this association indicates a medium grade metamorphic terrain but there are no garnets and the apatites have euhedral shapes and high F. Apatite and tourmaline are very low in the Cycle 1 and Cycle 2 sandstones (relative to zircon). This association is also characterised by chromite > TiO_2 and Ti > Fe. Most of this variation can be explained as a source from a deeply weathered protolith in which Fe has been largely removed, leaving a residue enriched in the more robust constituents. The Yolande River samples from the Strahan Road have high chromite, apatite ~ zircon but the chromite < TiO_2 and Ti > Fe suggests a weathered source area with less mafic/ultramafic rocks. The Higgins Creek and Westcott Argillite require a more actively eroding, less weathered western source.

The samples from along the Boco Road which are stratigraphically just above the Animal Creek Greywacke have some features of the Animal Creek signature modified by the volcanic input. The Huskisson Group sample (94/23) may be modified by alteration. The White Spur correlate (94/9) has higher apatite than typical CVC (apatite/euhedral zircon of 0.3) and TiO_2 > zircon.

MINERALS

Chromite

Chromite represents one of the most distinctive minerals within the heavy mineral suite. The data presented above suggests this material comes from the west and is sourced out of the Crimson Creek Formation and the mafic/ultramafic complexes (MUC). The MUC contain rocks which have a very refractory composition and have chromites with a very high Cr# (100*Cr/(Cr+Al+Fe3+)). The chromite in the Crimson Creek Formation is largely from basalt and the conventional view is that this will have a Cr# < 70. The Crimson Creek sample in this study has a small range of Cr# from 55 to 77 with a mode around 70 (Fig. 4). The trend to low Mg# in this figure is not a magmatic trend and is probably a metamorphic or metasomatic effect.

Three samples of Animal Creek Greywacke have been tested for chromite composition (Fig. 5). These all show a large range in chromite composition from 20 to 90. About 20% of grains lie in the very high Cr# range characteristic of MUC. The lower Cr#'s below 50 may reflect an evolved gabbroic source. The samples from the Yolande River Group (94/27, 94/38, 94/39) has a similar range in Cr# to the Animal Creek Greywacke (Fig. 6) . Sample 94/39 has a high proportion of grains in the distinctive high Cr# area suggesting a mainly MUC source but the zircon/chromite ratio does not support this. The Farrell Slate sample (Fig. 7a) has a similar range of chromite contents to 94/11 but none of the 8 grains analysed were above Cr# 80. These samples all support a well mixed composite source containing some MUC.

The chromite in the Higgins Creek sample 94/6 (Fig. 7b) is identical to chromite populations in the other samples and supports a continuation of the same source area for Middle and Late Cambrian.

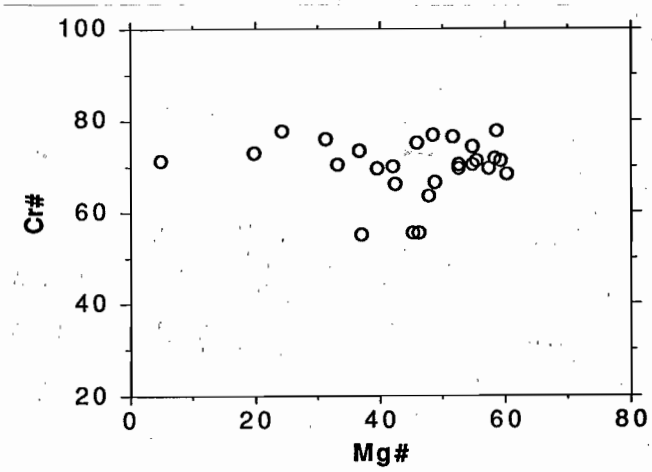

Figure 4. Chromite composition from Crimson Creek Formation (94/24).

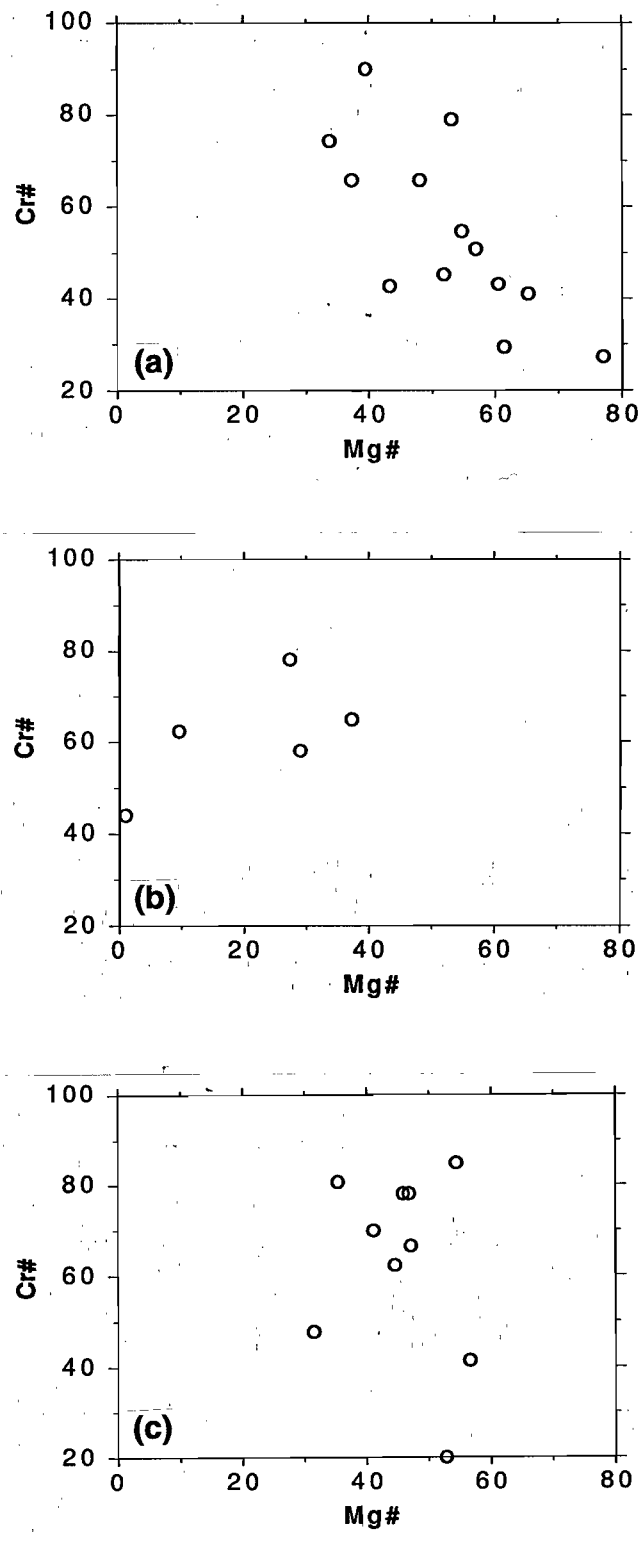

Figure 5. Chromites from the Animal Creek Greywacke. (a) 94/11, (b) 94/12, (c) 94/14.

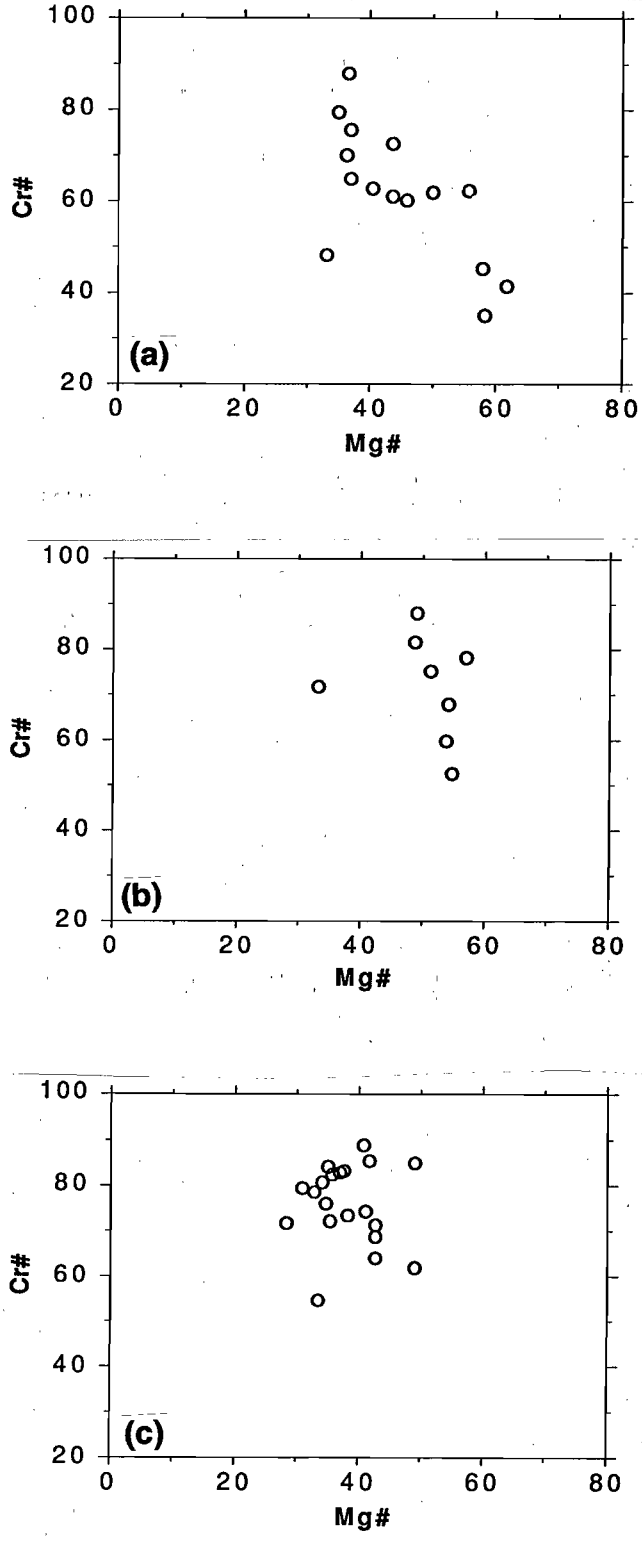

Figure 6. Chromites from the Yolande River Group on the Strahan Road. (a) 94/27, (b) 94/37, (c) 94/38.

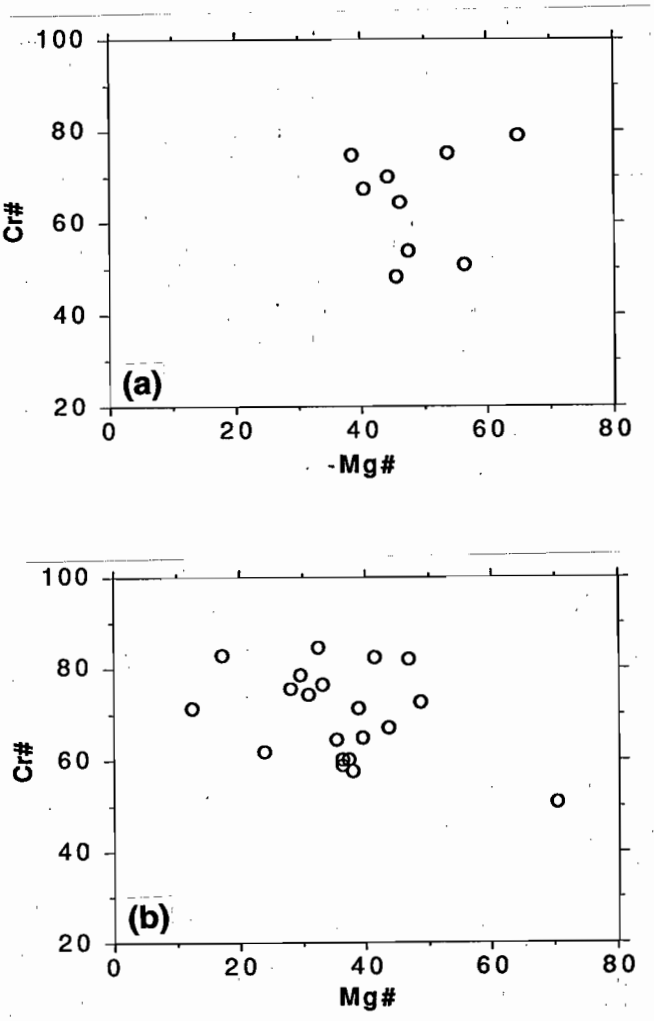

Figure 7. Chromites from (a) the Farrell Slate (94/1) and (b) Higgins Creek (94/6).

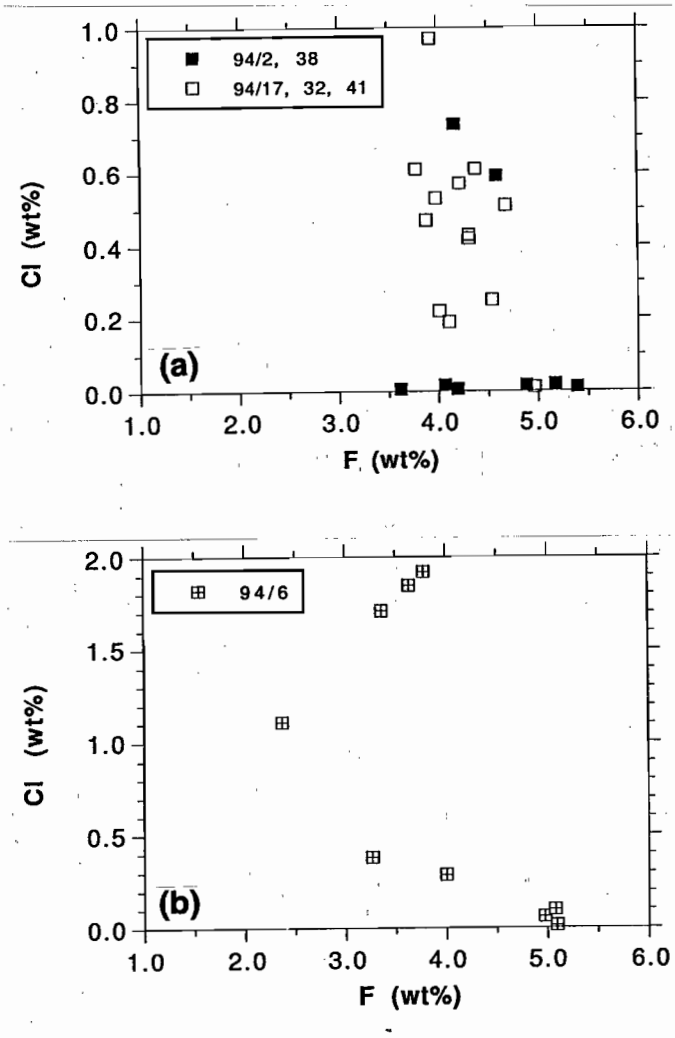

Figure 8. Apatite compositions. (a) Magmatic grain - 94/2, 94/38, alteration - 94/17, 94/32, 94/41; and (b) 94/6.

Apatite

Most apatites show fractured or euhedral shapes. No well rounded apatites were recognised. The compositions are mostly F-rich Cl-poor suggesting a magmatic origin, and combined with the textures, a proximal source from local magmatic activity is proposed.

Three samples contain a distinctly different apatite form. These apatites are broken grains and are full of fine grained inclusions. The apatites from these samples have higher Cl content than the magmatic apatites from other samples (Fig. 8a) and are probably formed by alteration. They were recognised from the Mt Cripps Subgroup on the Cradle Mountain Link Road (94/17), a volcaniclastic sandstone in the Yolande River sequence south of Lynchford (94/32) and the Tyndall Group (94/41). The alteration apatites also have marginally lower FeO and Sr than the clear apatites.

One sample (94/6, Higgins Creek) has been found with a population of apatites with much higher Cl contents (Fig. 8b). These samples contain 2% Cl and require a different source from the apatites found in other rocks in the area.

Zircon

Zircons have been found in most rocks. There is very little variation in composition. The ratio of rounded to euhedral zircons reflects the proportion of extrabasinal sediment represented in the sandstones. Some of the rounded zircons (especially in the Sticht Range Formation) are slightly metamict but the euhedral zircons are all clear and unaltered. This is consistent with detrital zircons including some very old grains.

Tourmaline

Tourmalines are largely euhedral or broken. No evidence was noted for rounded tourmaline. Some tourmalines have visible zoning in colour but this has not been investigated in detail. The compositions range in Mg#, with MgO varying from 5.8–11.3% but other elements are not very variable. Tourmaline is very common in the Animal Creek Greywacke, and forms part of the diagnostic mineralogy for this assemblage, but is rare in the Tyndall Group and younger rocks (e.g. Higgins Creek). The tourmaline analyses of samples from Animal Creek Greywacke, Farrell Slate and Stitt Quartzite are shown in Fig. 9. All the points plot in the fields 4, 5 and 6 of the Al, Mg and Fe diagram from Henry & Guidotti (1985). These fields are meta-pelites, meta-psammites, and quartz-tourmaline rocks. The Ca–Mg–Fe diagrams shows that these tourmalines are from a low Ca precursor. There is no evidence in this data for a granitic source. Taylor & Slack (1984) demonstrated that tourmalines from massive sulphide bodies have a very similar range in composition to the samples reported here.

Magnetite

Magnetite grains are all heavily altered with hematite rims and replacement. In many rocks there are only a few flecks of magnetite left. After coating for the microprobe it is difficult to distinguish the magnetite cores from the hematite and most of the oxide analyses have low totals indicating that they are largely hematite. TiO_2 is fairly low. The presence of ilmenite exsolution lamellae in hematised magnetite suggests titano-magnetite original compositions.

Fe oxides in the Farrell Slate(94/2) and Stitt Quartzite (SQ-1) are all hematite with very low TiO_2. Sample 94/41 (Tyndall Group) has a spread in Ti and Fe (Fig. 10) which reflects a titano-magnetite component and an ilmenite component. The spread in Ti among the "ilmenite" is unrealistic given the possible range of Ti at magmatic conditions and is interpreted here as the result of analysing edges of small exsolution patches of ilmenite associated with hematised titano-magnetite. The Mt Cripps sample (94/18) shows similar problems with a large and unrealistic spread in TiO_2 contents, suggesting that oxidised titano-magnetite is the major component (Fig. 11). The freshest Higgins Creek sample (94/5) has two distinct oxide populations (Fig.12), ilmenite and magnetite with scatter between them. These are compatible with a primary detrital grain population of ilmenite and magnetite which is partially hematised.

The observations of oxides in this project have direct implications for magnetic interpretation within the Mt Read Volcanics. Very high magnetite are found in both Tyndall Group rocks (up to 0.8%) and in rocks sourced directly from the Crimson Creek (up to 0.35%). However in many cases these magnetites are extensively hematised and other samples have no relict magnetite. At least for the Tyndall Group rocks this variation appears to be alteration rather than weathering. The very high magnetic signal over the eastern edge of the Mt Read Volcanics has often been linked to Cambrian granite but some of this signature may be the magnetic parts of the Tyndall Group. With variable alteration this can produce highly variable magnetic responses.

Hematite

The irregular form of hematite grains is interpreted here to indicate the hematite is not a primary detrital mineral but replaces the magnetite and possibly ilmenite.

Ilmenite

High ilmenite has been detected in the Crimson Creek Formation, Jukes correlate from the Murchison Gorge, and Higgins Creek. It is not typical of the Tyndall Group where ilmenite is largely found as a minor component due to exsolution and oxidation of original titano-magnetite. Much of this ilmenite could be attributed to the western source (Crimson Creek Formation) but the Jukes correlate is anomalous.

Some ilmenite grains are rounded and are detrital. They are weathered with alteration to TiO_2. The analyses are mainly too low in TiO_2 for ilmenite suggesting there is extensive hematisation of the ilmenites. In many rocks the fine grained patchy hematisation is visible in reflected light.

Rutile, anatase

TiO_2 is a common component in most rocks. Much of this especially in the Tyndall Group, is the result of weathering ilmenite and magnetite. In some samples, rutile is apparently a primary detrital phase. The Animal Creek Greywacke is the best example of this form of TiO_2. The dominance of TiO_2 over FeO in these rocks is best explained by preconcentration of TiO_2 in a weathering profile before erosion. In contrast Tyndall Group and Cycle 1 sandstones show evidence of oxidation after transport.

Garnet

Surprisingly, garnet has not been recognised as major contributor to the heavy mineral suite. This is

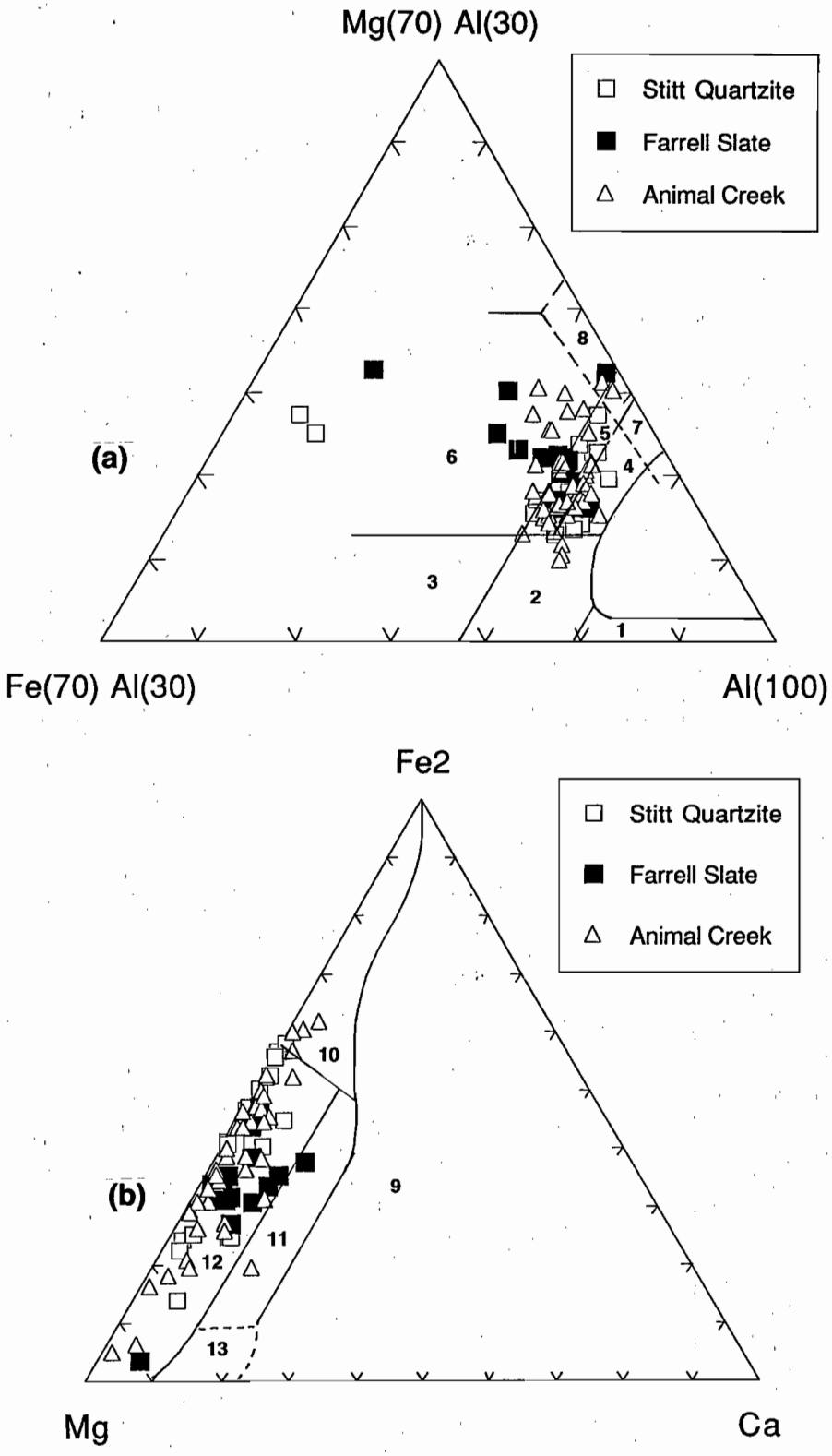

Figure 9. Tourmaline compositions: (a) Mg–Fe–Al and (b) Mg–Fe–Ca. Interpreted fields are from Henry & Guidotti, 1985. Types are 1: Li-rich granitoid pegmatites and aplites, 2: Li-poor granitoids, 3: Fe^{3+} qtz tourmaline rocks (altered granites), 4: Metapelites and metapsammites with coexisting Al-saturating phase, 5: Metapelites and metapsammites without coexisting Al-saturating phase, 6: Fe^{3+} rich quartz-tourmaline rocks, calc-silicates and metapelites, 7: Low Ca meta-ultramafics and Cr, V metasediments, 8: Metacarbonates and meta-pyroxenites (7 and 8 overlap 4 and 5). 9: Li-rich granitoid pegmatites and aplites, 10: Li-poor granitoids, 11: Ca rich metapelites, metapsammites and calc-silicates, 12: Ca poor metapelites, meta-psammites and quartz-tourmaline rocks, 13: Metacarbonates.

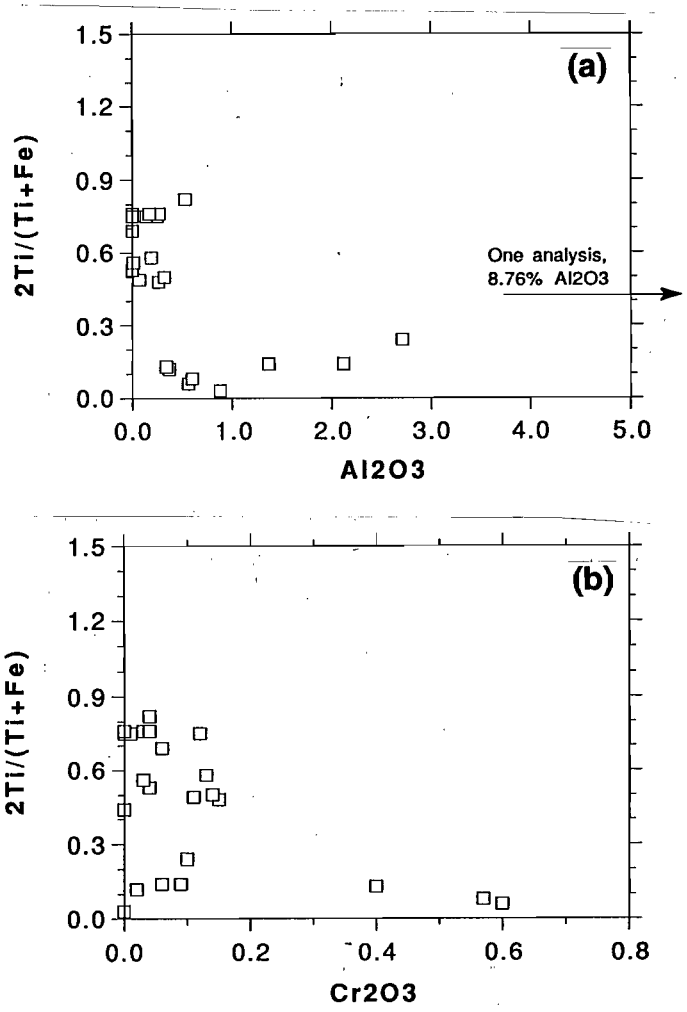

Figure 10. Oxide compositions from sample 94/41 (Tyndall Group). The y axis is a measure of the ilmenite component in an oxide.

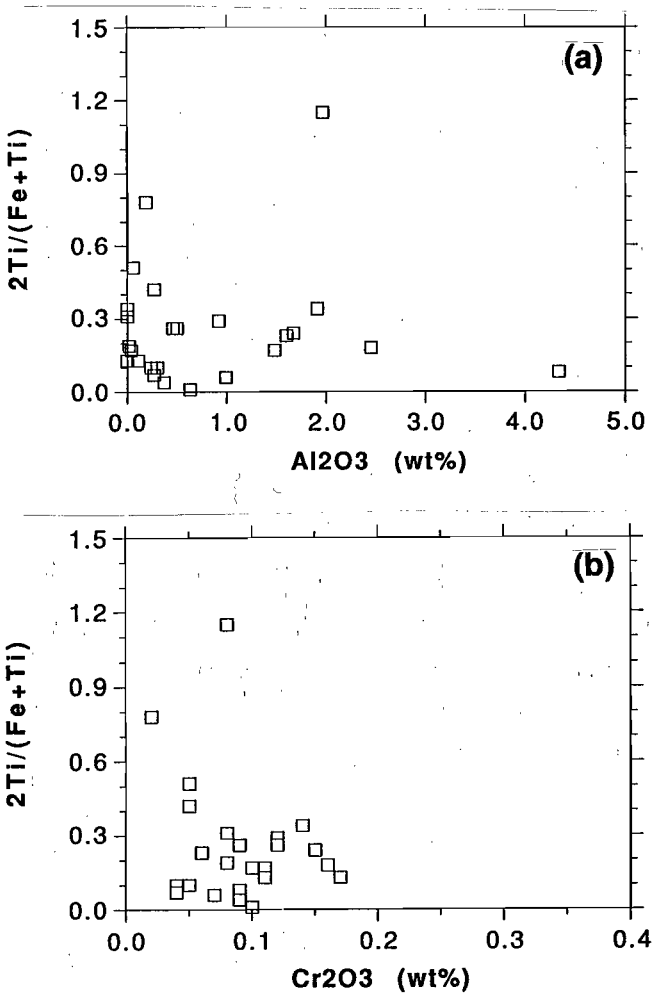

Figure 11. Oxide compositions from sample 94/18 (Mt Cripps Subgroup). The y axis is a measure of the ilmenite component in an oxide.

especially true for the Sticht Range Formation and more samples of this unit are needed to confirm this unexpected result. So far garnet has been recognised as a trace component in four rocks. The two samples of Yolande Group from the Strahan Highway have trace garnet. Sample 94/38 (Fig. 13) garnets have high MgO and low CaO, and are most probably sourced from granulites, but on the margin of the range of garnets from Nye Bay. This unusual, high-MgO-garnet composition has also been found in the Cycle 1 sandstone (94/6).

Another rock which contains garnet is the Crimson Creek Formation (94/24). In this rock the garnets have typical low to middle amphibolite compositions which could be sourced from the Tyennan region. No sources to the west are known but, in the Cambrian, Antarctica occupied this position and may be the source for both types of garnets.

Pyrite

Pyrite is a common heavy mineral. Most of the pyrite is euhedral but a minor proportion is in framboids. The more weathered samples may contain goethite after pyrite (e.g. Higgins Creek 94/7) and this blurs the distinction between Cycle 1 and Cycle 2 sandstones.

A few samples contain chalcopyrite and/or other sulphides.

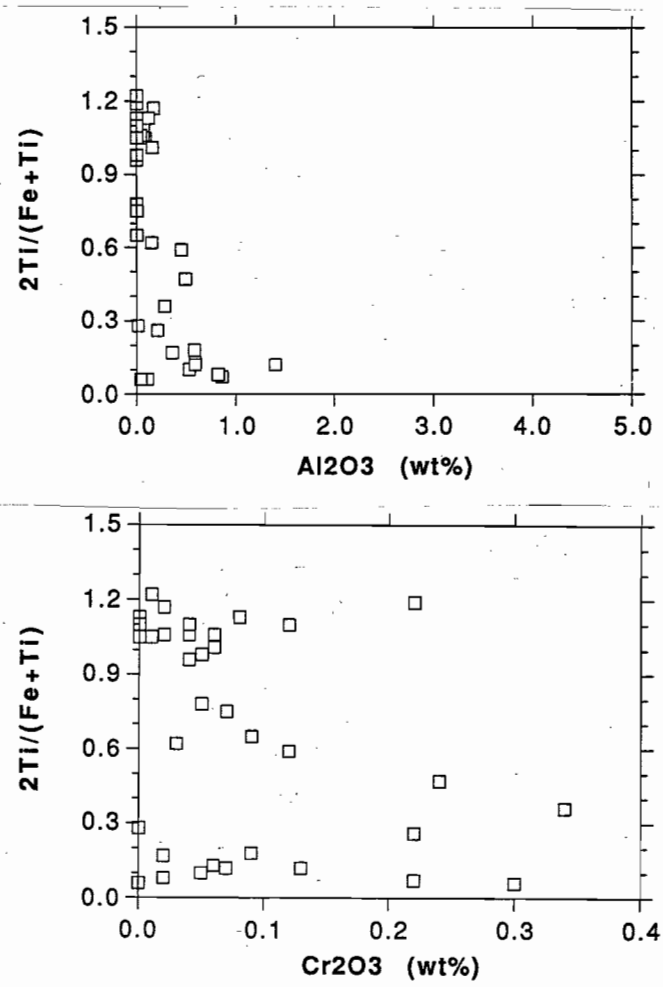

Figure 12. Oxide compositions from sample 94/5 (Higgins Creek) The y axis is a measure of the ilmenite component in an oxide.

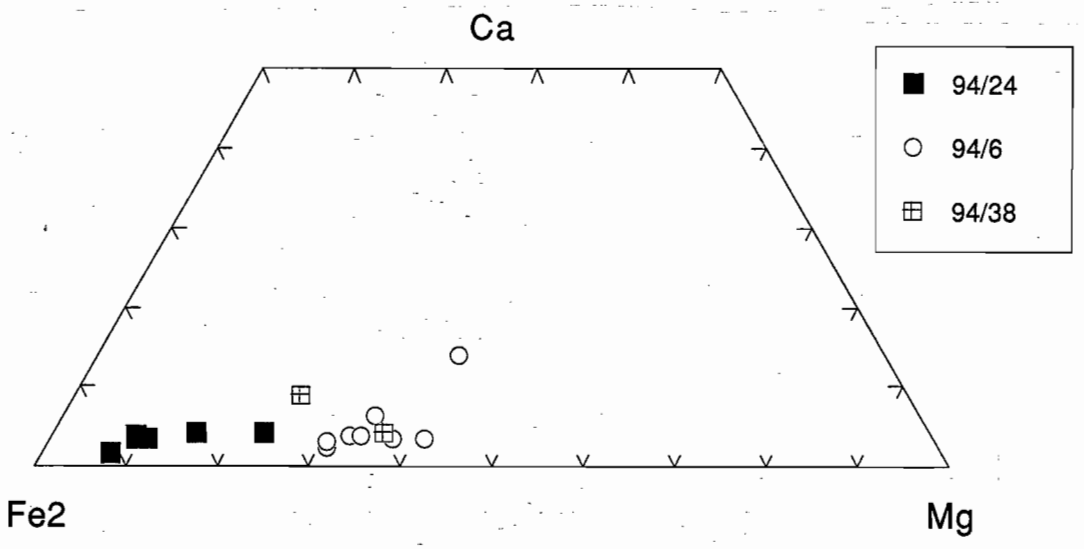

Figure 13. Octahedral components in pyralspite garnet from the Mt Read belt.

SUMMARY

1. The Tyndall Group is distinguished by high Fe oxide contents. These include magnetite, hematite and ilmenite plus the oxidised equivalents. The Tyndall Group samples also contain TiO_2, mostly as anatase where they are weathered, so that these rocks overall have $FeO \approx TiO_2$. The total heavy mineral suite is high, about 1% of sample. The rocks have low zircon and tourmaline, possibly due to dilution effects. On this basis the sample (94/20, ?Jukes Conglomerate) from Murchison Gorge, 7m below the Owen Conglomerate, has typical Tyndall Group heavy minerals with a very high ilmenite content. The high oxide content appears to be typical of all of the Tyndall Group and is not limited to the lower andesitic part.

2. The Animal Creek Greywacke has a distinctive association of high chromite, high TiO_2, very low Fe oxides, high zircon, tourmaline and apatite content. The Animal Creek Greywacke has rounded zircons forming a substantial part of the total zircon suite. Most micaceous sandstones throughout the Mount Read belt carry this signature. This signature is interpreted as a western to northern source from a low relief deeply weathered area with well mixed sources.

3. In contrast the Tyennan region, as exemplified by the Sticht Range Formation is deeply weathered or second cycle, but does not contribute very significantly to the samples analysed so far. At this stage the presence of a high proportion of rounded zircons, greater than 0.2 × chromite (ie greater than the western source), appears to be one of the best indicators of a contribution from the Tyennan source. This signature has not been recognised in other sandstones.

ACKNOWLEDGEMENTS

This project could not have proceeded without the heavy mineral separations carried out by Nilah Hlang. Andrew McNeill, Nathan Duhig and Rohan Hine have contributed extensively to the point counting and microprobe analyses. Their help, often at critical times, was much appreciated.

REFERENCES

Henningsen D 1967. Crushing of sedimentary rock samples and its effect on shape and number of heavy minerals. Sedimentology 8, 253–255.

Henty D J & Guidotti C V 1985. Tourmaline as a petrogenetic indicator mineral: an example from the staurolite grade metapelites of NW Maine. Am. Mineral.

Taylor B E & Slack J F 1984. Tourmalines from Appalachian-Caledonian massive sulfide deposits: Textural, chemical and isotopic relationships. Economic Geology 79, 1703–1726.

Catalog #	Field #	Rock name	Rock description	AMG grid	Locality	Area	Group	Formation/Member
130586	OC1	conglomerate	Immature, chert dominated,	370900E5355700N	Farrell River	Zeehan	Dundas Group	
130587	94/1	sandstone	massive, micaceous, coarse, many shale fragments	387700E5383300N	Lake Mackintosh	Tullah	Farrell Slate	
130588	94/2	sandstone	Med grained, feldspathic, load cast base	387400E5383100N	Mackintosh Spillway	Tullah	Farrell Slate	
130589	94/3	sandstone	laminated, volcanogenic	378400E5385000N	Boco Road	Boco	Central Volcanic Complex	
130590	94/4	sandstone	10-20cm beds in mudstone	376800E5384600N	Boco Road	Boco	Dundas Group	
130591	94/5	sandstone	mica, felds, qtz sst with hematitic veining	375300E5384400N	Boco Road	Boco	Dundas Group	
130592	94/6	sandstone	1-5 cm sst in fine sst - sltst package	375900E5384400N	Boco Road	Boco	Dundas Group	
130593	94/7	sandstone	30cm sst in sst dominated package	376100E5386100N	Boco 10 Spur Road	Boco	Dundas Group	
130594	94/8	sandstone	thin bedded volcanic derived	379300E5385300N	Boco Road	Boco	Dundas Group	
130595	94/9	sandstone	crystal rich with large qtz & coarse lithic fragments	379200E5385300N	Boco Road	Boco	Dundas Group	
130596	94/10	slate		379700E5385400N	Boco Road	Boco	Dundas Group	
130597	94/11	sandstone	micaceous sst within CVC	381100E5385300N	Boco Road	Boco	Central Volcanic Complex	
130598	94/12	sandstone	0.3-1m sst, massive, uniform, no grading or internal strat	384400E5389700N	Animal Ck	Boco	Mount Charter Group	Animal Creek Greywacke
130599	94/13	sandstone	f.g feldspathic sst, looks internally sratified	385500E5389800N	Animal Ck	Boco	Mount Charter Group	Animal Creek Greywacke
130600	94/14	sandstone	weathered	385300E5390300N	Animal Ck	Boco	Mount Charter Group	Animal Creek Greywacke
130601	94/15	sandstone	micaceous, m.g	391000E5398500N	Cradle Mountaint Link Road	Cradle Mountaint Link Road	Mount Charter Group	Animal Creek Greywacke
130602	94/16	conglomerate		397400E5399100N	Cradle Mountaint Link Road	Cradle Mountaint Link Road	Denison Group	Owen Conglomerate
130603	94/17	sandstone	c.g, red matrix	396700E5398700N	Cradle Mountaint Link Road	Cradle Mountaint Link Road	Mount Charter Group	Mount Cripps Subgroup
130604	94/18	sandstone	v. mixed lithic sst, low matrix	395700E5398700N	Cradle Mountaint Link Road	Cradle Mountaint Link Road	Mount Charter Group	Southwell Subgroup
130605	94/19	sandstone	c.g, micaceous sst; grey pebble conglomerate	394700E5398600N	Cradle Mountaint Link Road	Cradle Mountaint Link Road	Mount Charter Group	Southwell Subgroup
130606	94/20	breccia		386300E5376100N	Murchison Gorge	Tullah	Tyndall Group	Jukes Formation
130607	94/21	sandstone	qtz phyric volcaniclastic	387300E5375500N	Murchison Gorge	Tullah	Tyndall Group	Murchison Volcanics
130608	94/22	sandstone	f.g, pale grey, no obvious crystals	375800E5378500N	Pieman Dam Road	Pieman Dam Road	Dundas Group	
130609	94/23	sandstone	matrix rich	367700E5379400N	Merton Road	Merton Hill	Huskisson Group	
130610	94/24	sandstone	m.g with intraclasts	363400E5381300N	Pieman Dam Road	Pieman Dam Road	Crimson Creek Formation	
130611	94/26	sandstone	volcanogenic	375300E5349600N	Quarry at Loftus Hills Memorial	Yolande River	Yolande River Sequence	
130612	94/27	sandstone	less weathered core of micaceous sandstone	375600E5347500N	Zeehan Highway	Yolande River	Yolande River Sequence	
130613	94/28	sandstone	volcanogenic	375600E5346700N	Zeehan Highway	Langdon River	Yolande River Sequence	
130614	94/29	sandstone	m.g volcanogenic	378900E5343000N	Zeehan Highway	Queenstown	Yolande River Sequence	
130615	94/30	sandstone	crystal rich, matrix poor	379000E5337400N	Lynchford Road	Queenstown	Tyndall Group	
130616	94/31	sandstone	c.g crystal rich volcaniclastic	378900E5337800N	Lynchford Road	Queenstown	Tyndall Group	Lynchford Tuff
130617	94/32	sandstone	20 cm thick m.g volcanogenic sst	378000E5337800N	Lynchford Road	Queenstown	Tyndall Group	
130618	94/33	sandstone	qtz-feld crystal rich, sericite altered	379500E5331000N	Lynchford Road	King Power Station	Yolande River Sequence	
130619	94/34	sandstone	10cm sst in slates	380400E5330200N	Mt Jukes Road	Mt Jukes	Central Volcanic Complex	
130620	94/35	sandstone	largely vcc	382300E5331500N	Mt Jukes Road	Mt Jukes	Central Volcanic Complex	
130621	94/36	sandstone	v.c.g crystal rich lithic sst, slightly altered and cleaved	383800E5330600N	Mt Jukes Road	Jukes Pty	Eastern Quartz-Phyric Sequence	
130622	94/37	sandstone	v massive, c.g, crystal lithic sst, pebbly in part, cleaved	384600E5330300N	Mt Jukes Road	Jukes Pty	Tyndall Group Correlates	
130623	94/38	sandstone	1m massive, lithic sst, no visible grading,i/bdd with sltst	368400E5329700N	Lyell Highway	Four Mile Creek	Yolande River Sequence	
130624	94/39	sandstone	f.g sst 1m thick	366200E5332800N	Lyell Highway	Four Mile Creek	Yolande River Sequence	
130625	94/40	sandstone	i/bdd pebbly sst and sst	367500E5348600N	Road to Queensberry Mine	Professor Range	Yolande River Sequence	
130626	94/41	sandstone	chlorite, magnetite altered	387600E5341100N	Old Lyell Hwy, E end Linda Valley	Linda Valley	Tyndall Group	
130627	94/42	sandstone		388300E5369925N	Lake Murchison	Tullah	Sticht Range Beds	
130628	SQ1	quartz sst		377250E5375300N	Rosebery	Rosebery	Stitt Quartzite	
130629	SQ2	quartz sst		377300E5375310N	Rosebery	Rosebery	Stitt Quartzite	

Provenance of middle to late Cambrian polymict conglomerates of the Dundas Group

David Selley

Centre for Ore Deposit and Exploration Studies, Geology Department, University of Tasmania

ABSTRACT

Samples of coarse sandstone and fine conglomerates were collected from the Que River at the western margin of the Dundas stratigraphy and from the Dundas Group in the Dundas area. Detailed petrographic analysis of these rocks demonstrated that these coarser sediments were derived from the western margin of the basin (Crimson Creek Formation, Success Creek Group, Oonah Formation). This source was a major contributor to the deposition throughout the Middle and Late Cambrian. The CVC and Tyndall Group have a very minor contribution mainly in a few discrete volcaniclastic units.

INTRODUCTION

Source areas for sedimentary sequences within the Middle to Late Cambrian Dundas Group are poorly constrained for several reasons: (1) paucity of palaeocurrent indicators, (2) lack of extensive, fresh exposure, (3) poor knowledge of detrital composition and (4) complexity of the palaeogeography at the time of deposition. Although an eastern source (Mt Read Volcanics) is indicated from rapidly resedimented pyroclastic material within the late Middle Cambrian portion of the succession (Bull, this report), these deposits comprise only a small proportion of the stratigraphy. The bulk of the stratigraphic section is dominated by fine to coarse grained epiclastic sediments. Previous studies on the composition of these latter sediments have focused upon field description of clast lithotypes within conglomerate facies (e.g. Brown, 1986; Selley 1994). Although several important detrital components have been identified in these descriptions (eg. igneous fragments derived from the mafic-ultramafic complexes (MUC), basement-derived Precambrian quartzites), the bulk composition of these sediments remains poorly understood.

Recent studies of Cambrian fault geometries in western Tasmania suggest that the western margin of the Dundas Group was controlled by a N–S trending growth fault (Berry and Keele, 1993). This interpretation is based upon data from balanced cross sections (Rattenbury, 1990; Selley, 1992) and stratigraphic variations within the Middle to Late Cambrian succession (Berry and Keele, op. cit.). In order to test this hypothesis, samples have been collected for a petrographic study of detrital components from exposures which lie close to this proposed growth fault. Sampled formations involve several levels of the stratigraphy, ranging in age from mid Middle to Late Cambrian and occur in two regions. Lithologies from the Dundas region provide data adjacent to the southern extension of the proposed growth fault, while to the northern samples were collected from the western-most exposures of the Dundas Group in the Que River section.

The mapping and regional data reported here were collected for my PhD program outside the AMIRA project. The detailed petrographic data work reported here was carried specifically as part of the AMIRA project.

DUNDAS REGION

The type section of the Dundas Group, as defined by Elliston (1952), crops out in the Dundas River as a SW-facing, turbidite-dominated succession totalling about 2200 m in thickness (Fig. 1a). Packages involved in this study contain a very distinctive polymict

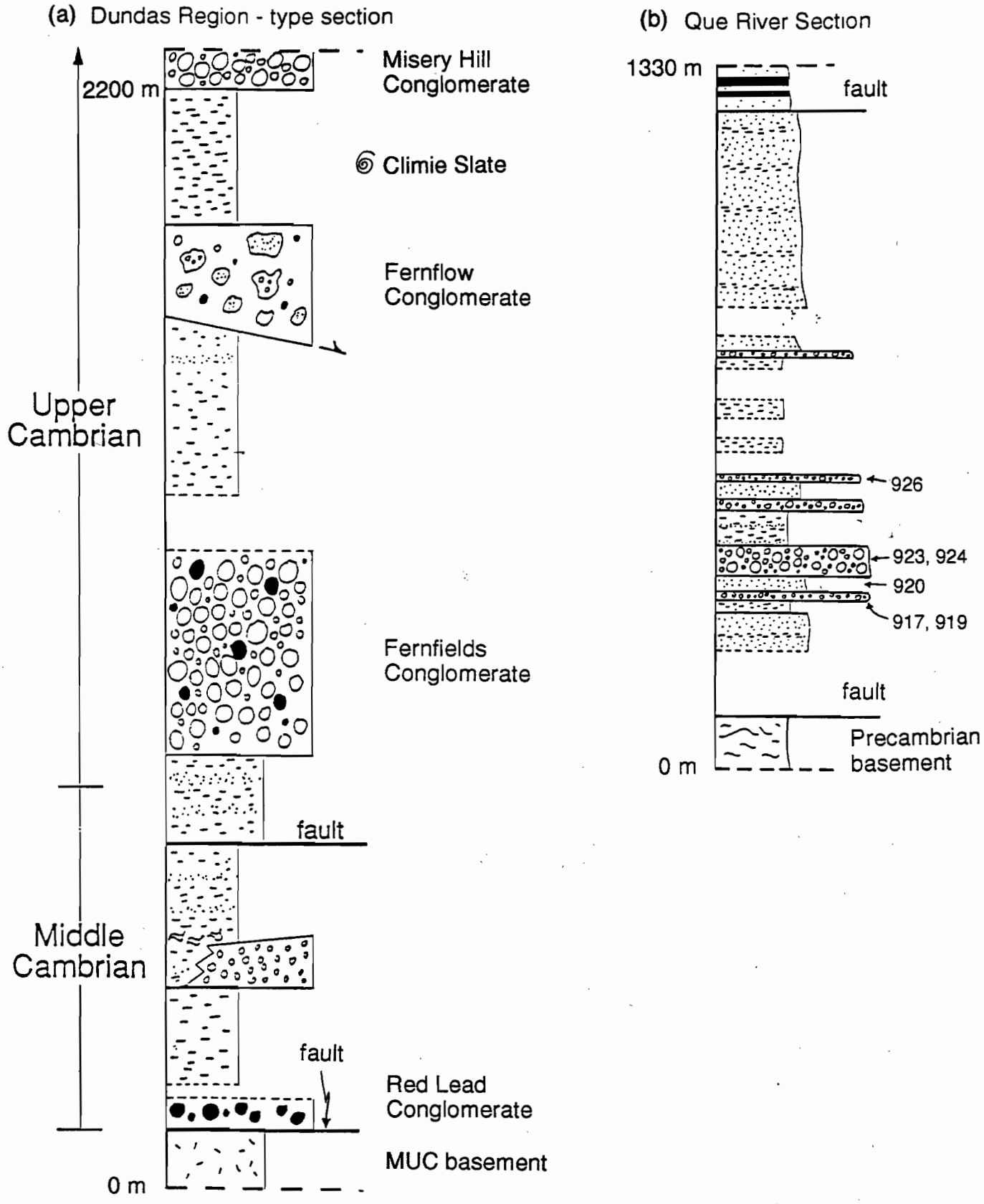

Figure 1. Stratigraphic columns for (a) Dundas region, (b) Que River section.

conglomerate facies which appears at three levels within the stratigraphy: Red Lead (RLC), Fernfields (FC) and Misery Hill Conglomerates (MHC). Although no datable fossils have been collected from these three conglomerates, age constraints can be derived from faunas in bounding mudstone-dominated sequences. These fossils indicate a middle Middle Cambrian age for the RLC, early Late Cambrian age for the Fernfields Conglomerate, and mid-late Late Cambrian age for the Misery Hill Conglomerate.

A similar depositional style is recognised in each of these conglomeratic packages which are characterised by thick, amalgamated beds of granule to pebble, framework-supported conglomerate intercalated with massive and normally graded lithic-rich sandstone and massive to delicately laminated mudstone. Conglomerate horizons exhibit tabular geometries with planar, or less common broadly channellised bases and crude internal stratification. Clasts are well rounded indicating erosion and reworking of source material in a fluvial or shallow marine environments. Facies associations are consistent with below wave-base deposition, probably in the upper or middle portions of submarine fans.

Additional facies types are associated with correlates of the basal Red Lead Conglomerate exposed in the Ring River. Towards the base of this section (Fig. 2a), coarse breccias and a thick unit of mud-supported conglomerate occur as fault bounded blocks or as lensoidal bodies within the framework-supported conglomerate facies. Breccia units are disorganised, generally matrix-poor and comprise angular blocks of gabbro and basalt derived from the MUC. They most probably represent talus breccias accumulating at the base of a fault scarp. The open framework conglomerate contains fragments and blocks of partially to totally disaggregated talus breccia, framework-supported conglomerate and mudstone, supported in a matrix of mud or fine sand. The close association of 'normal' Red Lead Conglomerate facies types with these mass failure deposits clearly indicates that sedimentation has occurred in an tectonically active environment characterised by fault scarps and/or unstable slopes.

Similar mass failure deposits are recognised from the Upper Cambrian portion of the succession in the Dundas River (Fernflow Conglomerate; Fig. 2b). Although this package is not included in the petrographic study due to its highly weathered nature, a brief discussion here is considered useful. It consists of approximately 130 m of intercalated pebbly mudstone, structureless mudstone and rare units of framework-supported pebble conglomerate. Bedding readings vary significantly both within the package and from the more coherently stratified bounding sequences. The base is defined by a layer parallel shear zone approximately 10 m in thickness which is sharply overlain by a crudely stratified unit folded into a large recumbent syncline. Ductile disaggregation of sandy layers within the fold hinge indicate that deformation took place while the sediment was unlithified. The disorganised nature of the package and the presence of local zones of soft sediment deformation suggest that the entire package was deposited as a slide sheet (or series of sheets). The geometry of the syncline towards the base (with the effects of the Devonian folding removed) indicates an ESE transport direction. These observations support the more general data above and are significant in terms of the provenance discussion below.

QUE RIVER SECTION

The western-most portion of the Dundas Group in the Que River comprises an E-facing, fault-bounded package dominated by turbiditic, lithic-rich sandstone and mudstone (Fig. 1b). The thickness of this package is approximately 1100 m. In many cases, A, B, D and E divisions of the Bouma sequence are preserved within individual units. In the lower portion of the succession, granule to cobble grade, polymict conglomerate occur, which are up to 15 m in thickness. These units become thinner and less common higher in the stratigraphy. Conglomerate units may show subtle normal grading, but are otherwise unstratified and commonly grade upward into massive lithic-rich sandstone. Their bases are generally planar and exhibit little evidence of channelling.

Although no fossils are reported from the Que River section, the succession appears to be structurally continuous towards the south, where a post-Idamean (Late Cambrian) fauna is described at Higgins Creek (Jell et al., 1991). Lithologies at this location are comparable with those mapped in the Que River, hence a Late Cambrian age is tentatively placed on the latter. Post Idamean fossils are also described from the Climie Slate in the Dundas Region (Jago, 1978; Fig. 1a) and provide a time line between the northern and southern successions. Chrono-stratigraphic equivalents of the coarse grained facies in the Que River are therefore likely to include Late Cambrian sequences in the type section of the Dundas Group (i.e. Fernfield through to Misery Hill Conglomerates).

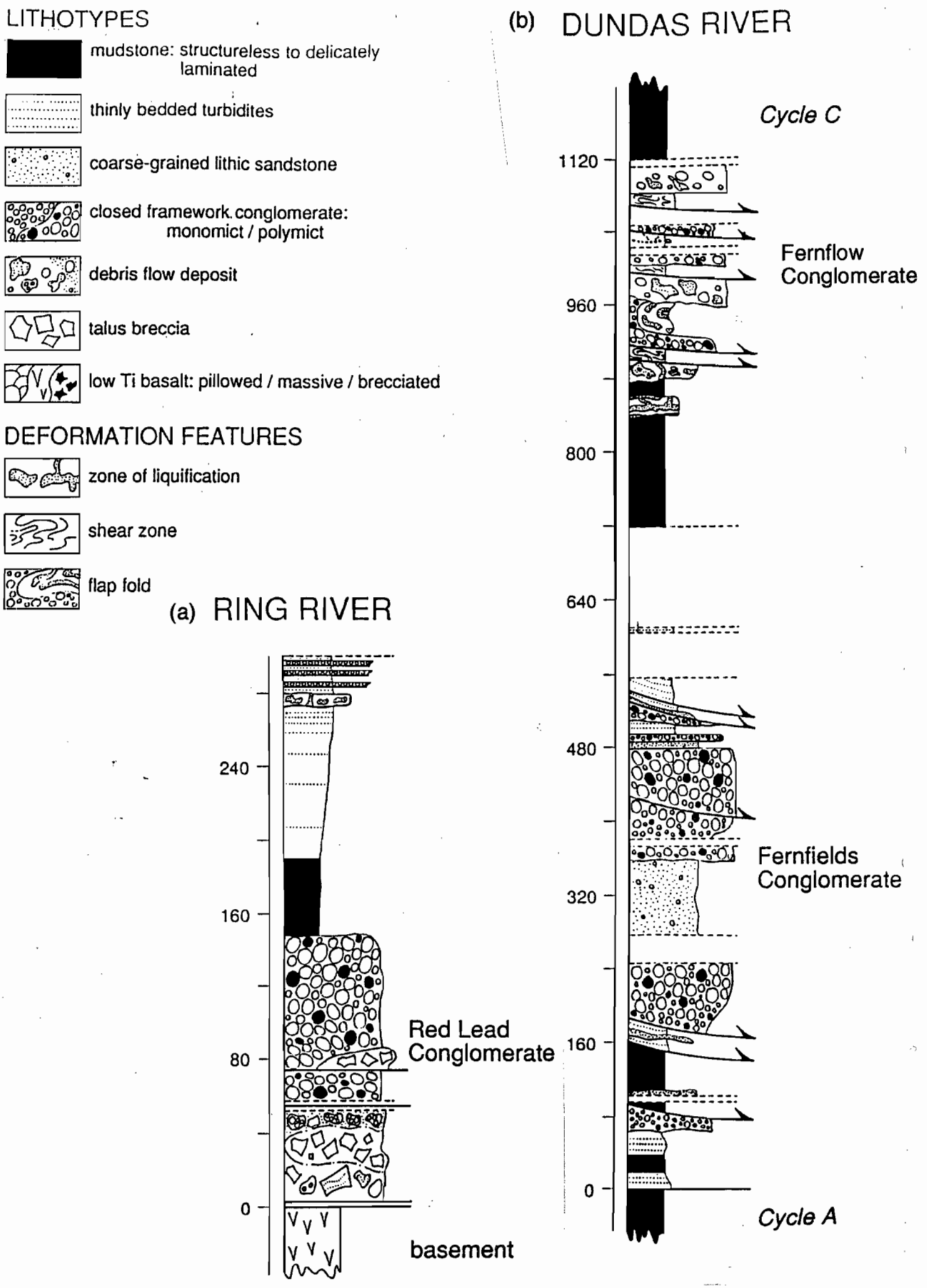

Figure 2. Stratigraphic positions of mass-failure deposits: (a) RLC correlate in the Ring River, (b) Fernflow conglomerate in Upper Cambrian portion Dundas River section.

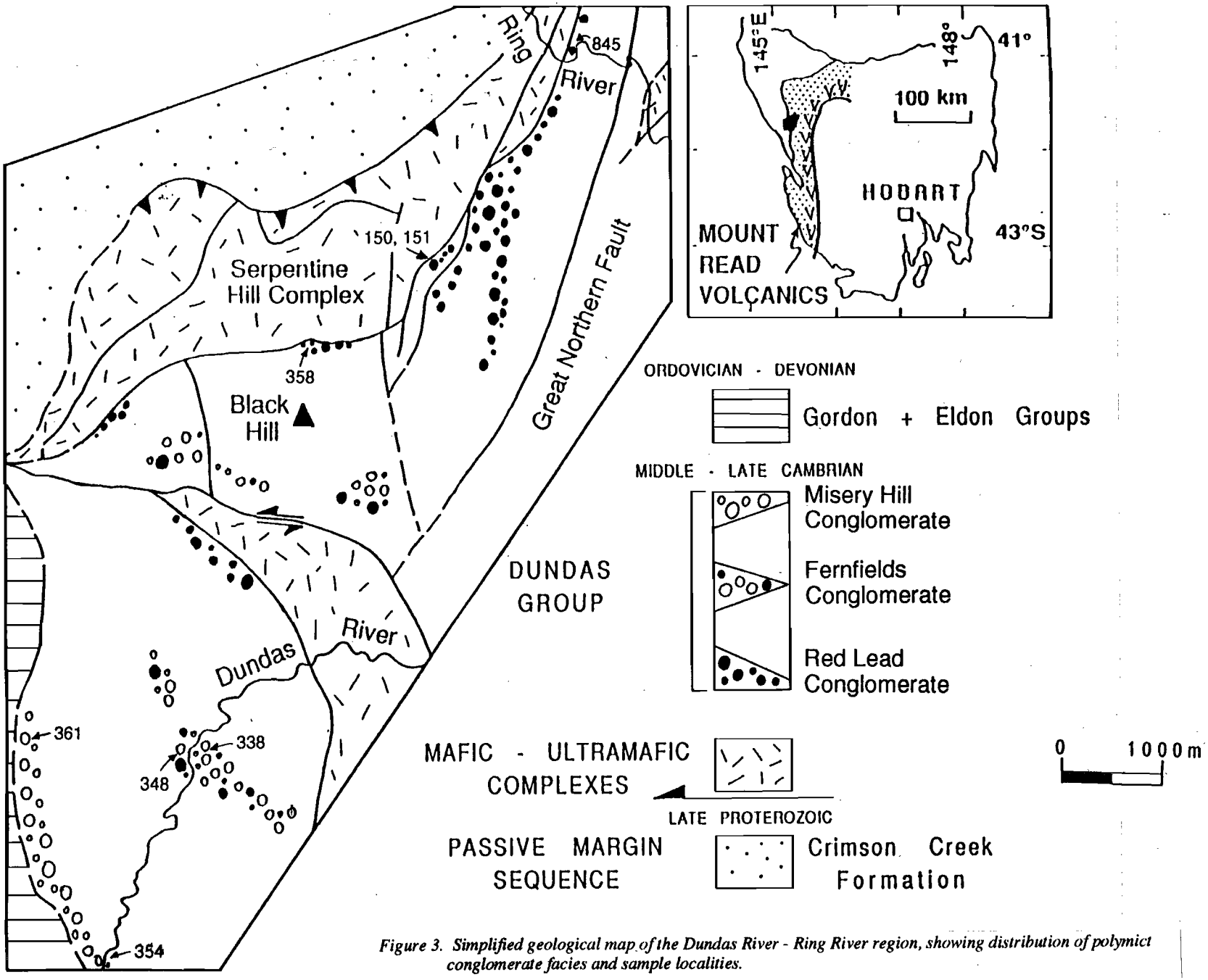

Figure 3. Simplified geological map of the Dundas River - Ring River region, showing distribution of polymict conglomerate facies and sample localities.

PETROGRAPHIC ANALYSIS

Detailed petrographic analysis involving a minimum of 380 counts per thin section, was carried out on 14 samples from each of the turbiditic packages. Six of these come from the lower portion of the Que River section (QRS), four from correlates of the Red Lead Conglomerate, two from the Fernfields Conglomerate, and two from the Misery Hill Conglomerate. Detrital modes for each sample along with averages and standard deviation for each of the packages are presented in Tables 1 and 2. Modal point counts and codes used in describing components are shown in Tables 3 and 4 respectively.

Due to the lithic-rich nature of the medium to coarse grained lithologies, special emphasis was placed on distinguishing and characterising the various types of rock fragments. In order to identify lithics with confidence, coarse grained sandstones and granule conglomerates were required. Thus poorly stratified A and B intervals of the Bouma sequence with thicknesses generally in excess of 2 m (thicker beds ensure more complete mixing of detrital components) provided the bulk of the sample selection.

A QFL plot (Fig. 4a) of the framework component shows close grouping of data from all packages and confirms the lithic-rich character of the rocks. In most samples, lithic rock fragments comprise 75–98 modal% , although one from the Red Lead Conglomerate and another from the Misery Hill Conglomerate appear considerably richer in quartz (Table 2). Apart from two samples mentioned above, quartz is present in relatively low abundances (< 1–10 modal%). It occurs most commonly as angular to subrounded monocrystalline grains with mild to intense undulose extinction (Qm). Rare grains show exhibit straight extinction and crude hexagonal habits. Although they superficially resemble grains of volcanic origin, in only one example were embayments, typical of resorbed volcanic quartz phenocrysts, clearly developed (Qi?). Feldspar occurs in roughly similar proportions to quartz in most packages (<1% – 8%) except Misery Hill Conglomerate, where it is absent.

Lithic fragments are initially subdivided into 'metamorphic', 'igneous' and 'sedimentary' categories (Fig. 4b). Fragments whose origins are unresolvable due to intense weathering, silicification or carbonate alteration are omitted from this subdivision. Their proportion of the framework component varies from 3% to 20% .

'Metamorphic' fragments comprise <1% to 3% of the detrital component in Red Lead Conglomerate, Fernfields Conglomerate and Que River section, and average 15 modal% in Misery Hill Conglomerate. The most common sub-category in all packages is metaquartzite (RMq; Fig. 4d). Fragments of this type involve relatively well sorted quartz grains, commonly with undulose extinction and sutured margins, set in a fine grained matrix of silica and white mica. Quartz-mica schist (RMqs) fragments consist of aligned, elongate grains of strained quartz and very fine muscovite, and occur as minor populations in all packages except Fernfields Conglomerate. Mylonitic quartzite (RMqm) occurs in only one Misery Hill Conglomerate sample and involves highly strained quartz porphyroclasts enclosed within a mosaic of recrystallised fine grained quartz.

'Igneous' fragments range from ?ultramafic to intermediate in composition and constitute between 4 (Misery Hill Conglomerate) and 24 (Red Lead Conglomerate) modal %. Clasts are generally well rounded and include gabbro, dolerite, diorite and basalt, with only the latter recognised in Misery Hill Conglomerate. Coarse grained fragments show slight to intense alteration, with replacement of columnar feldspar by sericite + calcite, and ferromagnesians by chlorite, and less commonly actinolite. Basaltic fragments contain rare feldspar phenocrysts, set in a groundmass of randomly or flow aligned microlitic feldspar and chlorite. They are occasionally vesicular and commonly exhibit spherulitic textures enclosed within a formerly glassy groundmass. Some fragments are completely replaced by fibrous chlorite (RCl) a few of which show subtle 'meshwork textures' similar to those developed in serpentine. Opaque Fe-oxides, and less commonly chromite occur as minor phases in many of the clasts.

'Sedimentary' fragments constitute approximately half of the framework component in all packages (48–63 modal%; Fig. 4b) and between 64% to 88% of the total resolvable lithic fraction (Table. 1). Sandstones are subdivided on the basis of their lithic content and relative proportions of quartz and feldspar. Although clean, quartz-rich and arkosic sandstones and silts (RQ, RA, RSq) occur conspicuously (15 modal%) in two samples (Red Lead Conglomerate: 358, Misery Hill Conglomerate: 361), they are subordinate to greywackes in all packages except Misery Hill Conglomerate (Fig. 4d). Quartz-rich sandstones consist of moderately well sorted, subrounded grains of low-strained quartz and rare chert, set in a quartz-sericite argillaceous matrix. Detrital muscovites occur up to 30 μm in width. Silty equivalents may possess a carbonate-rich matrix, and occasionally exhibit evidence of (?soft sediment) deformation. Greywackes and their fine grained equivalents exhibit feldspar-through to quartz- dominated compositions (RGSf–RGSqf–RGq). Feldspathic varieties are most abundant in Red Lead Conglomerate (24 modal%), Fernfields Conglomerate (37 modal%) and Que River section (40 modal%), but are absent within Misery Hill

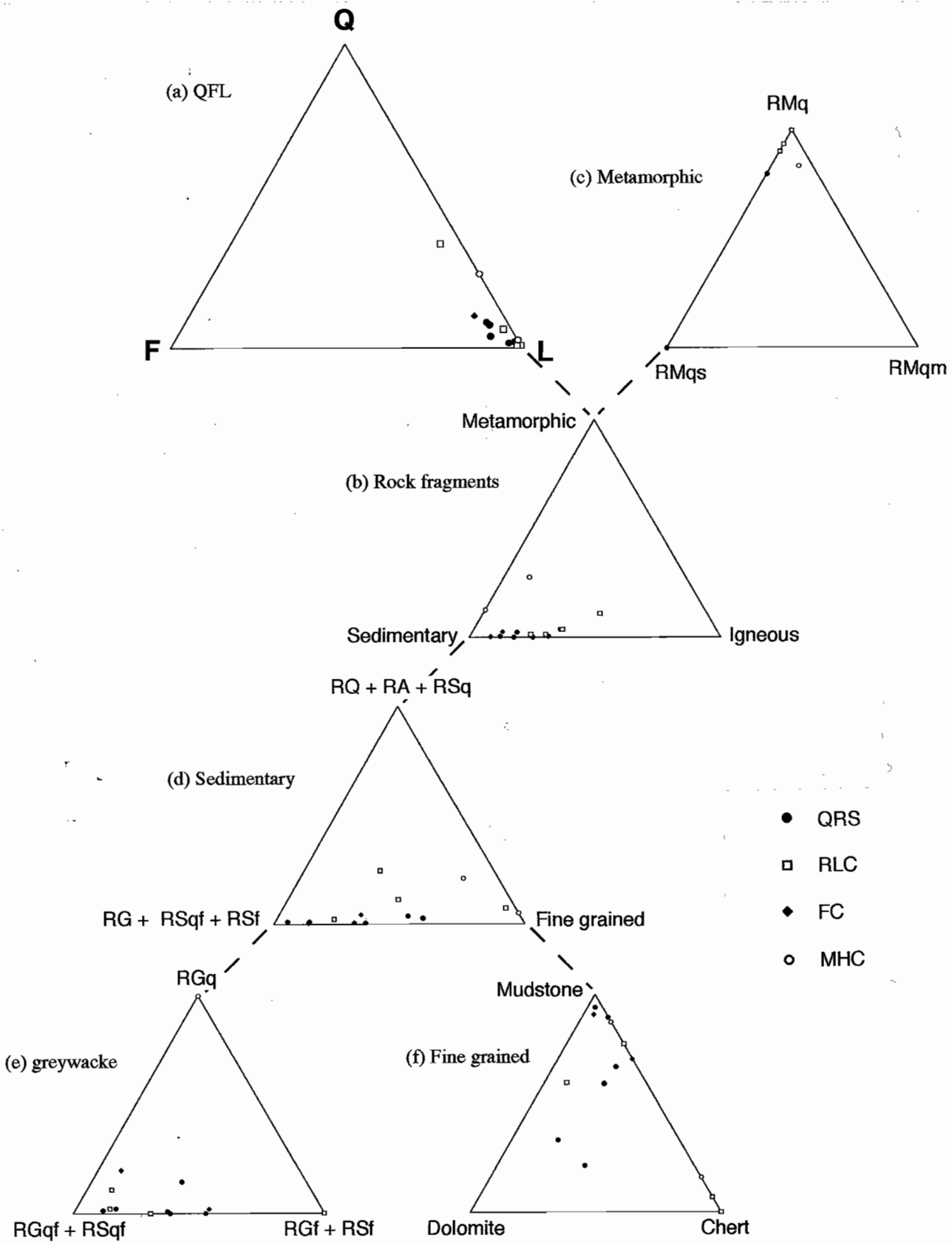

Figure 4. QFL plot and classification of the lithic component

Conglomerate (Fig. 4e). The most feldspathic end-members consist almost entirely of mafic to intermediate volcanic detritus and are characterised by angular grains of twinned feldspar, basalt fragments, chlorite-altered glassy fragments and opaques, set in a matrix of broken feldpar crystals. Basaltic fragments contained within these greywackes are texturally akin to those within the framework. Greywacke fragments are usually weathered and contain a haematitic cement, however a cloudy green chloritic groundmass is preserved in a few fresh clasts. As the quartz content increases, chert fragments and very coarse detrital muscovite are included within the framework component of the clasts. Quartz grains are texturally analogous to those within quartz-rich sandstone clasts.

Mudstone, chert and dolomite are grouped into a 'Fine-grained sediment' category. Clasts of this type comprise 15–20 modal% in Red Lead Conglomerate, Fernfields Conglomerate and Que River section, and average 44 modal% in Misery Hill Conglomerate. Mudstones are well rounded and most commonly deep red-brown in colour due to haematite staining. Dolomite is not recognised in Misery Hill Conglomerate and generally occurs rarely (<1–5 modal%) throughout the remainder of the packages. Two samples from Que River section however, show anomalously high populations of 12 modal%. Silicified oolitic textures are preserved in a few clasts. Chert occurs as both massive and laminated varieties and may be either grey or red in colour.

Accessory detrital minerals within Red Lead Conglomerate, Fernfields Conglomerate and Que River section include muscovite, chlorite, clinopyroxene and magnetite. Chromite is recognised in Red Lead Conglomerate and Que River section as both minor phases within chloritised igneous fragments and detrital grains within the matrix.

DISCUSSION OF LIKELY SOURCE REGIONS

Petrographic and modal analyses indicate gross consistency of sandstone compositions within Red Lead Conglomerate, Fernfields Conglomerate and Que River section. This is significant as it implies that similar source regions were active during both the mid Middle Cambrian and Late Cambrian. Sources are therefore of pre-mid Middle Cambrian age. The relatively unchanged proportions of quartz and feldspar within these packages suggests that the bulk composition of the source was not influenced by the introduction of siliciclastic and felsic volcaniclastic detritus during the late Middle Cambrian (LMC). The sediments do not appear to be affected by the wide variation in felsic volcanic activity which is recognised to the east in the Middle Cambrian but was not active during the Late Cambrian.

Large populations of volcaniclastic greywacke and igneous fragments within Red Lead Conglomerate, Fernfields Conglomerate and Que River section indicate that the bulk of the detritus contained within these packages is derived from one or more volcano-sedimentary sources. The high proportion of basaltic fragments, both within the greywacke clasts and the framework (Table. 1) is suggestive of a predominantly mafic composition. Additional, although relatively minor sources are required for the metamorphic and quartz sandstone clasts, and the more highly strained framework quartz grains. Taking into account these compositions and the absence of a clear CVC source, detritus is considered to be derived from a western 'basement' terrain. Lithologies contained within the Crimson Creek Formation (CCF) and underlying Success Creek Group (SCG) are consistent with many of the rock fragments. Felspathic greywackes, dolomite, mafic to intermediate volcanic and intrusive rocks are all characteristic of the Crimson Creek Formation (Patterson, 1979). Although Patterson indicates that quartz is uncommon in the Renison Mine sequence, correlates of the Crimson Creek Formation in the Pieman River exhibit abundant angular quartz, most probably derived from the Success Creek Group. Conspicuous abundances of deep red chromite (within Red Lead Conglomerate, Que River section; table. 3), both as a phenocrystal component in igneous fragments and as detritus within the framework of the sandstones suggests a source from either Crimson Creek Formation or MUC volcanics. Inclusion of MUC-derived talus breccias within the Red Lead Conglomerate (Ring River section) clearly indicates that the MUC acted as a local source during the mid Middle Cambrian.

Material derived from the Success Creek Group may include silicified oolitic dolomite, which has been reported from Nos. 2 and 3 dolomite (Newnham, 1975), and observed by the author as fragments within conglomerates of the Red Rock Member. Clasts of micaceous quartz sandstone and siltstone, and chert may have originated from portions of the Success Creek Group or Oonah Formation.

The overwhelming evidence from this study is that the western source terrane was exposed and actively eroding material throughout the history of the Dundas Group. In contrast the CVC and Tyndall Group were at most minor components for the conglomerates although a few volcaniclastic units probably are source from the east.

REFERENCES

Berry RF and Keele RA, 1993. Cambrian structure in western Tasmania. AMIRA P291 Report 5, 55–68.

Brown AV, 1986. Geology of Dundas–Mt Lindsay–Mt Youngbuck Region. Geol. Surv. Tasm. Bulletin 62.

Elliston JN, 1954. Geology of the Dundas district, Tasmania. Pap. Proc. R. Soc. Tasm. 88, 161–183.

Jago JB, 1978. Late Cambrian fossils from the Climie Formation, western Tasmania. Pap. Proc. R. Soc. Tasm. 112, 137–153.

Jell PA, Hughes NC, & Brown AV, 1991. Late Cambrian (post-Idamean) trilobites from the Higgins Creek area, western Tasmania. Mem. Queensland Mus. 30, 455–485.

Newnham LA, 1975. Renison Bell tinfield. Mon. Ser. Australas. Inst. Min. Metall. 1, 1006–1008.

Patterson Dj, 1979. Geology and mineralisation at Renison Bell, western Tasmania. PhD thesis, Univ. of Tasmania.

Rattenbury MS, 1990. Palaeozoic fault kinematics and a balanced cross section through the Husskisson–Que–Hellyer–Mackintosh region. AMIRA P291 Report 1, 1–16.

Selley D, 1992. A structural section through the Boco Road area. AMIRA P291 Report 4, 39–50.

Selley D 1994. Depositional cycles of the Dundas Group. P291a Second report October 1994, p41–45.

Table 1. Classification of lithic component. Av100 = proportions within each catagory.

	Que River Conglomerate									Red Lead Conglomerate							Fernfields Conglomerate					Misery Conglomerate				
	917	919	920	923	924	926	Av	SD	Av100	845	150	151	358	Av	SD	Av100	338	348	Av	SD	Av100	361	354	Av	SD	Av100
QFR																										
Qtot	0.77	1.80	2.06	6.96	8.12	3.64	3.89	3.00	4.19	6.00	0.68	30.94	0.79	9.60	14.44	10.38	9.81	1.84	5.83	5.64	6.30	2.53	22.53	12.53	14.14	13.27
F		2.84	0.77	5.15	5.84	5.97	3.43	2.62	3.70	2.13	0.17	5.23	1.06	2.15	2.21	2.32	7.48	1.32	4.40	4.36	4.76					
Rtot	97.44	91.24	88.69	78.35	80.96	76.10	85.46	8.31	92.11	84.53	95.60	52.94	89.97	80.76	19.09	87.30	75.23	89.21	82.22	9.88	88.94	94.18	69.62	81.90	17.36	86.73
ROCK FRAGMENTS																										
RMtot	0.26	1.55		0.26	2.54		0.77	1.04	1.05	2.90	1.18	4.58	1.06	2.43	1.66	3.28		1.84	0.92	1.30	1.29	10.89	18.48	14.68	5.37	19.4
Rsedtot	72.63	59.54	66.84	42.01	44.92	49.61	55.93	12.38	76.48	51.64	60.91	17.86	60.95	47.84	20.46	64.62	51.17	74.21	62.69	16.29	87.73	73.92	41.27	57.59	23.09	76.09
Rltot	9.97	13.14	14.40	19.07	25.13	16.88	16.43	5.28	22.47	29.98	26.23	19.61	19.26	23.77	5.24	32.10	4.91	10.79	7.85	4.16	10.98		6.84	3.42	4.83	4.515
OMITTED ROCK FRAGMENTS (RF,Rsil,RCa,Rop)																										
Total	14.58	17.01	7.46	17.01	8.38	9.61	12.34	4.37			7.28	10.89	8.71	6.72	4.72		19.16	2.37	10.76	11.87		9.37	3.04	6.20	4.48	
METAMORPHIC																										
RMq	0.256	1.546			2.03		0.639	0.909	83.35	2.708	1.184	4.139	1.055	2.272	1.454	93.52		1.842	0.921	1.303	100	10.89	15.44	13.16	3.222	89.66
RMqs				0.258	0.508		0.128	0.213	16.65	0.193		0.436		0.157	0.207	6.475							1.013	0.506	0.716	3.448
RMqm																							2.025	1.013	1.432	6.897
IGNEOUS																										
Rlga	1.79	6.70	4.11	0.52	1.02	2.34	2.75	2.30	16.71	0.58				0.15	0.29	0.61	1.17	2.63	1.90	1.03	24.21					
Rldo		1.80	1.80	1.03	1.78	4.94	1.89	1.65	11.51	15.47	0.51		0.53	4.13	7.57	17.36	0.93	2.63	1.78	1.20	22.72					
Rldi	0.26			0.77		1.30	0.39	0.54	2.36	2.71	5.58			2.07	2.67	8.72										
Rlb	6.65	2.58	6.17	7.47	15.48	3.90	7.04	4.52	42.85	10.83	18.10	15.03	7.12	12.77	4.80	53.74	2.57	5.26	3.92	1.90	49.91		5.57	2.78	3.94	81.48
Rlg	1.28	2.06	0.77	4.12	3.55	3.90	2.61	1.43	15.91	0.39	1.86	4.58	1.06	1.97	1.84	8.29	0.23		0.12	0.17	1.49					
RCl			1.54	5.15	3.30	0.52	1.75	2.08	10.67		0.17		10.55	2.68	5.25	11.28		0.26	0.13	0.19	1.68		1.27	0.63	0.90	18.52
SEDIMENTS																										
Rsand	0.51	0.52	0.26	0.26	1.27	1.82	0.77	0.63	1.38	5.80	1.35	1.31	15.04	5.88	6.46	12.28	0.23	3.16	1.70	2.07	2.71	15.44	2.03	8.73	9.49	15.16
Rgrey	62.15	55.93	57.58	26.55	17.51	22.08	40.30	20.30	72.06	23.21	45.69	0.65	27.44	24.25	18.51	50.68	34.58	46.58	40.58	8.48	64.73	10.38		5.19	7.34	9.011
Rfines	9.97	3.09	9.00	15.21	26.14	25.71	14.85	9.40	26.56	22.63	13.87	15.90	18.47	17.72	3.78	37.04	16.36	24.47	20.41	5.74	32.56	48.10	39.24	43.67	6.27	75.82
GREYWACKES																										
RGq	1.535	0.773		0.258	2.538		0.85	1.01	2.111	2.515	1.015			0.88	1.19	3.639	6.776	0.789	3.78	4.23	9.321	7.848		3.92	5.55	100
RGSqf	50.9	48.97	35.48	16.49	8.629	10.39	28.48	19.16	70.66	18.38	38.58		19	18.99	15.76	78.31	24.53	20.79	22.66	2.65	55.84					
RGSf	9.719	6.186	22.11	9.794	6.345	11.69	10.97	5.86	27.23	2.321	6.091	0.654	8.443	4.38	3.54	18.05	3.271	25	14.14	15.36	34.83					
FINES																										
RMudt	8.951	2.062	8.483	9.021	5.584	8.571	7.11	2.79	47.88	1.547	8.291		14.25	6.02	6.56	33.98	11.45	22.11	16.78	7.54	82.18	42.03	6.329	24.18	25.24	55.36
RDol,oo		0.26	0.26	2.58	11.42	12.47	4.50	5.85	30.27		4.40			1.10	2.20	6.207		1.32	0.66	0.93	3.223					
RCh	1.023	0.773	0.257	3.608	9.137	4.675	3.25	3.37	21.85	21.08	1.184	15.9	4.222	10.60	9.44	59.81	4.907	1.053	2.98	2.73	14.6	6.076	32.91	19.49	18.98	44.64

Table 2. Modal%, mean and standard deviation for detrital components.

	Que River Conglomerate								Red Lead Conglomerate						Fernfields Conglomerate				Misery Conglomerate			
	917	**919**	**920**	**923**	**924**	**926**	**Av**	**SD**	**845**	**150**	**151**	**358**	**Av**	**SD**	**338**	**348**	**Av**	**SD**	**361**	**354**	**Av**	**SD**
Qm	0.77	1.80	2.06	5.67	8.12	3.64	3.68	2.77	4.64	0.34	30.28	0.79	9.01	14.31	9.81	0.79	5.30	6.38	2.53	22.28	12:41	13.96
Qi				1.29			0.21	0.53	1.35	0.34	0.65		0.59	0.58		1.05	0.53	0.74				
Qv																				0.25	0.13	0.18
F		2.84	0.77	5.15	5.84	5.97	3.43	2.62	2.13	0.17	5.23	1.06	2.15	2.21	7.48	1.32	4.40	4.36				
Mu				0.52			0.09	0.21														
Cl				1.03		0.26	0.22	0.41	0.19	0.17		0.53	0.22	0.22	0.23	0.26	0.25	0.02		0.51	0.25	0.36
Mg										0.17			0.04	0.08						0.25	0.13	0.18
Py											0.44		0.11	0.22								
Rlga	1.79	6.70	4.11	0.52	1.02	2.34	2.75	2.30	0.58				0.15	0.29	1.17	2.63	1.90	1.03				
Rldo		1.80	1.80	1.03	1.78	4.94	1.89	1.65	15.47	0.51		0.53	4.13	7.57	0.93	2.63	1.78	1.20				
Rldi	0.26			0.77		1.30	0.39	0.54	2.71	5.58			2.07	2.67								
Rlb	6.65	2.58	6.17	7.47	15.48	3.90	7.04	4.52	10.83	18.10	15.03	7.12	12.77	4.80	2.57	5.26	3.92	1.90		5.57	2.78	3.94
Rlg	1.28	2.06	0.77	4.12	3.55	3.90	2.61	1.43	0.39	1.86	4.58	1.06	1.97	1.84	0.23		0.12	0.17				
RMq	0.26	1.55			2.03		0.64	0.91	2.71	1.18	4.14	1.06	2.27	1.45		1.84	0.92	1.30	10.89	15.44	13.16	3.22
RMqs				0.26	0.51		0.13	0.21	0.19		0.44		0.16	0.21						1.01	0.51	0.72
RMqm																				2.03	1.01	1.43
RQ				0.26		1.04	0.22	0.42		0.85	0.87	14.78	4.12	7.11		1.58	0.79	1.12	7.09	0.25	3.67	4.83
RA	0.26				0.76		0.17	0.31	4.06				1.02	2.03								
RGq	1.53	0.77		0.26	2.54		0.85	1.01	2.51	1.02			0.88	1.19	6.78	0.79	3.78	4.23	7.85		3.92	5.55
RGqf	36.57	35.31	29.56	13.40	5.08	8.83	21.46	13.99	16.83	21.49		14.25	13.14	9.26	18.69	17.11	17.90	1.12	1.01		0.51	0.72
RGf	6.39	4.38	11.57	3.87	2.79	1.56	5.09	3.56	0.97	2.20	0.44	3.96	1.89	1.56		12.37	6.18	8.75				
RSq	0.26	0.52	0.26		0.51	0.78	0.39	0.27	1.74	0.51	0.44	0.26	0.74	0.68	0.23	1.58	0.91	0.95	8.35	1.77	5.06	4.65
RSqf	14.32	13.66	5.91	3.09	3.55	1.56	7.02	5.58	1.55	17.09		4.75	5.85	7.75	5.84	3.68	4.76	1.53	1.52		0.76	1.07
RSf	3.32	1.80	10.54	5.93	3.55	10.13	5.88	3.70	1.35	3.89	0.22	4.49	2.49	2.03	3.27	12.63	7.95	6.62				
RMUDh	7.93	2.06	3.86	4.12	1.02	2.08	3.51	2.47		2.03		2.11	1.04	1.20	10.28	15.79	13.03	3.90	29.62		14.81	20.94
RMUDs	1.02		4.63	4.90	4.57	6.49	3.60	2.52	1.55	6.26		12.14	4.99	5.46	1.17	6.32	3.74	3.64	12.41	6.33	9.37	4.30
RF	11.00	2.84		6.44			3.38	4.52		0.34	10.68	1.58	3.15	5.06	6.78		3.39	4.79				
RCl			1.54	5.15	3.30	0.52	1.75	2.08		0.17		10.55	2.68	5.25		0.26	0.13	0.19		1.27	0.63	0.90
RCh	1.02	0.77	0.26	3.61	9.14	4.68	3.25	3.37	21.08	1.18	15.90	4.22	10.60	9.44	4.91	1.05	2.98	2.73	6.08	32.91	19.49	18.98
RDol			0.26	2.58	6.60	12.47	3.65	5.02		4.40			1.10	2.20		1.32	0.66	0.93				
Roo		0.26			4.82		0.85	1.95														
Rsil		5.15	1.03	1.80	1.02	6.75	2.63	2.69		4.40		2.90	1.83	2.19						3.04	1.52	2.15
Rca			3.86	2.32	1.27	0.52	1.33	1.52		1.52	0.22	0.26	0.50	0.69	5.84	2.11	3.97	2.64				
Rop	3.58	9.02	2.57	6.44	6.09	2.34	5.01	2.62		1.02		3.96	1.24	1.87	6.54	0.26	3.40	4.44	9.37		4.68	6.62
Mat	1.79	2.32	1.29	4.64	3.05	12.73	4.30	4.29	7.16	2.37	10.24	7.39	6.79	3.26	7.24	3.95	5.60	2.33	3.04	6.08	4.56	2.15
Cem		1.80	7.20	3.35	2.03	1.30	2.61	2.49		0.85	0.22	0.26	0.33	0.36		3.42	1.71	2.42	0.25	1.01	0.63	0.54
Total	100	100	100	100	100	100			100	100	100	100			100	100			100	100		
Counts	391	388	389	388	394	385			517	591	459	379			428	380			395	395		

Table 3. Modal point counts.

	Que River						Red Lead				Fernfields		Misery Hill	
	917	**919**	**920**	**923**	**924**	**926**	**845**	**150**	**151**	**358**	**338**	**348**	**361**	**354**
Qm	3	7	8	22	32	24	24	2	139	3	42	3	10	88
Qi?	-	-	-	5	-	-	7	2	3	-	-	4	-	-
Qv	-	-	-	-	-	-	-	-	-	-	-	-	-	1
F	-	11	3	20	23	23	11	1	24	4	32	5	-	-
Mu	-	-	-	2	-	-	-	-	-	-	-	-	-	-
Cl	-	-	-	4	-	1	1	1	-	2	1	1	-	2
Cr	10(t)	6(t)	14(t)	9(t)	2(t)	8(t)	3(t)	12(t)	1(t)	-	-	-	-	-
Mg	-	-	-	-	-	-	-	1	-	-	-	-	-	1
Py	-	-	-	-	-	-	-	-	2	-	-	-	-	-
Rlga	7	26	16	2	4	9	3	-	-	-	5	10	-	-
Rldo	-	7	7	4	7	19	80	3	-	2	4	10	-	-
Rldi	1	-	-	3	-	5	14	33	-	-	-	-	-	-
Rlb	26	10	24	29	61	15	56	107	69	27	11	20	-	22
Rlg	5	8	3	16	14	15	2	11	21	4	1	-	-	-
RMq	1	6	-	-	8	-	14	7	19	4	-	7	43	61
RMqs	-	-	-	1	2	-	1	-	2	-	-	-	-	4
RMqm	-	-	-	-	-	-	-	-	-	-	-	-	-	8
RQ	-	-	-	1	-	4	-	5	4	56	-	6	28	1
RA	1	-	-	-	3	-	21	-	-	-	-	-	-	-
RGq	6	3	-	1	10	-	13	6	-	-	29	3	31	-
RGqf	143	137	115	52	20	34	87	127	-	54	80	65	4	-
RGf	25	17	45	15	11	6	5	13	2	15	-	47	-	-
RSq	1	2	1	-	2	3	9	3	2	1	1	6	33	7
RSqf	56	53	23	12	14	6	8	101	-	18	25	14	6	-
RSf	13	7	41	23	14	39	7	23	1	17	14	48	-	-
RMUDh	31	8	15	16	4	8	-	12	-	8	44	60	117	-
RMUDs	4	-	18	19	18	25	8	37	-	46	5	24	49	25
RF	43	11	-	25	-	-	-	2	49	6	29	-	-	-
RCl	-	-	6	20	13	2	-	1	-	40	-	1	-	5
RCh	4	3	1	14	36	18	109	7	73	16	21	4	24	130
RDol	-	-	1	10	26	48	-	26	-	-	-	5	-	-
Roo	-	1	-	-	19	-	-	-	-	-	-	-	-	-
Rsil	-	20	4	7	4	26	-	26	-	11	-	-	-	12
Rca	-	-	15	9	5	2	-	9	1	1	25	8	-	-
Rop	14	35	10	25	24	9	-	6	-	15	28	1	37	-
Mat	7	9	5	18	12	49	37	14	47	28	31	15	12	24
Cem	-	7	28	13	8	5	-	5	1	1	-	13	1	4
Total	391	388	389	388	394	385	517	591	459	379	428	380	395	395

Table 4. Petrographic codes used in tables 1-3; fig. 4.

Qm = monocrystalline quartz
Qi = possible volcanic quartz
Qv = vein quartz fragment
F = feldspar
Cl = detrital chlorite
Mv = detrital muscovite
Py = detrital pyroxene
Mg = detrital magnetite
Cr(Tr) = phenocrystal or detrital chromite; (Tr) = not found with mechanical point count stage
Mat = matrix
Cem = cement, commonly haematite or carbonate

Rock Fragments

RI: igneous rock fragments
RIga = gabbro
RIdo = dolerite
RIdi = diorite
RIb = basalt-andesite
RIg = glassy volcanic rock fragment
RCl = chloritised rock fragment or grain of probable igneous origin

RM: metamorphic rock fragments
RMq = metamorphic quartzite
RMqs = quartz-mica schist
RMqm = mylonitic quartzite

sandstone rock fragments
RQ = quartz arenite
RQ = arkose

RG: greywacke rock fragments
RGq = quartz-dominated greywacke
RGqf = greywacke or lithic arenite with conspicuous quartz and feldspar grains
RGf = feldspathic greywacke, with abundant basaltic lithic detritus

RS: siltstone rock fragments
RSq = quartz-dominated siltstone with sericitic matrix
RSqf = siltstone with conspicuous fine grained quartz and feldspar
RSf = feldspathic siltstone with cloudy green or haematitic matrix

RMUD: mudstone rock fragments
RMUDh = haematitic mudstone
RMUDs = siliceous mudstone, usually altered to sericite or chlorite

fine-grained rock fragments
RCh = chert
RDol = dolomite
Roo = oolitic rock fragment or grain, usually silicified
Rop = opaque, irresolvable lithic fragment
RF = v. fine grained, irresolvable lithic fragment - commonly altered to chlorite, sericite or silica (glassy volcanic - mudstone - chert?)
Rsil = totally silicified rock fragment - precursor uncertain
RCa = fragment consisting of recrystallised carbonate (usually calcite) - precursor uncertain

Second report: Sedimentology of the Dundas Group and correlates with reference to a possible syn-depositional growth fault west of Rosebery

Stuart W. Bull

Centre for Ore Deposit and Exploration Studies, Geology Department, University of Tasmania

INTRODUCTION

This report follows Bull (1994), the main aim of which was to examine the sedimentology of the Stitt Quartzite in order to test the structural model that a N–S trending structure west of the Rosebery Fault near Rosebery was a Cambrian growth fault, with an associated WNW trending transfer (Berry and Keele, 1993; Fig. 1). The main conclusions of Bull (1994) were (i) that the Stitt Quartzite represents turbiditic sandstone and siltstone deposition in a fan system situated just below wave base; (ii) that the sections of the unit examined in the Rosebery region recorded no evidence of the erosion of a proximal growth fault scarp to the west; and (iii) that of the units of the Dundas Group observed in the study, the facies most likely to represent erosion of a fault scarp were the conglomeratic deposits intercalated with the Westcott argillite.

Two main problems were encountered which hampered the Stitt Quartzite study. Firstly, in the facies present in the unit, Bouma C division ripples are very rare. As a result, palaeocurrent evidence of the direction of the source of the Stitt Quartzite turbidites, which is critical in evaluating the structural model, is absent. Secondly, there is a lack of exposure of the Stitt Quartzite closest to the proposed growth fault (i.e. sections on the western limb of the N–S trending syncline in the Rosebery area; Fig. 1). As a result, relatively subtle manifestations of a growth fault (i.e. soft sediment deformation and/or slumping adjacent to the fault scarp), such as would occur if the fault was situated entirely within the sub-wave base environment which hosted the Stitt Quartzite could have been missed.

In order to address the problems encountered in testing the structural model outlined above, and to continue work on regional correlations of the Dundas Group, the main aims of the 1995 field season were:

1. To access the Pieman Gorge west of Rosebery to determine whether there is any outcrop of the Stitt Quartzite on the western limb of the syncline.
2. To examine a section through a correlate of the Dundas Group, the Huskisson Group, in the Huskisson River 7 km WNW of Rosebery. This section is adjacent to the WNW trending transfer fault of the Berry and Keele (1993) model (Fig. 1).

PIEMAN GORGE SECTION

The Pieman Gorge section was considered a high priority in terms of testing the Berry and Keele (1993) structural model, because it had the potential to provide exposures of the Stitt Quartzite immediately adjacent to the proposed growth fault (i.e. on the western limb of the N–S trending syncline; Fig. 1). In addition, both Green (1983) and Lees (1987) described disrupted bedding textures from the Stitt Quartzite in the Pieman Gorge, with the latter author describing the westernmost exposures as comprising "200 m of deformed melange-like quartzite and slate". Although much of this disruption is clearly tectonic (e.g. Lees, 1987; Fig 28), other examples cited (e.g. Green, 1983, Fig. 3.33) resemble soft-sediment deformation which, if it could be spatially related to the area adjacent to the proposed growth fault, would be consistent with slumping associated with a fault scarp.

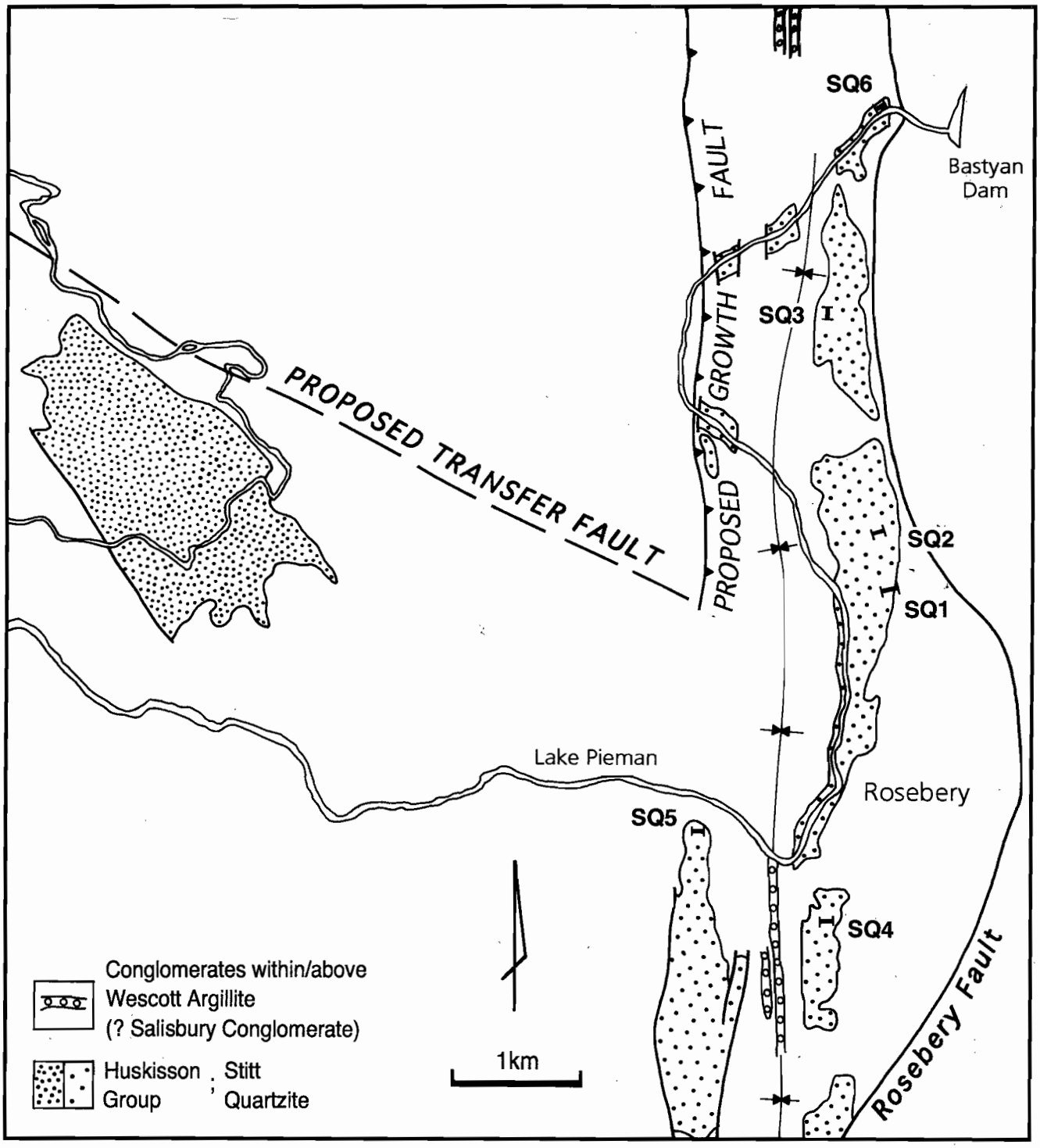

Figure 1. Locality diagram showing the extent of the Stitt quartzite in the Rosebery area (after Corbett and McNeill, 1986) and the Huskisson Group in the Huskisson River area (after Corbett and McNeill, 1986 and Brown, 1986).

Access to the Pieman Gorge section west of Rosebery was gained via boat launched from the ramp near the junction of the Ring and Pieman Rivers. Geological mapping (Lees, 1987; Corbett and McNeill, 1986) indicated that the Pieman Gorge section crossed the proposed growth fault on two bends 6 km NNW of Rosebery (Fig. 1). However, as a result of high water levels due to the damming of the Pieman River subsequent to the field work carried out for the studies of Green (1983) and Lees (1987), the sections examined by these authors are now inundated and exposure at the new higher lake level is minimal. On the southern of the two bends there is essentially no exposure. On the northern bend there is an exposure of interbedded sandstone and siltstone on the southeastern bank, however, it is essentially right on the N–S structure. As a result there is a very strong sub-vertical cleavage present which obscures much of the sedimentological detail. This outcrop superficially resembles a "normal" Stitt Quartzite facies (Bull, 1994), however, its interpretation during previous mapping is contradictory. Corbett (1986) places this exposure is on the eastern side of the fault where it should correspond to Stitt Quartzite or Westcott Argillite, while Lees (1987) puts it on the western side of the fault in which case it should be in the Crimson Creek Formation. In thin section the sandstone from this section has a distinctive mafic provenance in that it is feldspar-rich, with only scattered quartz grains, and contains mafic volcanic lithic fragments. It therefore has more affinity with the Crimson Creek Formation or parts of the Westcott Argillite (D. Selley, this report) than the quartz-rich Stitt Quartzite.

HUSKISSON RIVER SECTION

The Huskisson River section was considered a high priority in terms of testing the Berry and Keele (1993) structural model, because it had the potential to provide exposures thought to be correlates of the Dundas Group immediately adjacent to the proposed WNW trending transfer fault (Fig. 1). In overview, the section overlies a faulted contact with an ultramafic body, and consists of three main units (Jago and Brown, 1992). The basal unit is a 950 m thick conglomeratic sedimentary package which has a mixed sedimentary and volcanic provenance. It is overlain by a middle unit comprising 45 m of fossiliferous black pyritic mudstone, and an upper 200 m thick conglomeratic package which has a dominantly metasedimentary provenace. Palaeontological evidence indicates that the lower conglomeratic unit is Late Middle Cambrian (Boomerangian) and hence a bio-stratigraphic correlate of the Dundas Group, while the upper part of the middle mudstone unit is Late Cambrian (Idamean) in age (Jago and Brown, 1992). The fact that the Late Middle Cambrian (LMC) part of the section contained a considerable proportion of conglomeratic material was considered particularly significant in terms of testing the Berry and Keele (1993) structural model. In the absence of any palaeocurrent data from the Stitt Quartzite (Bull, 1994), it was hoped that provenance data from these conglomerates could provide some evidence of the direction of the source region for this material.

As was the case for the Pieman Gorge section, all previous work on the Huskisson River section (e.g. Brown, 1986; Jago and Brown, 1992) was carried out prior to the damming of the Pieman River. Current water levels are considerably higher, however, spaced weathered outcrops of the LMC part of the section, mainly of massive conglomeratic and volcaniclastic units, are still present. These were sampled, and examination of the hand specimens and thin sections, in combination with analysis of lithological descriptions from the previous work (especially that of Brown, 1986), allows significant interpretation of the Huskisson section.

Brown (1986) recorded a number of points about the LMC part of the Huskisson River section which are relevant to the current study which are as follows: (i) although the section is marked by the presence of numerous conglomerate units, the ambient background facies present throughout comprises laminated and thinly interbedded siltstone and mudstone with interbedded muscovitic sandstone beds up to 5 cm thick, which occasionally exhibit flame structures and ripple marks; (ii) the basal 70 m of the section above the contact with a structurally emplaced ultramafic unit is considerably disrupted by faulting, however, the basal units clearly have a sedimentary provenance. The first mixed provenance, in part volcanic-sourced material occurs approximately 150 up-section, after which such units are present throughout the middle Cambrian section; and (iii) the conglomerates in the LMC part of the section include both volcanic and mica schist clasts.

The ambient background deposits of the LMC part of the Huskisson River section were not observed during the current study, however, from the description outlined above they seem analogous to the facies which comprise the Stitt Quartzite in the

Rosebery region (Bull, 1994). Preliminary examination of the coarser-grained units via hand specimens and thin sections collected during this study confirm the basic provenance observations of Brown (1986), that they represent erosion of a mixed metasedimentary and volcanic source. However, some of the units noted by Brown (1986) as consisting "completely of epiclastic volcanic material" are crystal-rich felsic volcanic aggregates. Such units are now widely interpreted as essentially syn-eruptive volcaniclastic mass-flow deposits (e.g. Cas and Wright, 1987; McPhie et al., 1993), and their presence indicates that the active volcanism occurred synchronous with Middle Cambrian sedimentation in the Huskisson River region.

DISCUSSION

Sketch logs of the Dundas Group section in Pieman Gorge (after Lees, 1987) and the similarly aged Huskisson Group section in Huskisson River (after Brown, 1986 and this study) are shown in Figure 2. The Pieman Gorge section comprises the dominantly volcanic-derived White Spur Formation overlain by the Chamberlain Shale, Stitt Quartzite, Westcott Argillite and Salisbury conglomerate. In overview it can be considered in terms of three facies packages comprising: (i) lower volcaniclastic (probably in part syn-eruptive) mass flow deposits (the White Spur Formation), which in the absence of any evidence of reworking appear to have been deposited in a quiet, sub-wave base environment; (ii) a middle unit representing three different styles of quiet water, sub-wave base sedimentation, i.e. the Chamberlain Shale (suspension-dominated), the Stitt Quartzite (turbiditic) and the Westcott Argillite (carbonate-dominated); and (iii) an upper coarse-grained sequence comprising conglomerate units interbedded with the Westcott Argillite and the overlying Salisbury Conglomerate. Depending on whether these are mass-flow or tractional deposits they could represent either coarse-grained channelised deposition in the sub-wave base environment which hosted the underlying sequence, or alternatively, a change to more energetic shallow water conditions respectively.

As noted above, the Huskisson River section has an ambient background facies comprising suspension deposited siltstone and mudstone with interbedded turbiditic sandstones. This suggests that the whole sequence was deposited in a sub-wave base environment analogous to that which hosted the bulk of the Dundas Group sedimentation in the Pieman Gorge section. However, the Huskisson section has a markedly different facies and provenance profile. Brown (1986) considered that overlying a basal fault contact with an ultramafic unit, the Huskisson River section could be considered in terms of two broad packages: (i) a basal 150 m thick package which has a non-volcanic provenance and consists of thinly-bedded siltstone, sandstone and mudstone and includes a thick chert clast conglomerate horizon; and (ii) an overlying 900 m thick package of interbedded siltstone, mudstone, lithic wacke and sandstone which hosts numerous units of granule to coarse cobble conglomerate with a mixed metasedimentary and volcanic provenance.

Samples collected during field work for this study suggest that a further subdivision can be made of the upper mixed provenance interval of the LMC part of the Huskisson River section. Due to the high river levels, the lowest sample collected during this study was from approximately 280 m above the base of the section, well above the basal interval reported by Brown (1986) to have a non-volcanic provenance. It comprised an immature (i.e. glass shard-rich) volcaniclastic sandstone, and in fact all samples collected from five sites between approximately 280 and 515 m above the base of the section represented immature (i.e. shard- or crystal-rich), intermediate to felsic volcaniclastic units. The remaining samples collected from four sites in the upper part of the LMC section were siltstones, sandstone and conglomerates which all had an identical provenance. These units were dominated by metasedimentary clasts with only a minor volcanic component, and all of the constituent lithologies could have been derived from erosion of the regional basement (e.g. the Oonah Formation, Success Creek Group and Crimson Creek Group; D. Selley, this report).

Unless the lithological distribution outlined above is a sample bias due to the high river levels, it suggests that a middle interval of the LMC part of the Huskisson River section can be separated out as being characterised by potentially syn-eruptive, intermediate to felsic volcaniclastics (Fig. 2). In addition, one of the crystal-rich volcaniclastic samples from the middle interval of the section is distinctive in that although it dominated by feldspar, it also contains scattered large (up to 5 mm) quartz phenocrysts and sericite/chlorite replaced tube pumice fragments. This sample closely resembles volcaniclastic facies B of McPhie and Allen (1992),

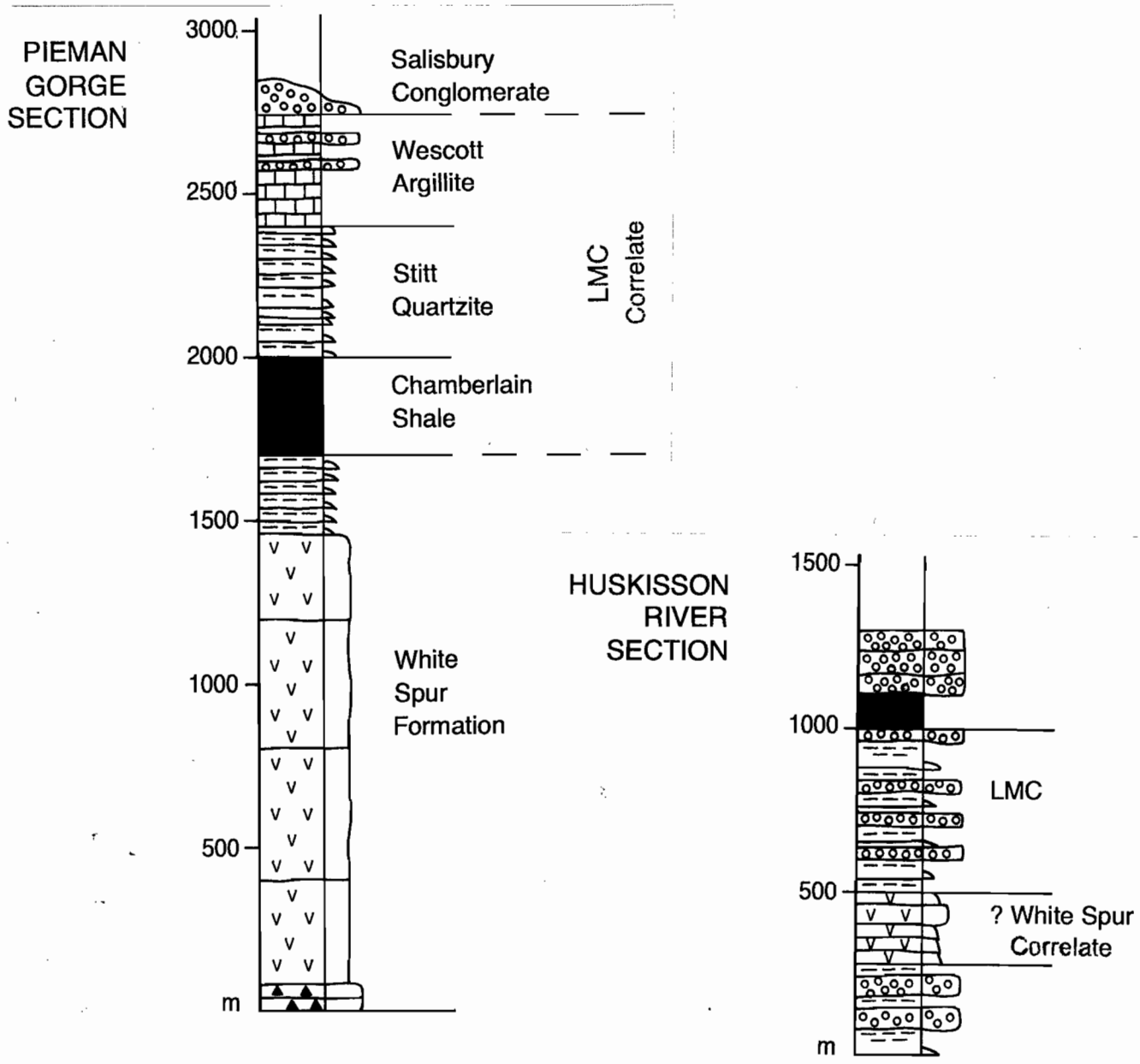

Figure 2. Sketch logs of the Dundas Group in the Rosebery area (after Lees, 1987), and the Huskisson Group in the Huskisson River area (after Brown, 1986 and this study).

which was first described from the Southwell Sub-Group in the Hellyer area 26 km NNE of Rosebery, and is thought to correlate to units within the White Spur Formation in the Rosebery region. The presence of this distinctive volcaniclastic unit in the LMC part of the Huskisson River section suggests that the immature volcaniclastic interval is a correlative of the White Spur Formation (Fig. 2).

If the above correlation is valid, the immature intermediate to felsic volcaniclastic horizon (White Spur Formation and correlates) provides a time line which links the Dundas Group in the Rosebery area and the Huskisson Group in the Huskisson River area. In this model, the units immediately above the volcaniclastic part of the White Spur Formation in the Rosebery area (i.e. the Chamberlain Shale, Stitt Quartzite and possibly part of the Westcott Argillite) correspond to the LMC part of the Huskisson River section. This chrono-stratigraphic correlation allows direct lithological comparisons to be made between the two sections which have important implications for the Berry and Keele (1993) structural model. In this comparative depositional model, following the emplacement of immature (i.e. at least partly syn-eruptive) intermediate to felsic volcaniclastic material in both areas, deposition of a relatively thinly-bedded and fine-grained sub-wave base succession comprising the Chamberlain Shale, Stitt Quartzite and Westcott Argillite occurred to the east of the proposed N–S growth fault (Fig. 1). At the same time, adjacent to the WNW transfer in the Huskisson River area, the upper mixed provenance, sub-wave base, partly conglomeratic part of the Huskisson Group was deposited.

The implications of this sedimentary facies distribution for the structural architecture of the system are, that during the Middle Cambrian minimal erosion of the proposed N–S growth fault west of Rosebery occurred. Instead, this structure seems to have controlled the deposition of relatively texturally mature clastic lithologies such as the quartz-rich sandstones of the Stitt Quartzite. At the same time, erosion was occurring either across the proposed WNW transfer, or across a the part of the N–S trending growth fault which had been offset to the west. The resultant texturally immature (i.e. footwall-derived) material was being deposited to form the conglomeratic units in the upper part of the LMC Huskisson Group section.

A possible explanation for the structural, sedimentary facies and provenance pattern outlined above is schematically illustrated in a block diagram (Fig. 3). This depicts LMC sedimentation patterns in the Rosebery/Huskisson River area based one the assumption that the WNW transfer zone in the Berry and Keele (1993) structural model is a synthetic inter-basin relay ramp (Gawthorpe and Hurst, 1993). The effect of the ramp structure, in addition to allowing the N–S trending growth fault in the Rosebery region to step to the west (Fig. 1), is that it also transgresses the level at which erosion is occurring in the basin (? storm wave base or palaeo-shoreline etc.).

In summary, the model depicted in Figure 3 explains:

1. The lack of erosion of the N–S growth structure in the Rosebery area, because the footwall block remains in the quiet sub-wave base environment. In fact, rather than being coarse-grained and immature as is likely if they had been the result of erosion of the footwall block, the clastic sediments adjacent to the N–S fault scarp are relatively fine-grained and texturally mature (i.e. the quartz-rich turbidites of the Stitt Quartzite). Textural maturity is in part dependant on the nature of the source region, however, the relatively fine grainsize and lack of lithic fragments suggests that these deposits are not locally derived. They would, therefore, seem to have been transported relatively large distances from their source. In a rift setting the longest sediment pathway will clearly involve longitudinal (i.e. rift-parallel) sediment transport in the axial graben region. This style of sedimentation is common in both subaerial (e.g. the East Africa Rift; Baker, 1986) and subaqueous (e.g. the Ventura Basin, California; Hsu et al., 1980) rift and basin settings. It is, therefore, proposed that rather than being eroded, the N–S growth structure in the Rosebery area is actually controlling the transport and deposition of sediment which is being transported considerable distances along the rift axis.

2. The erosion of the footwall block across the WNW trending transfer zone and/or the N–S growth fault which has stepped to the west, because the transfer ramp elevates the footwall block out of the quiet sub-wave base environment to a position above the level within the basin at which erosion can occur. The model depicted in Figure 3 shows that in addition to the transfer zone, the segment of the N–S growth fault which has stepped to the west is also elevated into the erosive regime. This precise configuration need not necessarily be the

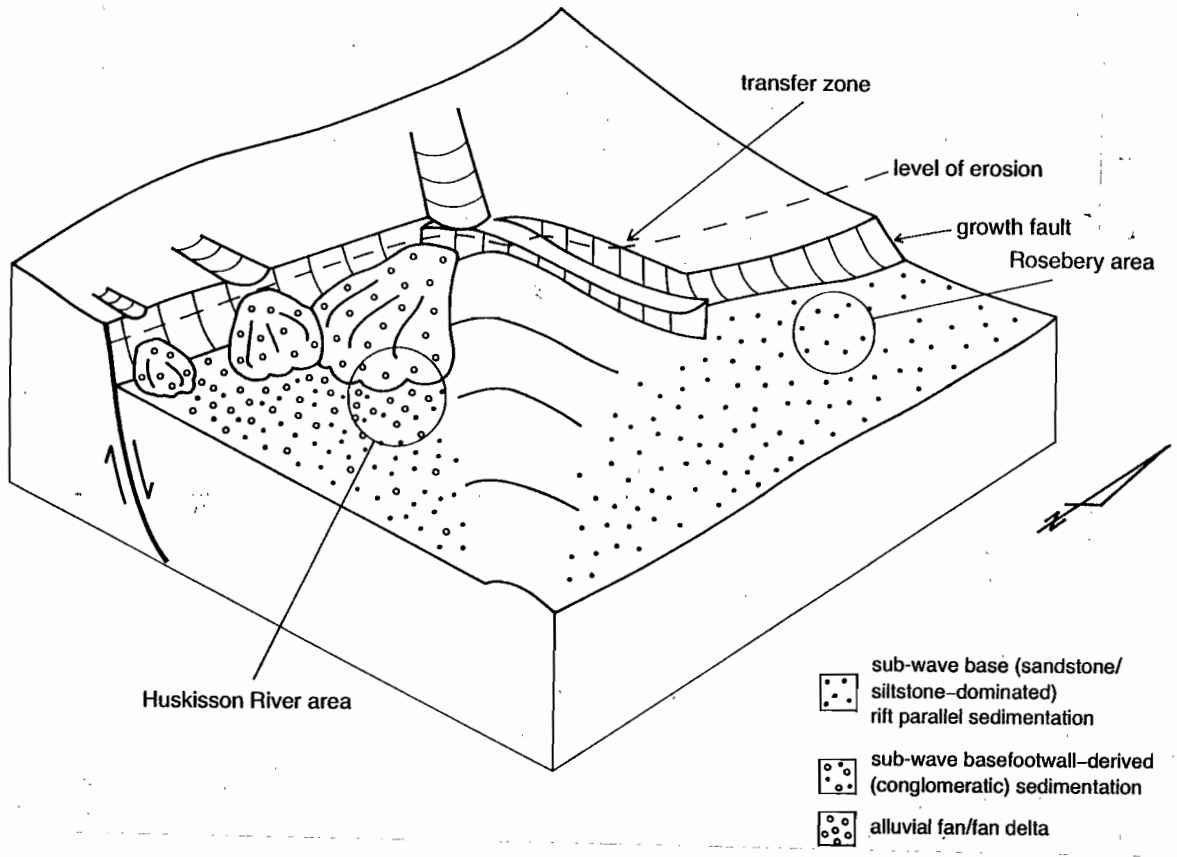

Figure 3. Block diagram depicting a model for LMC sedimentation in the Rosebery and Huskisson River areas.

case, however, because footwall-derived sediment influx into half grabens is an order of magnitude greater across major transfer zones than it is from erosion of footwall scarps adjacent to growth faults (Gawthorpe and Hurst, 1993). This reflects the fact that along graben-bounding normal faults (i.e. growth faults), the uplifted footwall block is tilted away from the graben depocentre. As a result, drainage along the outer side of the rift margin fault is directed away from the graben onto the rift flank. In general, the only sedimentological contribution from the bounding normal fault to the graben system is localised alluvial deposits resulting from direct slumping or erosion of the growth fault scarp. In contrast, transfer zones are often the sites where drainage systems established on rift flanks enter the axial graben region. These have the potential to drain large areas of uplifted footwall (i.e. the rift flanks) and, therefore, to introduce large volumes of footwall-derived sediment into the axial graben. In order to establish the configuration shown in Figure 3, where the N–S growth fault which has stepped to the west is also elevated in the erosive regime, it would be necessary to recognise localised alluvial deposits in the Cambrian succession which were spatially related to the N–S structure.

3. The reduced thickness of both the White Spur and LMC correlates in the Huskisson section relative to the area around Rosebery (Fig. 2). Transfer zones commonly form topographic highs which separate depocentres developed in the hanging wall of the main border fault (i.e. growth fault) segments (Gawthorpe and Hurst, 1993). In this model, deposition in the Huskisson area would, therefore, represent a condensed section on or near the topographically uplifted transfer ramp.

The main problems with the model presented in Figure 3 are firstly that is unclear what the basal non-volcanic interval of the Huskisson Group, which was not observed in this study, but which is reported to include thinly-bedded siltstone, sandstone, mudstone and a chert clast conglomerate (Brown, 1986) would represent. A lithic breccia zone is widely recognised at or near the base of the White Spur Formation associated with sandstones and shales (Lees, 1987), however, it has a partly volcanic provenance as it contains felsic tuffs and pumice clasts. Secondly, the significance of the conglomerate units which occur in the Westcott Argillite, which have a similar (i.e. immature basementally-derived) provenance to those of the Huskisson Group (D. Selley, this report), is also unclear. They apparently represent the onset of restricted footwall-block erosion much later than that occurring in the Huskisson River region.

CONCLUSIONS

1. No LMC outcrop exists in the Pieman Gorge section which is useful in testing the structural model of Berry and Keele (1993).

2. The LMC section in the Huskisson River can be subdivided into three sedimentary packages comprising a basal 150 m thick non-volcanic sequence, a 240 m thick middle package of immature (i.e. shard- or crystal-rich), intermediate to felsic volcaniclastics and a 650 m thick upper sequence of mixed metasedimentary and volcanic provenance.

3. The middle immature (i.e. potentially syn-eruptive), intermediate to felsic volcaniclastic sequence in the LMC Huskisson River section is tentatively correlated with the White Spur Formation in the Rosebery region. This correlation is proposed on the basis of intermediate to felsic composition, immature provenance and the recognition of a distinctive large quartz-bearing marker unit which closely resembles volcaniclastic facies B of McPhie and Allen (1992).

4. A model can be proposed which is consistent with the structures proposed by Berry and Keele (1993), and which also explains sediment facies and provenance patterns in the LMC units in the Rosebery and Huskisson River areas. In this model, the WNW transfer zone of the Berry and Keele (1993) is a synthetic inter-basin relay ramp. As a result of this configuration, the footwall block transgresses the level at which erosion is occurring in the basin and provides the basement-derived material which forms the conglomerates in the LMC Huskisson River section. Because the relay ramp is a elevated relative to the axial graben area of the rift, the LMC succession in the Huskisson River area represents a condensed section. In contrast, the proposed N–S growth fault in the Rosebery area controls rift-parallel

transport and deposition of a thicker sequence of relatively texturally mature clastic sediments (i.e. the quartz-rich turbidites of the Stitt Quartzite) in the axial graben.

FUTURE WORK

Given the poor exposure encountered in field work for this project, an obvious avenue for future work involves examining a number of relevant drill cores. Green (1983) refers to Department of Mines Natone DDH (or MD1?) which intersects the Salisbury Conglomerate interfingering with the Natone Volcanics. Examination of this core could resolve the question of whether these conglomeratic deposits are mass flow or tractional deposits. Another potentially important intersection is a drill core from several kilometres along strike to the south from the Huskisson River section. This hole (DDH RBE D1), from the Exe Creek area, was drilled by Comstaff and is held at the RGC core yard in Zeehan. It is currently being studied as part of an honours project which is focused on mineralization in the area, however, it is also significant from a sedimentological viewpoint in terms of its potential for comparison with the Huskisson River section.

REFERENCES

Baker, B. H. 1986. Tectonics and volcanism of the southern Kenya Rift Valley and its influence on rift sedimentation.. In Frostick, L. E. et al. (eds.). Sedimentation in the African Rifts. Geol. Soc. Spec. Publ. No. 25, p. 45–57.

Berry, R. F. and Keele, R. A. 1993. Cambrian structure in western Tasmania. In Structure and mineralization of western Tasmania, AMIRA Project P.291 Final Report. p. 55–68.

Bouma, A. H. 1962. Sedimentology of some flysch deposits. Amsterdam: Elsevier. 168p.

Brown, A. V. 1986. Geology of the Dundas–Mt Lindsay–Mt Youngbuck region. Tas. Dept. of Mines, Geol. Surv. Bull. 62, p. 45–49.

Bull, S. W. 1994. Preliminary report: sedimentology of the Dundas Group with reference to a possible syn-depositional growth fault west of Rosebery. AMIRA Project P.291A Report No. 1, p. 1–14.

Cas, R. A. F., and Wright, J. V. 1987. Volcanic successions modern and ancient. Allen and Unwin Ltd., London. 528p.

Corbett, K. D. 1986. Geological Survey of Tasmania-Department of Mines Hobart, Mt Read Volcanics Project, Map 3. Geology of the Henty River–Mt Read area.

Corbett, K. D. and McNeill, A. W. 1986. Geological Survey of Tasmania-Department of Mines Hobart, Mt Read Volcanics Project, Map 2. Geology of Rosebery–Mt Block area.

Gawthorpe, R. L. and Hurst, J. M., 1993. Transfer zones in extensional basins: their structural style and influence on drainage development and stratigraphy. J. Geol. Soc. London v. 150, p. 1137–1152.

Green, G. R. 1983. The geological setting and formation of the Rosebery volcanic-hosted massive sulphide orebody, Tasmania. unpublished PhD thesis, Geology Department, University of Tasmania.

Hsu, K. J., Kelts, K. and Valentine, J. W. 1980. Resedimented facies in the Ventura Basin, California, a model of longitudinal transport of turbidity currents. AAPG Bull, v. 64, no. 7, p 1034–1051.

Jago, J. B. and Brown, A. V. 1992. Early Idamean (Late Cambrian) agnostid trilobites from the Huskisson River, Tasmania. Papers and Proceedings of the Roy. Soc. Tas., v. 126, p. 59–65.

Lees, T. C. 1987. Geology and mineralization of the Rosebery–Hercules area, Tasmania. unpublished MSc thesis, Geology Department, University of Tasmania.

McPhie, J. and Allen, R. 1992. Facies architecture of mineralized submarine volcanic sequences: Cambrian Mt Read Volcanics, western Tasmania. Econ. Geol. v. 87, p. 587–596.

McPhie, J., Doyle, M. and Allen, R. 1993. Volcanic Textures. Centre for Ore Deposits and Exploration Studies. 198 p.

A new structural section between Queenstown and Zeehan: preliminary results on structure and unconformity relationships between the Upper Dundas Group and Zeehan Conglomerates

by Richard A. Keele

Centre for Ore Deposit and Exploration Studies, Geology Department, University of Tasmania

INTRODUCTION

The purpose of this report is to present data on a new structural section between the Firewood Siding and Zeehan sections (Berry 1990, 1991; Keele 1991b). This section is intended to track the change in strain south of the Rosebery Fault in the region of Cambrian transfer fault No. 5 (see P.391 final report). Preliminary results suggest that E–W structures were at least as important in controlling Late Cambrian/ Early Ordovician deposition, as the N–S structures were. Two E–W sections through the Upper Dundas block show that the siliciclastics thicken towards: (1) the east trending Firewood Siding Fault, and (2) north trending late Late Cambrian synclines.

UPPER DUNDAS SILICICLASTICS

The Upper Dundas beds that crop out over a 50 km^2 area between the Professor Range and the Murchison Highway (Brown et al. 1994, Baillie and Corbett 1985) contain rocks that are equivalent in age and type to the largely marine Newton Creek Sandstones further east (K. Corbett pers. comm. 1995). The lower part of this sequence is dominated by siltstone–sandstone interbeds. A thick sandstone unit marks the actual base to the sequence and may correlate with the Stitt Quartzite. The upper part is characterised by conglomerate–sandstone interbeds indicating that the sequence is part of a coarsening upwards cycle. A total thickness of 2000 m is indicated from the sections (Fig. 2). Broadly, the block is tilted to the north with the base of the sequence sitting hard up against the Firewood Siding Fault, with the top of the sequence resting unconformably beneath the Zeehan Conglomerates at its northern end (Fig. 1). The central region is dominated by a small (2 km x 2 km) dome that exposes the lower siltstone–sandstone interbeds; this is considered to be an interference effect between Cambrian and Devonian folding. A marked unconformity surface separates these siliciclastics from the overlying Zeehan Conglomerates along the eastern and northern flanks of the outcrop. This is due to open folding in the Dundas Group rocks during the final stages of the Delamerian Orogeny; during this period the anticline crests were being actively eroded whilst the synclinal cores were acting as sites of deposition, i.e. they were growth folds. In contrast, the same surface on the western side is a disconformity that appears to have suffered little, if any, erosion (Baillie and Corbett 1985).

CAMBRIAN FOLDING

Previous workers in the region have speculated on the presence of Cambrian folds in the Mount Read Volcanic belt (e.g. Corbett and Lees 1987, Baillie and Corbett 1985). In a summary of deformation events in western Tasmania, Berry (1994) described two periods of folding in the Cambrian: an initial episode of E–W folding during the middle Late Cambrian, followed by N–S folding at the close of the Late Cambrian. The doubly plunging folds along nearby Howards Road (where the limbs of the folds plunge in opposite directions) has been suggested to be due to an initial (E–W) Cambrian compression followed

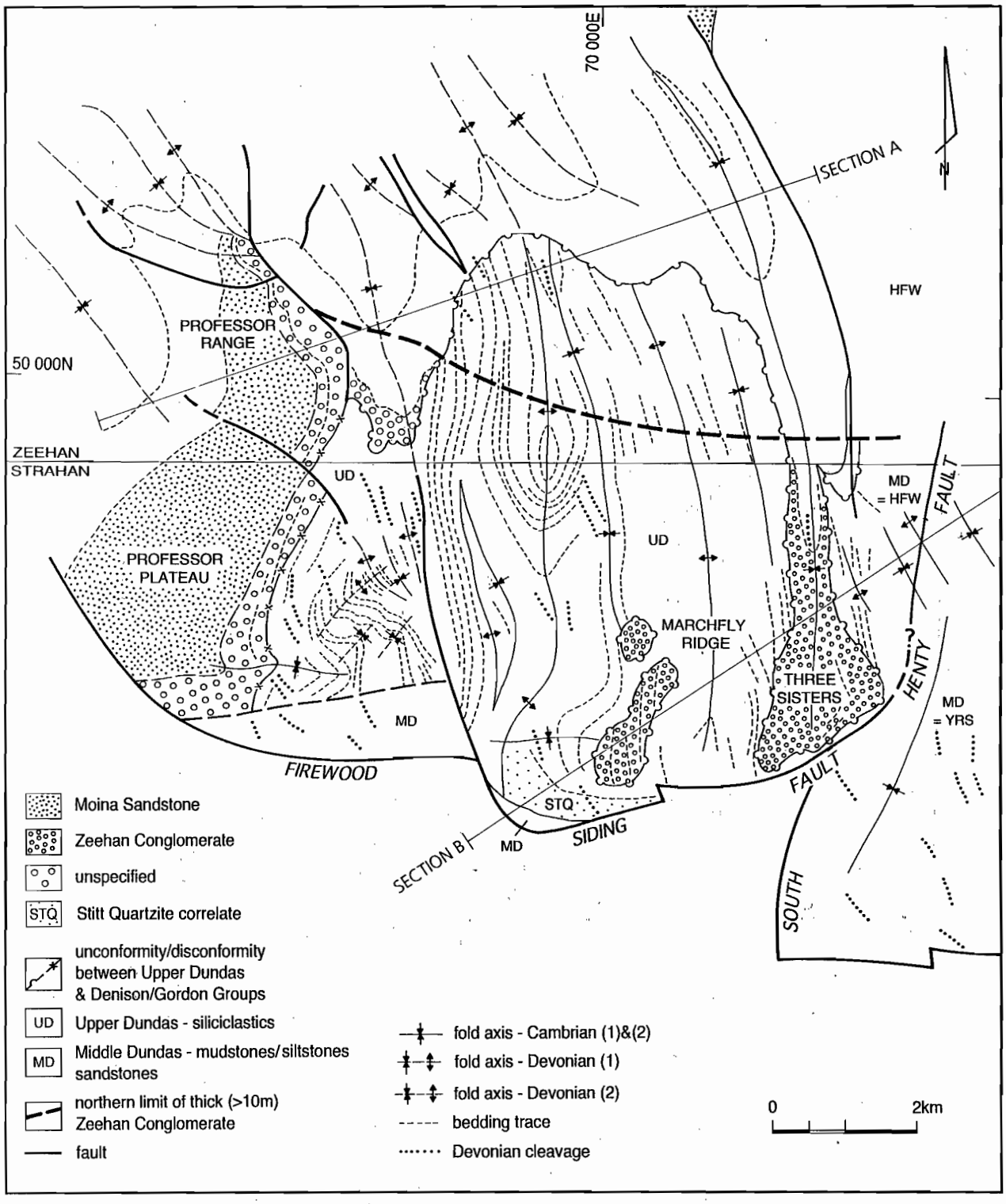

Fig. 1 Simplified geological map of the siliciclastic Upper Dundas sequences north of the Firewood Siding Fault (FSF) showing the positions of sections A and B. The Zeehan Conglomerate thins northwards away from the Firewood Siding Fault suggesting it exerted a strong control on sedimentation during the Late Cambrian; however, the thickest conglomerates are to be found in the keels of the N–S trending Late Cambrian folds that were subsequently tightened during the Devonian compression event . The outcrop of sandstones sitting up against the FSF, at the end of section B, is tentatively correlated with the Stitt Quartzite part of which is just visible at the top of the map.(Geology from Corbett & Baillie 1985, Brown et al. 1994).

by an oblique (NE–SW) Devonian compression (Keele 1991a); in this case, the later compression tightened the folds and rotated their limbs in opposite directions during this process. Since these particular Cambrian folds occur in the middle Dundas beds this means that one of the true tests for determining the amount of Cambrian versus Devonian folding, namely how much and to what extent the unconformity is folded, cannot be applied here. However, no such problems exists with the Upper Dundas block between the Professor Range and the Murchison Highway where the unconformity is exposed on three sides of the block (Fig. 1).

Two periods of Cambrian folding are recognised in this block. The first comprises an E–W synclinal fold related exclusively to the Firewood Siding Fault; the second forms a series of N-trending anticlines and synclines (Figs 1, 2). The single E–W syncline, which is offset in its centre by a dextral fault of Devonian age, is probably related to a shallow trough which was mildly inverted during the middle Late Cambrian compression event. By virtue of its continuation and eventual decay onto the Professor Plateau to the west, this particular fold is seen to be tightened as a result of Devonian movements on the Firewood Siding Fault. East of the wrench fault, the syncline interferes with the main N–S folds, causing plunge changes in the latter: the most obvious effect of this can be seen at the Marchfly Ridge outlier where the E–W syncline crosses one of the N–S later Cambrian synclines to form a depression into which thicker sediment accumulated.

Two pairs of N–S trending anticline-synclines of Cambrian age, with half wavelengths of approximately 1000m, dominate the main central part of the block. None of these Cambrian folds — with the exception of the central anticline — continue northwards into the overlying Denison and Eldon Group sequences. Such evidence for the existence of two main periods of folding, viz. of Cambrian and Devonian age, would be hard to find any where else in the Dundas Trough. To illustrate this further, some Cambrian folds have no counterpart in the overlying sequences and one Cambrian anticline actually lies directly beneath a Devonian syncline!

DEVONIAN FOLDING

Devonian folds are ubiquitously developed throughout the region. The majority are first generation folds, however, some second generation folds are also present.

First generation folds

The orientations and wavelengths of the first generation folds, caused by NE–SW compression, are greatly influenced by: (1) their stratigraphic level, and (2) the rheology of the rocks involved in the folding. For instance, the folds in the Ordovician, Silurian and Devonian sequences trend north westerly — the typical Devonian trend in the west coast terrain — whereas the same generation of folds in the Cambrian rocks trend more northerly (Fig. 1); this is because the Devonian folds in the Cambrian rocks are generally more influenced by the pre-existing grain in the rocks. The folds in the 'basement' (in part tightened Cambrian folds) have half wavelengths of 2–3 km, whereas the folds in the Eldon Group have half wavelengths of 500–750 m (Figs 1, 2). It should be noted that the synclines are generally much tighter than the anticlines (see Fig. 2b, especially). This is due to the enhanced rheological differences imparted to the rocks by the thicker than normal conglomerate beds in the synclines. It is also noted that tight basement folds with overturned limbs are restricted to these Devonian keels.

Second generation folds

A second generation of Devonian folding, indicating a NW–SE compression, is present in a triangular shaped block sitting on the western side of the block of Upper Dundas siliciclastics (Fig. 1). These folds, which number three in total, appear to bend the Devonian cleavage; they are sandwiched between the E–W Cambrian fold and a number of small amplitude NNW-trending Devonian folds to the north. A NW-trending wrench fault has acted as a *decollement* between these two domains of folding.

Interference between the N–S Cambrian folds and the NE–SW Devonian compression has produced a small dome in the centre of the block. The double plunge to this structure was largely controlled by the zones of strong cleavage that occur at both ends of the dome, e.g. the headwaters of Malcolm Creek.

LATE-CAMBRIAN UNCONFORMITY SURFACE

Given the limitations of this study, where dip angles across the unconformity are generalised from the cross-sections, rather than measured directly in the field, some features are worthy of note:

1. The angular discordance across the unconformity varies from 0–45°, with the bulk of the values in the range 15–25°.
2. The angle decreases (to zero) in the west.

In a study of bed dips above and below the mid-Devonian unconformity in the Lachlan fold belt (Powell and Edgecombe 1978), it was found that the sub-unconformity beds had been folded into a series of open concentric folds with a maximum bed dip of 30°. A slightly higher maximum bed angle (say 35–40°) would seem appropriate for the Cambrian folds here.

The conformable nature of the contact between the Tyndall Group (along the western side of the Henty Fault Wedge) and the overlying Late Cambrian–Early Ordovician sequences to the west, implied by the work of Poltock (1992), contrasts with the unconformable nature of the contact north and south of the wedge (Fig 2, sections A, B). This indicates that a considerable amount of movement took place along the North and South Henty Faults prior to the close of the Late Cambrian period. The Middle Dundas to the north and the Yolande River sequence to the south, have been uplifted with respect to the HFW, thus the lack of any Tyndall Group rocks in these sequences is due to: (1) uplift during the Late Cambrian whereby the Tyndall was stripped off by erosion, or (2) the existence of topographic features that did not allow deposition of Tyndall Group in the first place.

FIREWOOD SIDING FAULT — A LATE CAMBRIAN/ORDOVICIAN GROWTH FAULT

The Firewood Siding Fault had clearly been active during late Cambrian times because both the Zeehan Conglomerate and the Moina Sandstone thicken towards the fault (Baillie and Corbett 1985). A marked change in thickness of the latter is noted across the western end of the Firewood Siding Fault in the south western corner of the Professor Plateau. Similar increases in thickness of the Zeehan Conglomerate occur towards the Little Henty Fault (Pitt 1962). The conglomerates at Zeehan have a source to the north west, whilst the conglomerates in the Professor Range have a different (probably eastern) source from the Tyennan block (D. Seymour pers. comm. 1995). This tends to confirm that the Little Henty and Firewood Siding Faults were bounding structures to two southward deepening clastic wedges which, during the main conglomerates fill stage, were quite distinct and separate entities (Fig.3).

It is considered rather unlikely that the Upper Dundas siliciclastics were as strongly fault controlled as the overlying sequences. However, Fig. 2b shows that major thickness changes, with lensing out of individual units, has to be assumed in order to avoid putting in faults for which there is little direct evidence.

MINERALISATION

Vein mineralisation at the Queensberry Ag–Zn–Pb mine (described by G.R. Green in Baillie and Corbett 1985) shows all the hallmarks of a syn-, to late-D_2 (Devonian) hydrothermal deposit related to movement on the Firewood Siding Fault. Green describes a complex paragenesis involving two phases of quartz-sulphide mineralisation and attributes the deformation to post-Devonian movements on the fault. The possibility of fluid activity along the fault during Ordovician times is not discussed, although it may have been a reality given the evidence presented in this report.

IMPLICATIONS FOR FURTHER WORK

- Further study is required to determine the relative importance of the E–W and N–S structures in controlling the shape of the basins in the Late Cambrian times.
- Further work is required to determine whether the Stitt Quartzite correlate at Farrell Rivulet can be extended south to the Firewood Siding Fault area. This will help establish whether the east-trending structures had influenced sedimentation during late middle Cambrian times or not (either as transfers or extensional growth faults).
- The three closely spaced structural sections (Figs 2a, b, c; the latter is not shown), and an earlier section across the south west corner of the HF wedge (Keele 1991b), will be integrated with the available geophysics by next meeting. Further field work, including following up some of the work by

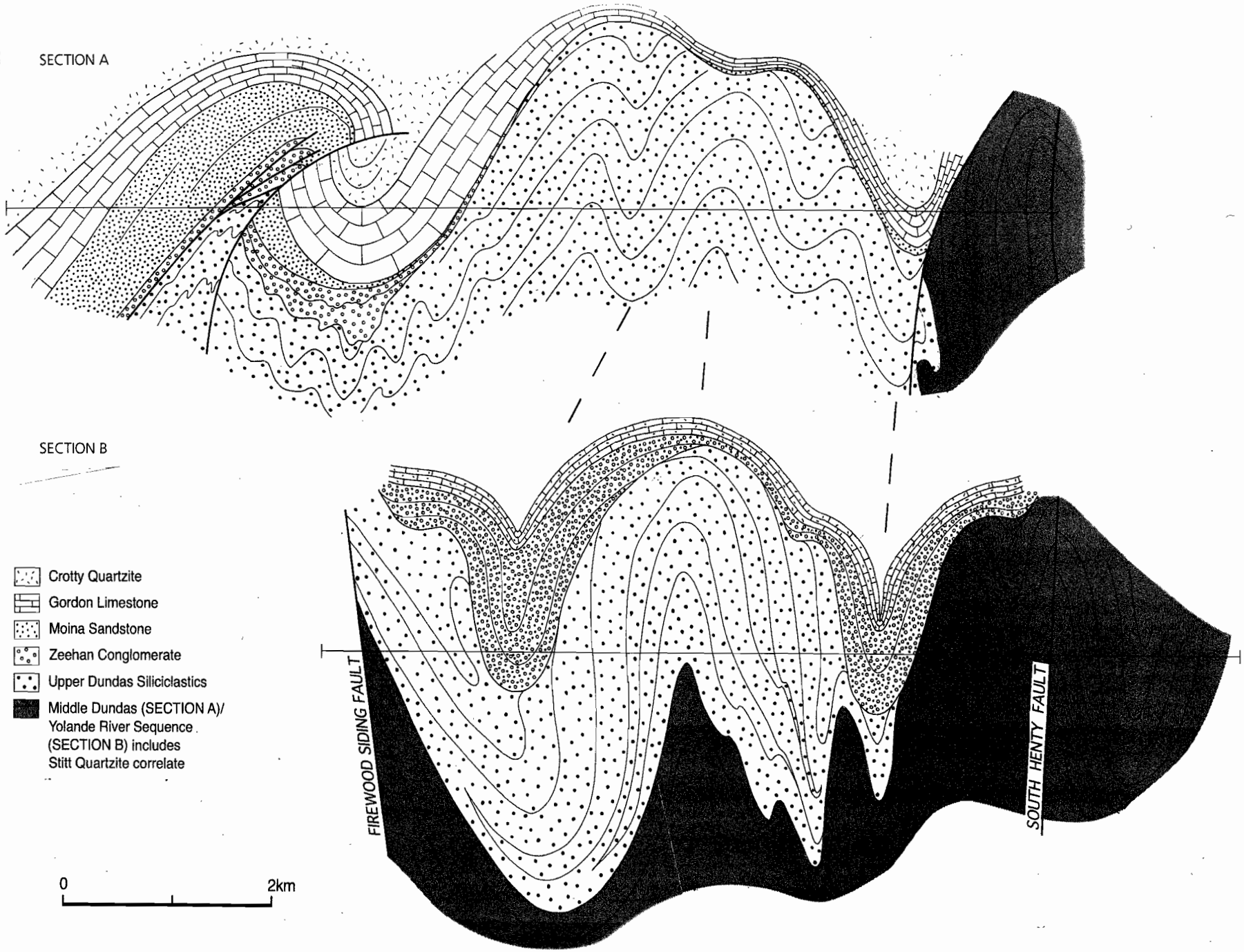

Fig. 2 Structural sections across the Upper Dundas block between the Professor Range and the Murchison Highway (refer to Fig. 1). The mudstone–siltstone–fine sandstone ± volcaniclastic sequences at the eastern end of section A belong to the Middle Dundas Group; a similar sequence at the eastern end of B belongs to the Yolander River sequence. The strong similarities in their structure might suggest that these are one, and the same, sequence.

Poltock (1992) in the HFW, would be desirable. If the top of the HFW sequence, thought to be Tyndall Group, *does* pass conformably up into the Ordovician, this implies that the HFW is primarily a Late Cambrian, rather than Devonian, structure.

ACKNOWLEDGMENTS

The author is grateful to Keith Corbett, David Seymour, Roger Poltock and Ron Berry for useful discussions on the geology of the area.

REFERENCES

Baillie P.W. and Corbett K.D., 1985. Strahan; Geological Survey Explanatory Rept. Sheet 57. Tasmania Department of Mines. 76 pp.

Berry R.F., 1991. Victoria to Queenstown regional section. CODES:AMIRA Project P.291 Structure and mineralisation of western Tasmania, 22–30.

Berry R.B. 1994. Tectonics of western Tasmania: Late Precambrian–Devonian. Geological Society of Australia, Tasmania Division. Contentious issues in Tasmanian Geology: a symposium; 5–8.

Brown A.V., Findlay R.H., Goscombe B.D., McClenaghan M.P. and Seymour D.B. 1994. 1:50 000 Geological map of the Zeehan Sheet (2nd ed.). Geological Survey of Tasmania, Department of Mines, Hobart.

Corbett K.D. and Lees T.C., 1987. Stratigraphic and structural relationships and evidence for Cambrian deformation at the western margin of the Mt Read Volcanics, Tasmania. *Australian Journal of Earth Sciences* 34, 45–67.

Keele R.A. 1991a. A description of the Howard's Road traverse. CODES/AMIRA Project P291, Structure and Mineralisation of western Tasmania. Rept. No. 2, 23–30.

Keele R.A., 1991b. The Zeehan–Red Hills–Lake Selina traverse — a domain approach to the analysis of structural data. CODES:AMIRA Project P.291 — Structure and mineralisation of western Tasmania, 40–73.

Pitt R.B.P., 1962. The geology of the Zeehan area. B.Sc. (Hons) thesis, University of Tasmania, 117 pp.

Poltock R.A., 1992 Geology of the Henty Fault Wedge, western Tasmania. M. Econ Geol. thesis, University of Tasmania, 76 pp.

Powell C. McA and Edgecombe D.R. 1978. *Jour Geol. Soc. Aust*, v 25, 165–184.

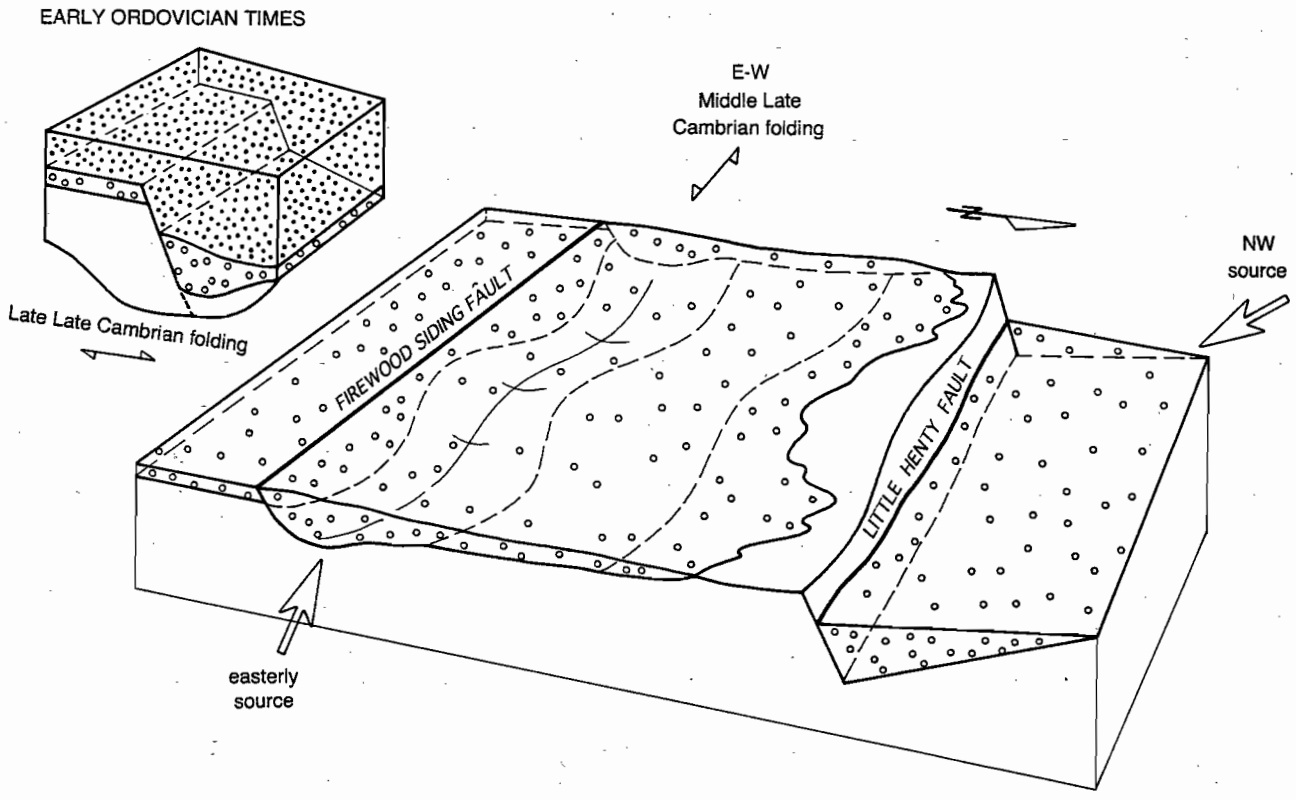

Fig. 3 Block diagram showing how E–W folding, N–S folding and faulting in Late Cambrian–Early Ordovician times probably affected the thicknesses of Zeehan Conglomerate. The Firewood Siding Fault is shown becoming more active during deposition of the Moina Sandstone.

Progress Report 3: Detecting Cambrian structures in the Mt Read Volcanic Belt using sulfur isotopes — on-going work at Rosebery

Garry J. Davidson and Paul Kitto

Centre for Ore Deposit and Exploration Studies, Geology Department, University of Tasmania

ABSTRACT

A second phase of infill laser-based sulfur isotope work has detected greater complexity in the 2 km of footwall north of the Rosebery B-lens. Seventy four analyses were obtained, mainly on holes 49R and109R, which lie 150 m and 580 m north of B-lens respectively, between previously sampled holes 60R (in mineralisation), and 71R (968 m north of B-lens). The disseminated pyrite in the footwall of both the latter holes has "ore signature" pyrite with a mean of $\delta^{34}S$ = 11.5‰. Holes 49R and 109R are similar to one another but have very heterogeneous sulfur isotope patterns (–3 to ~+45‰), av. 16.57‰ (n = 3) and 16.17‰ (n = 13) respectively. The data are better viewed in their spatial context. In hole 109R the ore position and the underlying 70 m of stratigraphy contain both very isotopically heavy ***and*** ore-signature pyrite, giving a range here of 5–46‰, with a mean of 23.5‰. The underlying 310 m of stratigraphy is characterised by B-lens to lower-than-B-lens values (–7 to +11‰), and within 30 m of the Rosebery Fault there is a second zone of heavy sulfur (11–25‰). In the previous report a picture was emerging of B-lens-values extending in the top 70 m of footwall out at least 1 km north of B-lens itself, and then rising to an average 15‰ 1.9km north of B-lens. Now it is apparent that the top 70 m of the footwall 500 m north is characterised by even heavier sulfur, indicating a local zone of direct and near-complete seawater sulfate reduction. In terms of Cambrian structures and seawater circulation, this area must be considered an area of shallow downflow, possibly imposed on a previously higher temperature alteration zone evidenced by the wide band of 5–12‰ sulfur below 70 m. By the same logic, the area around hole 71R, 968m north of B-lens, could be a separate hydrothermal upflow zone.It is identical to the B-lens variation. On the basis of isotopic heterogeneity, including values as heavy as 25‰ which are comparitively rare in the Rosebery footwall, the Rosebery Fault has experienced sulfur precipitation during during the Cambrian and during the Devonian; heterogeniety may be the hallmark of such histories.

In other work, regional Cambrian faults have been sampled for sulfides, but no results are yet available. The areas sampled are "Moxons" Fault (a splay of the Henty Fault north of Henty), Zigzag Hill north of Mt Lyell, faults on the shores of Lake Macintosh, a projected splay within the Rosebery township, and the Carters Prospect in the Back Peak area west of Cradle Mountain. Uncertainty over the timing of veining at Carters Prospect has been allayed by identification of a Cambrian Pb-isotope signature, slightly less radiogenic than Hellyer .

INTRODUCTION

This is the third progress report investigating the usefulness of sulfur isotopes in the identification of Cambrian brittle structures. It reports the results of a second phase of sulfur isotope work at Rosebery, and sampling details of regional Cambrian faults through the Mt Read Volcanics. Reviews of previous isotopic work at Rosebery, and of the general usefulness of sulfur isotopes, are presented in reports 1 and 2.

WORK DONE

Rosebery

Previously the Rosebery sequence was sampled below B-lens, 1 km north of B-lens, and 1.8 km north of B-lens. Analyses of sulfur in the hangingwall epiclastics, the Rosebery Slate, the host sequence, and the footwall sequence were obtained, but the greatest interest was and is in the footwall variation, which is likely to have been most influenced by the circulation of Cambrian hydrothermal fluids. It was found that the footwall down to about 70m below the ore position had a mean of $\delta^{34}S$ = 11.5‰ beneath the ore, a signature which extended 1 km north to hole 71R, but hole 107R, 1.8 km north, contained heavier sulfur, $\delta^{34}S$ = 11–21‰. This was interpreted to reflect an increase in the amount of locally reduced Cambrian seawater sulfate, such as might occur in a broad region of seawater downflow.

The second phase has tested the uniformity of the sulfur signature in the 1 km-wide upflow zone. Seventy-four analyses were obtained, mainly on holes 49R and109R, which lie 150 m and 580 m north of B-lens respectively, between previously sampled holes 60R (in mineralisation), and 71R (968 m north of B-lens). It has also examine the isotopic variation approaching the Rosebery Fault, in hole 109R.

Regional Cambrian Faults

Cambrian faults have been sampled for sulfur isotopes at six locations, as outlined in Table 1. The faults were identified Ron Berry. Faults with both Cambrian and Devonian movements were avoided to minimise the complexity of the geochemical signature. The sampling strategy was to surface-sample these faults within and at intervals of 1, 5, 10, 20 and 50 m from the trace. In practice the exact location of the trace could not always be found, but was inferred from changes in stratigraphy. Nor were materials always available for systematic sampling. Table 1 documents the sampling details.

These samples are currently being processed for sulfur isotope analysis. They were divided into two groups for the purposes of finding sulfides in the samples; (1) those with no visible sulfides, which will be crushed and sieved before heavy liquids are used for sulfide separation, and (2) those with visible sulfides, which have been submitted for laser thin-sections. These groups will be combined for laser S analysis in the coming months.

RESULTS

Regional Faults

Pb-isotope geochemistry was undertaken at Carter's Prospect to ascertain that the system was indeed Cambrian, due to doubts raised by previous Mineral Resources of Tasmania work. Three pure galena samples were obtained from the vein system, over an area of 30 m. These were sent to the University of Western Australia, and were analysed on a collaborative basis by Dr Neal McNaughton.

The analyses indicate that the lead at Carter's Prospect is Cambrian, slightly less radiogenic than the Hellyer field. Data is presented in Table 2.

Rosebery sulfur isotopes

Holes 49R, 57R, 109R and 71R were analysed in this phase of sulfur work. Results are presented in Table 3.

Footwall variation: The new work has shown that the footwall between B-lens and hole 71R 1km north is more complex than previously realised. It contains zones of heavy near-surface sulfur in the top 70 m of the sequence, overlying a region at least 310 m thick of ore-signature pyrite (Figs 1 and 2), as determined in holes 49R and 109R (the latter is the deepest hole in the sample set to date). In detail, the range and averages in 49R and 109R are similar (–3 to ~+45‰), av. 16.57‰ (n=3) and 16.17‰ (n=13) respectively, but in hole 49R there is no mode coincident with the mean, and in 109R there is a distinct mode between 5‰ and 12‰, i.e,, within the B-lens ore signature (Fig. 1). The number of samples from hole 49R is too small to determine the real downhole $\delta^{34}S$ pattern, and will be enlarged.

The data in hole 109R are better viewed in their spatial context. The ore position and the underlying 70 m of stratigraphy contain both very isotopically heavy AND ore-signature pyrite, giving a range here of 5–46‰, with a mean of 23.5‰ (n = 13 analyses from 6 samples). Given that Cambrian $\delta^{34}S$ is ~35‰, much of this data is actually heavier than the likely contemporary seawater sulfate. The underlying 310 m of stratigraphy is characterised by B-lens to lower-than-B-lens values (–7 to +11‰), and within 30 m of the Rosebery Fault there is a second zone of heavy sulfur (11–25‰) (Fig. 2).

The morphology of the heavy pyrite is 40–50μ diameter sub- and euhedra, in relatively unstrained

Table 1. *Sampling details of regional Cambrian Faults.*

Fault	Location	AMG coordinates	Sampling Details	Nature of samples
Carters Prospect	2km NW of Back Peak, vein-systems transecting the Precambrian/Cambrian contact	406500mE 5394400mN	Fault not directly sampled. Samples mainly 30 m east of probable fault trace.	Some visible disseminated py and galena in silicified areas; Pb-isotopes indicate Cambrian age
"Moxons" Fault (a Henty Fault splay)	2km NW of Henty mine, on the Tyndall-CVC contact	381500mE 5365850mN	100m wide zone of intense shearing with severe chlorite, pyrite and sericite alteration	Visible pyrite. Samples taken at ~20 m intervals across the shear.
"Tullabardine" Fault (a Henty Fault splay)	On the northern shore of Lake Macintosh, on the CVC-Dundas Group contact	388650mE 5385300mN	Fault not directly sampled. Obtained Dundas Group 100m east, and CVC 50m west, and an isolated silica pod in the fault. Heavy vegetation.	Visible pyrite nodules in the Dundas Group. No visible pyrite elsewhere.
"Dalmeny St" Fault	Rosebery township	379400mE 5373200mN	A brittle fault dipping 80°/076° was sampled, likely to be Devonian, but this corresponds to the Cambrian location	No visible sulphides; Sample intervals: 0, 1, 5m; weathered.
Pieman River	Details in next progress report			
"ZigZag Hill" Fault	Comstock Valley, 6 km north of Queenstown	382200mE 5345800mN	Fault not exposed. Separates Tyndall Group andesites from volcaniclastics. Associated with strong red-K-feldspar alteration	Minor visible py. RGC drillhole with abundant py still needs to be sampled. Have sampled 5, 10 and 100m from fault.

Table 2. *Pb-isotope analyses of pure galenas from Carter's Prospect, Back Peak area.*

Sample	206/204	207/204	208/204
PKGD1a	18.284	15.608	38.148
PKGD1b	18.272	15.606	38.144
PKGD1c	18.274	15.601	38.147

fabrics. Only laser thin-sections have been inspected to date, but in a subsequent progress report correct-thickness thin-sections will be studied to determine if the heavy sulfur samples have a particular mineral or textural association.

Black Slate/hangingwall epiclastic variation: A detailed synthesis of this will be presented in a subsequent progress report. Black Slate pyrite is routinely analysed, resulting in 36 analyses to date, with an average $\delta^{34}S$ value of 10.4‰ (range $\delta^{34}S$ = –6.5 to +26.0‰). The current work-phase determined that where both nodular (up to 1 cm diameter) and dispersed fine pyrite were present in slate, the dispersed pyrite was ~ 20‰ lighter than the nodular variety. A smaller variation was obtained within the nodules, with the margins being~2‰ heavier than the cores. Raw values are presented in Table 3, but no attempt has been made to separate "Devonian" pyrite in veins.

DISCUSSION

In the previous report a picture was emerging of ore-values extending in the footwall out at least 1 km north of B-lens itself, and then rising to an average 15‰ 1.9km north of B-lens. Now it is apparent that the top 70 m of the footwall 500 m north is characterised by much heavier sulfur, indicating a local zone of direct and near-complete seawater sulfate reduction. In terms of Cambrian structures and seawater circulation, this area must be considered an area of shallow downflow, possibly imposed on high temperature alteration, evidenced by the wide band of 5–12‰ sulfur below 70 m, and by sporadic "ore signature" values within the heavy zone (Fig. 2).

By the same logic, the area around hole 71R, 968m north of B-lens, could be a separate hydrothermal upflow zone. Additional hole 71R data obtained during this work-phase, and reported in Table 3, indicates that the top 60 m of footwall has an average of $\delta^{34}S$ = 11.5‰, and a range of 3.6–13.2‰ (n=6, 11analyses), which is identical to the B-lens variation.

These relationships are sketched in Fig. 3. The unknowns in the area are shown with question marks. Firstly, how extensive is the heavy sulfur facies which occurs between B-lens and the upflow in hole 71R? Hole 109R has clearly shown that the zone has a distinct depth limit, but its lateral exent is uncertain. This will be rectified in the final infill phase, by analysing footwall samples from hole 57R (120 m north of B-lens). What is the relationship between the upflow zone of hole 71R and the adjacent downflow in hole 109R? This question awaits further infill drilling. Lastly, what is the real significance of the increase in $\delta^{34}S$ found in hole 107R 1.8 km from B-lens, now that other zones of heavy sulfur have been located? The $\delta^{34}S$ range in 107R is far more restricted than in hole 109R and 49R, and unlike these, has very little overlap with "ore signature" values. On this basis fluid circulation may have been better mixed, with mixing occurring between deep upwelling reduced sulfur, and pure reduced seawater sulfate, as might occur towards the edge of a regional upflow cell.

The Rosebery Fault data represents an interesting variation on this theme. Hole 109R finishes in the fault, and the passage of Devonian fluids is recognised by abundant carbonate–tourmaline–pyrite/pyrrhotite veins. Our previous work recognised a Devonian signature in some texturally distinct areas of $\delta^{34}S$ = 1–4‰, whereas Khin Zaw (1991) has shown that where Devonian fluids contact Cambrian sulfides, their innate sulfur content is so low that there is no net isotopic change, and a homogenised Cambrian signature remains. It is yet to be demonstrated that Devonian fluids scavenge and transport Cambrian sulfur to new sites, although this is possible, given that they clearly scavenge large quantities of Pb and Zn. Carbonate–tourmaline-bearing veins in and near to the Rosebery fault in hole 109R contain $\delta^{34}S$ = –3.5 to 25.3‰ (Fig. 2); this consists of a discrete vein zone 54m from the fault with a narrow range of $\delta^{34}S$= –3.5 to –2.4‰, grains of pyrite 3m from the main trace with $\delta^{34}S$ = 25.3‰, and pyrite in the main fault with $\delta^{34}S$ = 11.3–15.0‰. Hence some carbonate–tourmaline zones contain the Devonian light S signature, whereas the main fault trace contains heterogeneous ore signature as well as heavy sulfur, which can only have originated by Cambrian seawater reduction. There is support here for the Rosebery Fault as a Cambrian entity, that at times even experienced downflow of Cambrian seawater to achieve values as high as $\delta^{34}S$ = 25.3‰. If the sulfur signature was purely Devonian, it would be either similar to the identified Devonian signature, or consist of a homogenised Cambrian signature. In fact it is mainly similar to Cambrian values, it is very heterogeneous, and it includes heavy values which are comparitively rare in the Rosebery deposit. It is possible that heterogeneity may be a useful criteria in discriminating faults with both Devonian and Cambrian fluid movement histories.

CONCLUSIONS

1. Areas of very heavy Cambrian sulfur are the signature of shallow Cambrian seawater downflow within 500 m of major upflow zones. The only known Rosebery downflow zone extends 70 m below the ore horizon.

2. The Rosebery Fault contains a mixed Devonian-ore Cambrian and heavy-S Cambrian signature, suggesting it was fluxed with Devonian magmatic fluids, as well as downwelling Cambrian waters. The signature of a multiple fluid history may be sulfur isotope heterogeneity.

3. Whereas the region 1 km north of B-lens was previously thought to be all dominated by the upflow ore signature ($\delta^{34}S = 11.5‰$ on average), it is now known to be divided into two regions in which the top 70 m of stratigraphy contains the ore signature, separated by a region of heavy sulfur alluded to in point 1. An explanation for this is that two upwelling zones were originally present, one of which was overlain by B-lens.

FUTURE WORK

At Rosebery

1. A final infill and check laser isotope phase is required, mainly on holes 49R and 57R.
2. Further samples of sulfur in the Rosebery Fault should be obtained and analysed, to evaluate the heterogeniety of sulfur isotopes in the fault plane.
3. More careful sampling of the hostrock–footwall contact is required, to determine the extent of heavy sulfur zones in the Rosebery sequence. Have they been missed in any of the other holes?
4. Transmitted and reflected light study of existing samples, to develop better criteria for recognising Devonian sulfides in hand-specimen, and to determine if there are mineralogical or textural means of identifying zones of heavy Cambrian sulfur.

Regionally

5. Stage 1. Analyse regional fault samples now collected for sulfur isotopes.
6. Stage 2. If the results warrant further work, resample the well-exposed faults from this group, to determine what lateral changes can be expected along Cambrian faults. The "Moxons" Fault–Henty Fault zone is likely to be the best area, on the known distribution of outcrop, availability of sulfides, and location of prospects.

REFERENCES

Khin Zaw (1991) The effect of Devonian metamorphism and metasomatism on the mineralogy and geochemistry of the Cambrian VMS deposits in the Rosebery–Hercules district, western Tasmania. PhD thesis, University of Tasmania (unpublished).

Updated Rosebery sulfur isotope data

DDH/METRES	MINE SEQUENCE	SAMPLE DESCRIPTION	anal. no.	Machine ∂34S	Corrected value	Corr'd value (laser)	Corrected sample mean	Comment	hole diam µ
DDH 107R									
107R-546.6m	Black Shale	Py in 2mm veinlet	1048	2.70	0.51	6.26	7.60	Vein py edge	300
			1049	5.20	3.19	8.94		Vein py centre	300
107R-558.5m	Black Shale	Disseminated Py in epiclastic sandstone							
107R-601.1m	HW epiclastics	Disseminated Py in Qz-Fels phyric volcanoclastics							
107R-621.0m	HW epiclastics	Disseminated Py in Qz-phyric volcanoclastics							
107R-639.7m	HW epiclastics	Disseminated Py in Qz-Fels phyric volcanoclastics							
107R-651.4m	Host rock	Laminated Fels-phyric shales	1052					Too small	
			1053	11.77	10.26	16.01	16.64	1mm py vein, Cambrian	250x3
			1054	12.95	11.52	17.27		Same vein; 1cm to 1053	400x2
107R-652.5m	Host rock	Disseminated Py in Qz-Fels phyric volcanoclastics	1069	0.46	-1.91	3.84	3.84	Anhedral clot 2mmx3mm: Dev.?	400
107R-661.1m	FW volcanics (Pumiceous Breccia)	Disseminated Py in semi-massive Fels-phyric sandstone	1070	10.90	9.32	15.07	15.07	Recryst. Cambrian py; 200µ av.	300x2
107R-669.9m	FW volcanics (Pumiceous Breccia)	Disseminated Py in siliceous Fels-phyric volcanoclastic/epiclastic	1082	8.64	6.88	12.63	12.63	Recryst. Cambrian py; 70µ av.	250X7
			1083					Too small	
107R-677.3m	FW volcanics	Disseminated Py veined by late carbonate	1064	12.71	11.26	17.01	17.01	Recryst'd py; 400µ av.	300
			1065	12.70	11.25	17.00		Recryst'd py; 400µ av.	300
107R-688.3m	FW volcanics (Pumiceous Breccia)	Disseminated Py in massive pumiceous breccia	1073	7.83	6.02	11.77	12.42	Recryst'd py; 400µ av.	250x2
			1074	9.04	7.32	13.07		Recryst'd py; 100µ av.	250x5
107R-711.1m	FW volcanics (Pumiceous Breccia)	Disseminated Py in massive pumiceous breccia	1071	10.82	9.24	14.99	14.15	Recryst'd py; 400µ av.	400
			1072	9.25	7.55	13.30		Recryst'd py; 400µ av.	250
107R-722.3m	FW volcanics (Pumiceous Breccia)	Disseminated Py in massive pumiceous breccia & 5cm siderite	1066	15.65	14.43	20.18	15.41	Recryst'd py; 700µ av.	300
		alteration zones	1067	7.82	6.01	11.76		Recryst'd py; 700µ av.	250
			1068	10.18	8.54	14.29		Recryst'd py; 100µ av.	250x5
107R-728.0m	FW volcanics (Pumiceous Breccia)	Disseminated Py in massive pumiceous breccia with silicified Fels	1051	9.49	7.80	13.55	15.75	Recryst'd py; 500µ av.	300X2
		phyric texture	1050	13.58	12.20	17.95		Recryst'd py; 300µ av.	300
DDH 49R									
49R-800.0'	HW epiclastics	Disseminated Py in turbiditic mass flows?	1540	4.68	5.45	11.20	11.20	Large std. dev. One piece of anhedral py	
49R-815.0'	Black Shale	Black shales with Py-nodules	1552	12.32	14.65	20.40	20.40	Large std. dev.-UNCERTAIN SAMPLE NO.	
49R-840.0'	Black Shale	Black shales with abundant Carb-Py veining	1524	18.15	20.23	25.98	25.98	3 mm long py veinlet	
49R-898.0'	Black Shale	Black shales with abundant Carb-Py veining	1544	10.96	13.02	18.77	8.97	2-4 mm wide massive py & qutz	
			1545	-5.11	-6.33	-0.58		as again, 0.5 cm along	
			1546	2.62	2.98	8.73		as again, midway between the others	
49R-925.0'	Black Shale	Py-black shales	1505	3.71	4.06	9.81	10.41	Py in black shale concretion	
			1506	5.24	5.26	11.01		concretion margin	
49R-935.0'	Host rock (split)	Thin epiclastic layers interbedded with Py-black shales	1500	-14.24	-17.84	-12.09	-4.86	high std. dev.	
			1502	-2.39	-3.39	2.36		high std. dev.	
49R-954.0'	FW volcanics (Pumiceous Breccia)	Disseminated Py in pumiceous breccia	1503	-6.85	-8.83	-3.08	-2.50	subhed. py extending from straight vein	
	(pyrite adjacent to straight vein)		1504	-7.10	-9.13	-3.38		anhedral: Dev.?	
			1529	-6.10	-7.89	-2.14		py vein	
			1530	-5.45	-7.14	-1.39		py euhedra: 7 grains in all	
49R-956.0'	FW volcanics (Pumiceous Breccia)	Disseminated Py in pumiceous breccia							
49R-984.0'	FW volcanics (Pumiceous Breccia)	Disseminated Py in pumiceous volcanoclastic	1553	1.67	1.83	7.58	6.02	high std. dev. Fine anhedral py/po in vein	
			1554	-0.92	-1.29	4.46		high std. dev. A.a.	
49R-998.0'	FW volcanics (Pumiceous Breccia)	Disseminated Py-Po in pumiceous breccia	1483	29.42	35.42	41.17	46.19	po?	
			1486	35.92	43.35	49.10		300µ blebs of po?	
			1487	34.28	41.35	47.10		200µ blebs of po?	
			1499	34.51	41.63	47.38		200µ blebs of po?	
DDH 57R									
57R-2250.0'	Black Shale	Black shales with thin laminated turbidite layers containing	1513	-8.10	-10.22	-4.47	-4.47	Large Std. dev. Massive region+carb.Dev?	

Updated Rosebery sulfur isotope data

DDH/METRES	MINE SEQUENCE	SAMPLE DESCRIPTION	anal. no.	Machine ∂34S	Corrected	Corr'd value	Corrected	Comment	hole diam μ
57R-2273.0'	Black Shale	Black shales with disseminated Py cubes	1479	6.98	8.05	13.80	13.60	Coarse 2-3 mm py; dissem cpy also	
			1480	6.64	7.63	13.38		a.a.	
57R-2290.0'	Black Shale	Disseminated Py in laminated epiclastics	1551	-5.36	-6.64	-0.89	-3.68	Schistose py	
			1569	-9.97	-12.18	-6.48		anhedral py within chlorite alteration	
57R-2301.0'	Mineralised Black Shales	Graphitic?-Py black shales cut by 15cm wide Qz-Rhod vein	1471	7.05	8.13	13.88	13.94	meta-vein of py	
			1473	7.14	8.24	13.99		meta-vein of py, 1 cm from last	
57R-2325.0'	Host Rock	Disseminated Py±Sph±Qz in fine grained epiclastic	1541	-7.43	-9.12	-3.37	0.64	X-cutting late? vein with ab. fine py	
			1542	3.93	4.55	10.30		X-cutting late? vein with ab. fine py	
			1543	-8.79	-10.77	-5.02		Large Std. dev. A.a	
57R-2362.0'	FW Volcanics?	Siliceous epiclastic with Py-Sph-Chl veinlets							
57R-2437.0'	FW Epiclastics	Disseminated Py in Qz-Fels phyric sequence							
57R-2437.0'	FW Epiclastics	Disseminated Py in Qz-Fels phyric sequence							
N.B. THE EARLY SAMPLES FROM THIS HOLE MAY BE FROM A DEFLECTION									
57R-2391.0'	Ore Zone	Disseminated Py-Sph-Gal in chloritised host							
57R-2424.0'	FW Volcanics	Disseminated Py in fels-phyric chloritised volcanics							
57R-2460.0'	FW Volcanics	Disseminated Py in epiclastics							
57R-2495.0'	FW Volcanics	Disseminated Py(±Po) in volcanoclastics							
57R-2535.0'	FW Volcanics	Disseminated Py-Sph in volcanoclastics							
57R-2546.0'	FW Volcanics	Disseminated Py-Sph in volcanoclastics							
DDH 109R									
109R-510.0m	Black Shale	Disseminated Py in turbiditic-conglomeric mass flow with black	1547	-2.01	-2.60	3.15	3.16	800μ patch of anhedral py	
		shale clasts	1548	-1.99	-2.57	3.18			
109R-530.0m	Black Shale	Disseminated Py in calcite veined black shale	1565	8.98	10.64	16.39	23.75	schistose py 2mm across in black shale	
				15.86	18.92	24.67		high std. dev. Background fine py	
				20.45	24.45	30.20		high std. dev. 3 grs in a thin veinlet	
109R-550.0m	Black Shale	Disseminated Py in laminated Black shale with minor calcite veinlet	1537	12.07	14.35	20.10	13.80	coarse strained pyrite	
			1538	-3.75	-4.69	1.06		fine background pyrite: 8 blasts	
			1539	12.19	14.50	20.25		coarse strained pyrite	
109R-559.5m	Host Rock	Disseminated Py in a pumiceous Fels-phyric epiclastic with	1562	0.47	0.38	6.13	5.24	A single 200μ py in a clump of grs.	
		chloritic-calcite veins	1563	-2.35	-3.01	2.74		high std. dev.	
			1564	1.05	1.09	6.84		a.a.	
109R-569.6m	Transition Zone	Disseminatd Py in pumiceous mass flow	1514	34.17	38.81	44.56	45.09	a 2-3mm cluster of fine py-cpy	
			1515	35.08	39.87	45.62			
109R-580.0m	Transition Zone	Disseminatd Py in pumiceous mass flow with chloritic veinlets	1517	2.81	2.44	8.19	8.19	high std. dev. anhedral py in thin vein	
109R-591.2m	FW Volcanics	Disseminatd Py in pumiceous mass flow with prolific Qz-Chl	1531	24.28	27.34	33.09	34.90	internally intricate py-po: Dev?	
		crack-seal veins	1532	27.40	30.96	36.71		internally intricate py-po: Dev?	
109R-599.2m	FW Volcanics	Disseminatd Py in pumiceous mass flow with both chloritic							
		veinlets and Qz-Carb veins							
109R-611.3m	FW Volcanics	Fels-phyric mass flow with minor Py in a chloritic interval	1519	4.31	4.18	9.93	12.06	high std. dev. Massive py in 1mm x 2mm zone	
			1520	0.57	-0.16	5.59		high std. dev.	
			1521	5.69	5.78	11.53		euhedral 200μ pyrite	
			1523	14.01	15.43	21.18		anhedral pyrite	
109R-620.5m	FW Volcanics	Fels-phyric mass flow with Py disseminated along fractures	1507	10.86	11.77	17.52	20.17	Large anhedral clot	
			1509	15.41	17.06	22.81		Other end of same	
109R-629.4m	FW Volcanics	Fels-phyric mass flow with minor disseminated Py	1477	15.18	18.05	23.80	24.58	euhedral py x 2, 0.4 cm apart	
			1478	16.45	19.60	25.35		euhedral py x 3, 0.5 cm apart	
109R-642.0m	FW Volcanics	Fels-phyric mass flow with Py disseminated along fractures							
109R-649.6m	FW Volcanics	Disseminated Py in Fels-phyric mass flow with Chl-Qz veining	1474	0.69	0.37	6.12	6.12	2 mm long collection of subhedra: Dev?	
109R-671.5m	FW Volcanics	Disseminated Py in Fels-phyric mass flow with chloritic alteration	1516	0.93	0.26	6.01	6.01	high standard dev. Late? X-cutting py	

Updated Rosebery sulfur isotope data

DDH/METRES	MINE SEQUENCE	SAMPLE DESCRIPTION	anal. no.	Machine ∂34S	Corrected	Corr'd value	Corrected	Comment	hole diam μ
109R-738.7m	FW Volcanics	Chloritic-Kfels alteration of Qz-Kfels phyric mass flow similar to Anthony Rd.							
109R-790.1m	FW Volcanics	Disseminated Py in siliceous Fels-phyric mass flow	1533	0.33	-0.43	5.32	5.17	Veins and strings of py as euhedra	
			1534	0.08	-0.72	5.03		Veins and strings of py as euhedra	
109R-839.5m	FW Volcanics	Disseminated Py in Fels-phyric mass flow	1535	3.80	3.58	9.33	9.93	Recryst'd py in high strain zone	
				4.82	4.77	10.52		Recryst'd py in high strain zone	
109R-841.4m	FW Volcanics	Tour-Qz veining and brecciation together with Py veinlets (Dev.)	1527	-7.24	-9.22	-3.47	-2.96	Vein 2 mm wide	
			1528	-6.35	-8.19	-2.44			
109R-871.5m	FW Volcanics	Fels-phyric mass flow with disseminated Py	1475	9.48	11.09	16.84	15.57	Large Cambrian py xtal	
			1476	7.39	8.54	14.29		Same grain, other end	
109R-892.0m	FW Volcanics-5m from Rosebery	Pumiceous Fels-phyric mass flow with carbonate overprint	1555	16.42	19.59	25.34	25.34	high standard dev. 7 subhedral grains	
	Fault								
109R-895.0m	Rosebery Fault	Siliceous brecciation zone with Carb(±Tour) overprint	1549	7.87	9.29	15.04	13.18	strongly fractured, py on cracks	
			1550	4.77	5.56	11.31			
DDH 60R									
60R-2827.0'	Black Shale	Disseminated Py in laminated black shale with carbonate veinlets	1035	1.16	-1.15	4.60	5.64	Vein in black shale: 3 large grns.	300X3
		parallel to schistocity	1036	3.10	0.93	6.68		8 disseminated grns, 50–100μ	300X8
60R-2850.0'	Black Shale	Disseminated Py in laminated black shale with carbonate veinlets	1032					Too small	
		parallel to schistocity	1033	13.97	12.62	18.37	18.80	Recryst'd & dissem'd;large grains	300X3
			1034	14.77	13.48	19.23		Recryst'd & dissem'd;large grains	300x4
60R-2890.0'	Black Shale	Disseminated Py at the contact between black shales and minor	013, 15, 17					Too small	
		mass flow unit	1014	2.45	0.23	5.98	5.05	Vein pyrite in black shale	400
			1016	5.02	3.00	8.75	8.75	Recrystallised euhedra; 100μ av.	300
			1018	5.07	3.05	8.80		Recrystallised euhedra; 500μ av.	300X5
			1019	0.71	-1.63	4.12		Vein py, 2 grains	300X2
60R-3001.0'	Porphyry????	Disseminated Py in Fels-phyric(Porphyry?) unit with Qz-Carb	1024	-7.18	-10.12	-4.37	-4.01	Recryst'd;100μ av.	6x250
			1025-1027					Too small	
			1028	-6.52	-9.41	-3.66		Big euhedra in deformed vein	250X2
60R-3095.0'	Ore Zone	Massive Py-Sph Gal	1031	5.85	3.89	9.64	9.64	Massive pyrite; analysed one gn	400
60R-3106.0'	Ore Zone	Py-Sph vein	1039	7.02	5.15	10.90	10.90	Abundant pyrite, recrystallised	300x3
60R-3154.5'	FW Volcanics	Disseminated sulphides and stringer veins	1058	12.60	11.14	16.89	17.25	Recrystallised;150μ	300x3
			1059	13.12	11.71	17.46		Recrystallised;150μ	300x3
60R-3197.0'	FW Volcanics	Disseminated Py and Qz-Carb veining	1010	5.24	3.23	8.98	10.56	Recrystallised, single gn; 300μ	400
			1009					Too small	
			1011	8.06	6.26	12.01		Recrystallised, single gn; 300μ	300
			1012	6.84	4.95	10.70		Recrystallised, single gn; 200μ	300x2
60R-3213.0'	FW Volcanics	Disseminated Py in chloritic volcanoclastic	1029	3.57	1.44	7.19	7.25	Recrystallised, single gn; 500μ	300
			1030	3.66	1.54	7.29		Recryst'd; 800μ; 1cm from 1029	300
60R-3253.0'	FW Volcanics	Disseminated Py in chloritic volcanoclastic	1022	8.92	7.19	12.94	12.29	Recrystallised, single gn; 1000μ	300
			1023	7.72	5.90	11.65		Recrystallised, two gn;400μ	300X2
60R-3290.0'	FW Volcanics	Disseminated Py in chloritic volcanoclastic	1007	9.71	8.04	13.79	14.09	Recrystallised, single gn;200μ	150
			1008	10.27	8.64	14.39		Recrystallised, single gn;200μ	350
60R-3325.0'	FW Volcanics	Disseminated Py in sericitised Qz matrix	1020	6.64	4.74	10.49	9.56	Recrystallised, two gn;400μ	250X2
			1021	4.91	2.88	8.63		Recrystallised, single gn;400μ	300
60R-3346.0'	FW Volcanics	Disseminated Py in siliceous volcanoclastic							
60R-3368.0'	FW Volcanics	Disseminated Py in siliceous volcanoclastic	1037	5.46	3.48	9.23	10.06	Recrystallised, 5 gns;150μ	300x3
			1038	7.02	5.15	10.90		Recrystallised, 3 gns;150μ	300X5
60R-3385.0'	FW Volcanics	Disseminated Py in volcanoclastic	1046	8.56	6.80	12.55	12.28	Recrystallised;150μ	300X2
			1047	8.06	6.26	12.01		Recrystallised;200μ	300X2
DDH 71R									
71R-1648.0'	Black Shale	Disseminated Py in carbonate veinlets	1003	12.79	11.35	17.10	16.21	Primary 4mm grain	300

Updated Rosebery sulfur isotope data

DDH/METRES	MINE SEQUENCE	SAMPLE DESCRIPTION	anal. no.	Machine ∂34S	Corrected	Corr'd value	Corrected	Comment	hole diam µ
			1004	11.13	9.57	15.32		Primary 0.5mm grain	320
71R-1707.0'	Black Shale	Laminated Black shale with Py veinlets. Po disseminated through-	995	11.71	10.19	15.94	14.15	Gape-fill: single crystal	300
		out core but not in this piece	996	7.01	5.13	10.88		500 µ from 995; same crystal	300
			997	11.28	9.73	15.48		thin short vein; 0.5cm from 995	300
			998	9.03	7.31	13.06		thin short vein; 1 cm from 995	200
			999	11.20	9.64	15.39		same vein as 998; 300µ away	200
71R-2096.5'	HW epiclastics	Disseminated Py in Qz-Fels phyric pumiceous breccia							
71R-2107.0'	HW epiclastics	Disseminated Py in Qz-phyric pumiceous breccia	1005	-2.07	-4.62	1.13	1.13	2mm grain	200
			1006					Sample too small	
71R-2133.0'	Host Rock	Disseminated Py in cherty siltstone	1042	0.19	-2.19	3.56	3.35	Filagree pyrite....Devonian?	250x3
			1043	-0.37	-2.79	2.96		Filagree pyrite....Devonian?	250x2
71R-2174.0'	Host Sequence	Disseminated Py in Fels-phyric pumiceous breccia	1075	4.93	2.90	8.65	10.74	recrystallised py;250µ av.	250X2
			1076					Sample too small	
			1079					Sample too small	
			1080	8.24	6.45	12.20		recrystallised py;250µ av.	200X4
			1081	6.59	4.68	10.43		recrystallised py;250µ av.	200X4
71R-2210.0'	FW Volcanics	Disseminated Py in chloritic Fels-phyric pumiceous breccia	1040-1041					Sample too small	
71R-2210			1481	5.04	5.68	11.43	12.30	450µ euhedral py	
			1482	6.47	7.42	13.17		450µ euhedral py	
71R-2245.0'	FW Volcanics	Disseminated Py nodules in chloritic Fels-phyric pseudo	1056	8.72	6.97	12.72	12.72	recrystallised py xtal; 50µ av.	250x8
		pumiceous breccia							
71R-2286.0'	FW Volcanics	Disseminated Py in pumiceous breccia	1044	6.34	4.42	10.17	10.60	recrystallised py xtal; 2-300µ	250x2
			1045	7.15	5.28	11.03		recrystallised py xtal; 2-300µ	200x5
71R-2325.0'	FW Volcanics	Disseminated Py nodules in chloritic Fels-phyric pseudo	1057	12.67	11.22	16.97	16.97	recrystallised py xtal; 50µ av.	250x8
		pumiceous breccia with Qz-Chl crack-seal veins in core of zone							
71R-2351.0'	FW Volcanics	Disseminated Py in Kfels-Chl altered fels-phyric pseudo	1000-1002					Sample too small	
71R-2351			1526	-0.40	-1.29	4.46	4.03	anhedral pyrite	
			1526	-1.14	-2.14	3.61		euhedral pyrite	

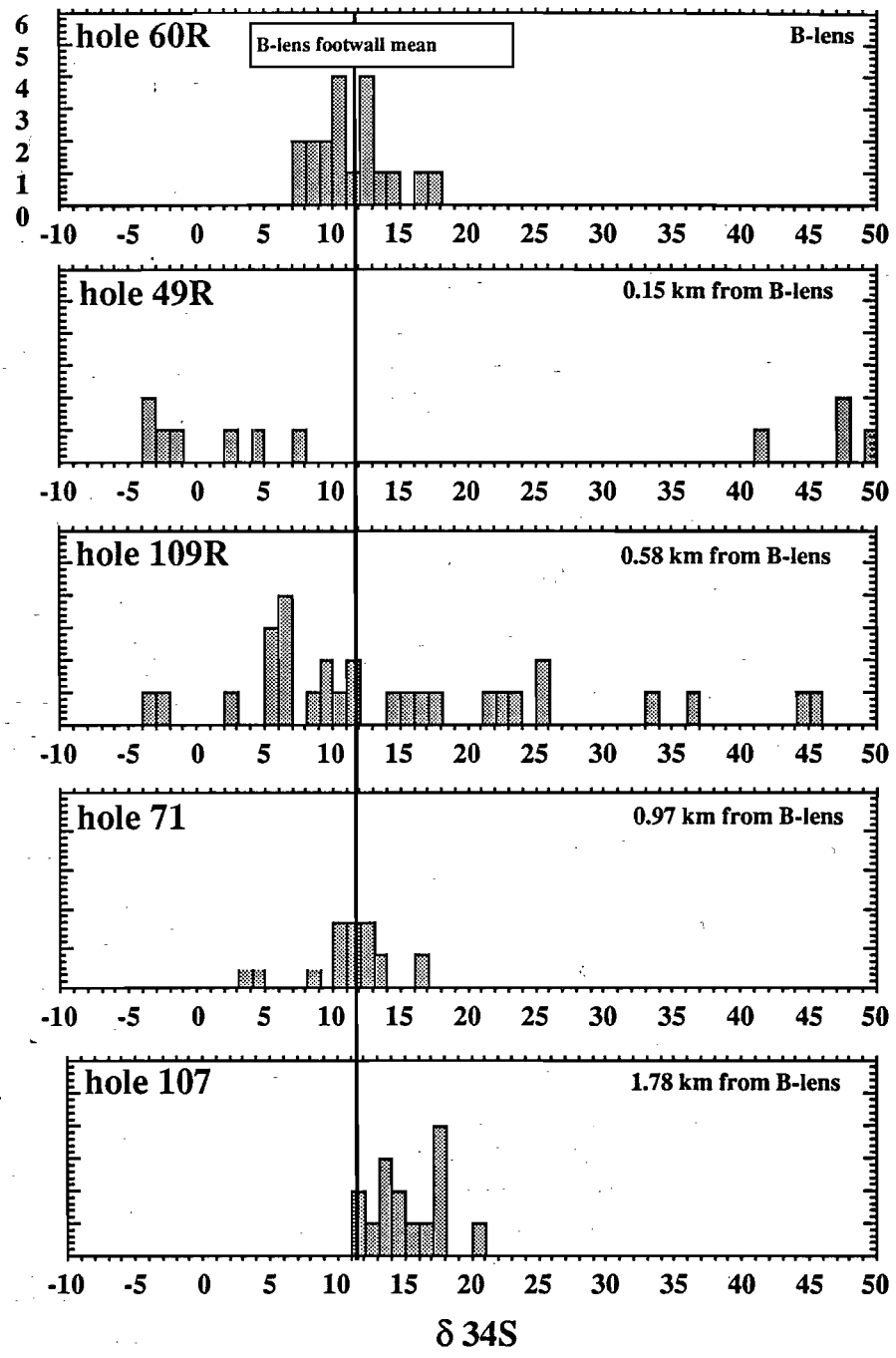

Figure 1. Frequency histogram summary of the sulfur isotope variation in five holes north of Rosebery B-lens. Data include footwall, hostrock and ore pyrites, but specifically exclude hangingwall and Devonian sulfur, where it is clearly identified.

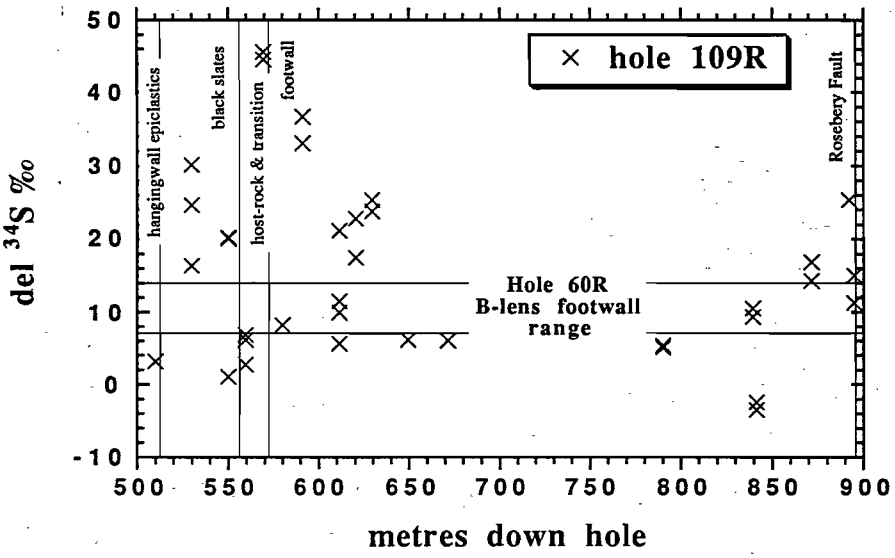

Figure 2. Total downhole $\delta^{34}S$ variation in hole 109R.

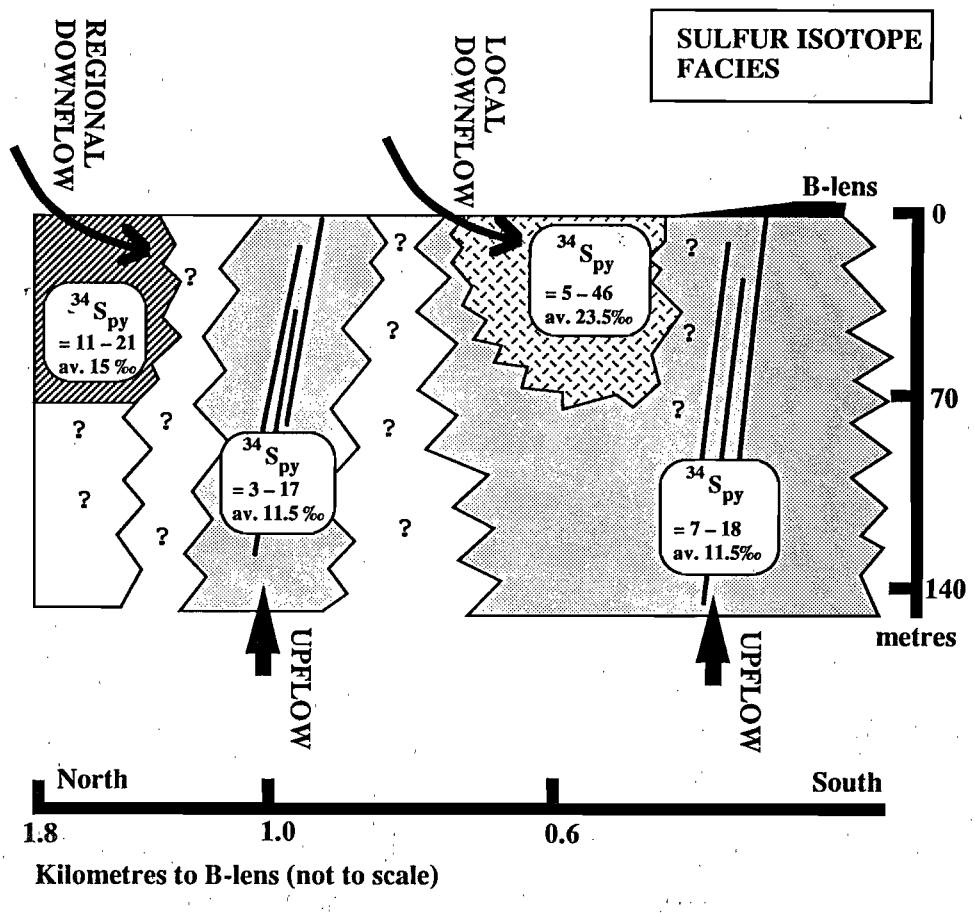

Figure 3. Sulfur isotope facies of the Rosebery footwall, a schematic section.